Exploring the Mechanics of Golgi-localized Tul1 Selective Degradation

by

Devon Danielle Dennison

A dissertation submitted in partial fulfillment
of the requirements for the degree of
Doctor of Philosophy
(Cellular and Molecular Biology)
in the University of Michigan
2024

Doctoral Committee:

Assistant Professor Ryan D. Baldridge, Chair
Professor Phyllis I. Hanson
Professor Patrick J. O'Brien
Professor Melanie D. Ohi
Professor Lois S. Weisman

Devon Danielle Dennison

devond@umich.edu

ORCID iD: 0000-0002-3229-0343

Dedication

In memory of Virginia (Ginny) Ewell, who taught
me how to unapologetically break glass ceilings
(and that singing “Eye of the Tiger” before any
presentation is a recipe for success).

Rising up, straight to the top;
Had the guts, got the glory;
Went the distance, now I’m not going to stop;
Just a woman and her will to survive.

Acknowledgements

I have had the great fortune of spending my time here at Michigan under the mentorship of Dr. Ryan Baldridge, whose generosity, support, and incomparable wealth of knowledge continues to motivate me to be the best and smartest version of myself. Ryan started every meeting with "How are you doing?" and ended every meeting with "Is there anything I can do?" – phrases that are seemingly routine but were exactly what I needed to hear sometimes. Thank you, Ryan, you've made it very hard to leave Michigan.

I would like to thank members of my thesis committee, Dr. Phyllis Hanson, Dr. Patrick O'Brien, Dr. Melanie Ohi, Dr. Lois Weisman, and Dr. Kaushik Ragunathan, for their insights and support. I have been very lucky to have the opportunity to present my work and receive guidance from such an esteemed and inspiring group of scientists. I would also like to thank Dr. Matt Chapman and Dr. Lyle Simmons, who played large roles in my decision to come to Michigan. I came here prepared to continue my love for western blotting thanks to the stellar mentorship of Dr. Misol Ahn during my undergraduate research at UCSF. Thank you to Dr. Tanya Parish for giving me the opportunity to join her TB Drug Discovery group in Seattle, where I continued to hone my skills under her great leadership and from working with Dr. Matt McNeil.

I would also like to thank members of the Baldridge lab, past and present, for their contributions and constructive feedback. I would especially like to thank Dr. Jiwon Hwang and Dr. Rachel Sharninghausen for their mentorship and friendship, I miss you both immensely. To Dr. Brian Peterson – I always say that you walked so I could run, and that's not just because you're an extremely fast walker. You have set a strong precedence for research greatness in the Baldridge lab; your friendship, intelligence, and advice has shaped my work and my life for the better. To Jenn Russ – I'm a little upset that you waited so long to come to Michigan so we could meet, but I look forward to celebrating your successes in and outside of the lab for years to come, and, more importantly, to keeping you company on the phone during those late nights concentrating protein.

To the wonderful friends I met in Ann Arbor: Amanda Ames –your ability to say exactly the right thing to make my day better continues from afar, though I miss having you right around

the corner. Denise Poltavski – you were my first friend here and my first favorite thing about Ann Arbor, our virtual movie nights are a highlight of my week. Martina Fraga – your generosity and loyalty is unmatched, thank you for constant support, advice, and unlimited access to the candy bowl. Shannon Lacy – you made our apartment home and they say that home is where the heart is, thank you for lighting up my life much like the lights on Main Street. I would also like to acknowledge Nick Urban (someday we'll finish Ted Lasso, I promise!), Kevin Toolan, Jeff Knupp, Madison Pletan, Katy Speckhart, Sarah Katz, Emily Eberhart, Tyler Hoard, Evan Arnold, Lwar Naing, Jack Ryan, Andi Bustamante, Allie Duensing, and Mike Nagy for their friendship, support, and advice throughout the years. Go Blue!

To my Berkeley friends: Alex Trantham, Tori Bird, Lauren Hogrewe, Adrienne Wedel, Ashley Young, Megan Delzell, and Brittany Hanson – ladies, we've made it. Life wouldn't be the same without each and every one of you and the memories from our annual reunions never fail to put a smile on my face. I especially would like to thank Alex and Tori for doing what no Californians should do and traveled to Michigan in December to be front row at my defense; thank you for bringing the literal and metaphorical sunshine with you. Sarah Healy –your dedication to the bit is one of the many reasons I'm so grateful that you're in my life, and for all of the joy and support you give me, I hope we can be neighbors again someday. Michelle Leeds –we first met at Cal, but fate brought us together in Seattle and you got me through some particularly hard times, which wasn't just while helping me practice vocab for the GRE. I would also like to acknowledge Rachel Hoffman, Geof Leeds, Collin Raff, Sage Purkey Cioto, Brendan Cioto, the Trantham family, and the Bird family for their continued support and friendship. Go Bears!

To my Seattle friends: Katya Selivanoff – our phone calls never fail to make my day and your presence at any and all milestones in my life is something I will always treasure; Melia Albrecht – your confidence is contagious, your laugh infectious, and your motivational speeches effective, thank you for always being there for me; Dr. Kayla Robinson – your brilliance, loyalty, and kindness, among many other amazing traits, make you the scholar, partner, and mother that I aspire to be (and thank you for bringing Chris and Avery into my life). Thank you all for making the trip out here for my defense, but also for sticking with me since middle school; our friendships will continue to transcend time zones for decades to come. Lindsay Flint – I look forward to our hikes every time I'm home and your science memes never fail to make me laugh. Amanda Garza – music is therapy, and the concerts we go to together heal my soul. Jen, Mike, Dan, and Ben

Pinkowski – keep a seat open at the kitchen counter because I'll be ready for my victory lap and fist bump soon, thank you for your unending support throughout the years. To the Thanksgiving crew, Lauren, Colin Briskman, and Renee and Paul Hein – your friendships continue to expand the list of things I am grateful for, which extends far beyond our holiday gatherings. I would also like to acknowledge Elise Sobotka, Katie Tinkham, the Selivanoff family (especially Nikita and Nina), the Graue family, and the Mendel family for being amazing cheerleaders and their continued support.

I would like to thank my tiny but mighty family, curated by my grandparents Dave and Shirley Dennison and Gwen and Ray Ewell, whose influences in my life transcended genetics. On the Dennison side, Aunt Lilli and Uncle Brian – thank you for creating the perfect soundtracks for my life and for keeping me 'cool' all these years. Uncle Scott – your catalogue-worthy photos from your trips were a form of escapism for me and I always enjoyed when you shared them, I'm glad that I got to show you this before you were taken from us too soon. Family celebrations will never be the same without you; you, and your generosity to share your photos and your good fortunes, will be forever missed. On the Ewell side: Aunt Ginny – I always envisioned you sitting front row at my defense because you were one of my biggest cheerleaders, which made losing you too early in your life a few years ago particularly difficult. I can't begin to express how much I wish I could tell you about something I've learned in class or a great article I've read. Thank you for bringing Uncle Ned into our family, who carries on your legacy in his love and unending support. Ned – thank you for traveling back to your alma mater to support me during my defense and in all moments in my life preceding and proceeding my time at Michigan; I'm so proud to share the 'Ph.D. from Michigan' title with you. To my Aunt Nancy and Uncle Ray – your love for music, reading, and making people laugh continues in our family and in our memories of you. To my cousins, the Michigan Sharps: Jeff, Julianne, Griffin, Dillon, Connor, and Evie – thank you for ensuring a continued healthy sports rivalry all these years (Go Blue) and for jokes that always liven up the family group chat (and Jeff: "Lasers"). To my other cousins, the Ohio Sharps: Greg, Colleen, and Addie – you have become a home away from home for me and even if my next steps take me a little further away than driving distance, I hope I can still visit often and I look forward to our Fourth of July tradition for years to come. It's a little silly, but I would be remiss not to say something about my cats, Sally and Rosie, for their company during the late nights while writing

this thesis and for being the best kitties I could ask for (most of the time), and something about my 'little brother' Max the dog, for his uncontained and infectious excitement whenever I come home.

And finally, to my parents: words escape me for how to properly express my gratitude. You gave me life, literally and metaphorically. Everything that's to come, in the following pages of this thesis and also in my life, is because of you. Thank you and I love you.

Financial Acknowledgements

Work performed by D.D.D. was supported in part by the NIH Cellular and Molecular Biology Training Grant (T32-GM007315). This work was also supported by the University of Michigan Biological Sciences Scholars Program (BSSP) and NIH/NIGMS award (R35GM128592 to R.D.B.).

Table of Contents

List of Tables

List of Figures

Abstract

The eukaryotic proteome is in constant flux, as cellular proteins are continuously synthesized, folded, post-translationally modified, trafficked, and degraded to maintain a healthy proteomic balance. Maintaining this balance is critical to organismal health and disrupted cellular protein homeostasis is omnipresent in human disease. Cellular proteostasis is maintained and/or restored by networked protein quality control systems. Endoplasmic reticulum (ER) quality control surveils nascent secretory and membrane proteins synthesized into the ER lumen before trafficking through the secretory pathway. Organelles that receive ER-synthesized proteins contain additional quality control systems that recognize and respond to proteostatic threats by either rerouting substrates and/or facilitating their degradation.

In *S. cerevisiae*, two examples of post-ER degradative quality control systems are the Tul1 (transmembrane ubiquitin ligase 1) sub-complexes, which cycle through the Golgi apparatus/endosomal compartments or localize to the vacuole (the yeast lysosome). Two features of the Golgi-localized Tul1 system distinguish it from all other degradative quality control systems. First, Tul1 is the only known integral membrane ubiquitin ligase that localizes to the Golgi/endosomes in yeast. Second, Golgi-localized Tul1 complexes facilitate protein substrate degradation through two different pathways: the vacuole and the cytosolic proteasome.

Our current understanding of Golgi-localized Tul1 substrate degradation is quite limited. However, the pathway by which a substrate is degraded seems fixed and specific to the recognized protein; proteasomal substrates are not re-routed for degradation in the vacuole and vice versa. We sought to elucidate how Tul1 complexes specify a substrate for the proteasome versus the vacuole, beginning with a dissection of the central component in the complex the Tul1 ubiquitin ligase. In this thesis, we established deep mutational scanning tools and biochemical characterization assays to perform a residue-level structure-function analysis of Tul1. From our efforts, we defined lumenal mutations that impaired Tul1 complex formation and inhibited its function, meaning it was unable to degrade proteasomal and vacuolar substrates.

Surprisingly, we identified mutations within the Tul1 RING domain that changed substrate specificity. These mutants were nonfunctional for degradation of proteasomal substrate, but hypomorphic for vacuolar substrate degradation. We did not identify Tul1 single-residue mutants that were singularly functional for only proteasomal or only vacuolar substrate degradation, which led us to conclude that Tul1 is important for selecting substrates for either degradation pathway, but there are likely other factors involved.

Based on our results, we propose models for how the Golgi-localized Tul1 system can selectively degrade substrates. Of these, we favor a model in which differing interactions with the ubiquitin conjugating enzyme Ubc4 influences Tul1 to selectively conjugate differing lengths of ubiquitin chains on to proteasomal and vacuolar substrates, which ultimately directs selective substrate engagement with degradation machinery. Further exploration of this, and other proposed models, can be easily achieved by applying or adapting tools that we introduce. In summary, the work presented in this thesis lends further insight into how the Golgi-localized Tul1 protein quality control system contributes to maintaining cellular proteostasis by selectively degrading substrates through proteasomal and vacuolar pathways.

Chapter 1
Introduction

1.1 Proteostasis in eukaryotes

Cells are the fundamental unit of life and responsible for creating and sustaining organisms. Central to their function, cells contain intricate libraries of genetic information that encode and regulate protein synthesis [1]. Protein homeostasis (proteostasis) within a cell is essential for cell health and the overall health of organisms; loss of cellular proteostasis is omnipresent in, arguably, all types of human disease [2–4]. Cellular proteostasis is maintained by diverse, networked protein quality control systems that function in both eukaryotic and prokaryotic cells. The work in this thesis focuses on protein quality control mechanisms that operate at membrane-bound organelles in the eukaryotic secretory pathway, though prokaryotic protein quality control shares several features with cytosolic eukaryotic systems [5–7].

The composition of the cellular proteome is in constant flux; protein synthesis, folding, post-translational modification, and degradation must be in precise balance to maintain proteostasis. This balance is easily disrupted by many naturally occurring intrinsic and extrinsic factors, to which quality control systems respond. There are multiple opportunities for protein folding errors during and after synthesis. Some misfolded proteins are a result of pre-translational events, including mutations in the genetic code, mistakes made during transcription, or modification of the messenger RNA [3,8,9]. Errors also arise post-translationally, such as from improper protein folding or aberrant protein modification [3,10,11]. Extrinsic environmental stressors, such as oxidative stress or exposure to toxins, can also disrupt protein folding or stability [12,13]. The dangers of mutant protein to cellular proteostasis extends beyond lost or gained function: improperly folded proteins can be prone to aggregation [11,14–16]. Accumulation of protein aggregates can change protein activity, impair organelle function, and even trap essential, properly folded proteins, further exacerbating the imbalance of aggregated insoluble protein in a cell – consequences of which have been linked to numerous diseases including diabetes and cancer [3,11,14–18].

Chronic proteostasis imbalance caused by an influx of misfolded protein and associated insoluble aggregates overwhelm protein quality control systems to ultimately impair cell function and even cause cell death [19,20]. Depending on the affected cell-type or cellular pathway, a variety of protein-related pathologies (proteopathies) can develop, including neurodegenerative, metabolic, cardiac, and oncological disorders [3,14,21]. These misfolded protein diseases are particularly prominent in aging populations due to age-related increases in protein misfolding risk factors [4,8,22]. Importantly, perpetual pre- and post-translational errors are not the only causes of proteostatic imbalance and disease; failure of protein quality control systems to survey and maintain proteome health are found to be equally complicit, as reviewed in the next section.

1.2 Membrane and secretory protein quality control in human health and disease

Secretory and membrane proteins synthesized at the endoplasmic reticulum (ER) comprise one third of the entire eukaryotic proteome and participate in many essential cellular functions [19,20,23]. Correspondingly, these proteins and the associated quality control systems are frequently implicated in the development and progression of many human diseases [2,21,24,25]. Systems involved in the quality control of membrane and secretory proteins are found at all eukaryotic organelles and serve as important checkpoints as proteins traverse the secretory pathway. Each system recognizes certain types of substrates and responds with one of three strategies to relieve misfolded protein burdens: refolding, degradation, or distribution (Figure 1.1). The interconnected networks of protein quality control in a eukaryotic cell allow a series of coordinated systems at multiple organelles to respond to disrupted proteostasis. These systems can also be considered part of protein 'quantity' control measures to maintain proteostasis by acting in response to environmental or metabolic cues and prevent excess protein accumulation [19,20,23].

1.2.1 ER protein quality control

Secretory and membrane proteins are immediately subjected to folding quality control upon co-translational or post-translational translocation into the ER. Chaperones in the ER lumen, such as the lectins calnexin and calreticulin, are the first line of defense in preventing the aggregation and/or misfolding of nascent membrane and secretory proteins (Figure 1.1A) [25,26]. In addition to folding nascent protein, chaperones prevent their distribution into the secretory pathway until they are properly folded. ER chaperones are undoubtedly critical to cell health, with

dysfunction implicated in many human diseases, as they are responsible for the proper folding of most proteins that enter the secretory pathway [10,24,27]. However, up to 80% of certain proteins translocated into the ER never achieve a properly folded state despite the activity of chaperones [28].

To prevent accumulation of misfolded protein in the ER, proteostasis is also maintained through degradative quality control responses, either through bulk lysosomal degradation to dispose of protein buildup en masse, or by disposing individual aberrant proteins via the proteasome to preclude aggregation risk. It is important to briefly distinguish lysosomal and proteasomal degradation in mammalian systems. Lysosomes are organelles containing a variety of proteases that are active in the acidic lysosomal lumen. Lysosomal degradation occurs upon fusion of the lysosome with entire organelles or vesicles, such as autophagosomes in autophagy, resulting in bulk degradation of its contents by exposure to lysosomal proteases [1,28]. Proteasomes are multi-enzymatic soluble complexes that localize to the cytosol, either as the 20S proteasome core or the 26S proteasome, the latter of which includes a 19S regulatory particle capping the 20S core [29]. The proteasome interacts with and degrades substrates in the cytosol, generally targeting a specific protein for degradation.

Proteasomal degradation of proteins in the ER functions to prevent elevated ER stress via ER-associated degradation (ERAD) of misfolded or overabundant proteins (Figure 1.1A). ERAD systems are, conceptually, centered on ubiquitin ligase proteins, which recognize target proteins (substrates) and mark them for degradation by the cytosolic proteasome through a process called ubiquitination, detailed later in Section 1.3. Many ERAD substrates have been linked to human disorders and diseases that occur when ERAD fails [30]. Contributing to this, ERAD system capacity can be saturated if misfolded protein production is unmitigated, which can increase protein burden in the ER and further inducing ER stress. While ERAD specifically degrades proteins to prevent aggregates from forming, autophagy can target aggregated protein masses within the ER for bulk degradation by sequestering substrates in autophagosomes that bud from the ER membrane, fated for lysosomal fusion (Figure 1.1A) [19,31,32]. This process of ER autophagy is found to be important in several metabolic and neurological disease models, among other human disease implications [33,34]. Some ER chaperones participate in multiple functions that maintain ER proteostasis by correcting unfolded proteins and facilitating autophagy; GRP78/BiP, from the heat shock protein

chaperone family, sequesters misfolded protein for coordination with autophagy factors in response to elevated ER stress [35].

Failure to properly fold or degrade misfolded proteins increases ER protein burden, and therefore ER stress. ER stress triggers the unfolded protein response (UPR). Briefly, the UPR comprises a cascade of networked quality control responses that can 1) upregulate lipid biosynthesis, chaperone, ERAD, and autophagy activities, 2) attenuate nascent protein synthesis, and 3) increase export of proteins from the ER (Figures 1.1A & 1.1B), all of which aim to relieve ER protein burden [36]. If proteostatic stress is unattenuated, sustained UPR induction results in cell death, therefore proper UPR function is important to human health [36]. Aberrant UPR function is associated with several diseases, with cardiovascular disease as one clear example [36,37].

One branch of the UPR increases export of membrane and secretory proteins to alleviate ER protein burden [36]. This allows opportunity for misfolded proteins to evade ER quality control systems or for ER-resident proteins to leak into the secretory pathway (Figure 1.1B). Entry of misfolded proteins into the secretory pathway can also occur if they are simply not recognized by ER quality control systems [19,20,38–41]. Fortunately, these proteins are subjected to quality control systems in organelles that receive proteins from the ER. These post-ER protein quality control systems can either re-localize substrates to other organelles, including retrograde trafficking back to the ER, or can simply degrade proteins using systems localized to their membranes [19,20]. Dysfunction of these systems also hold many human disease-related implications [19,20,42,43].

1.2.2 Post-ER protein quality control

Proteins that exit the ER in COPII coated vesicles are shuttled to the Golgi apparatus, where they can receive further post-translational modifications, such the removal or addition of sugars, phosphate groups, and/or other moieties important to protein function, prior to distribution to other organelles [28]. Golgi-localized protein quality control systems compose the next stage of quality control for misfolded or mislocalized proteins as they enter the secretory pathway (Figure 1.1C) [19,20]. The exact systems involved in degradative quality control systems that function at the mammalian Golgi remain to be well-characterized, though the activity of these systems has been noted with a number of misfolded or aggregation-prone proteins [42,44]. For example, prion proteins, commonly associated with the development of neurodegenerative disorders, are found to localize to the Golgi prior to degradation by lysosomal systems through unknown mechanisms [45].

There are numerous protein candidates likely involved in degradative Golgi quality control systems, though their substrates and mechanisms are unknown outside of basic domain-based conclusions [42,44]. Furthermore, the current understanding in the field is that mammalian Golgi-localized quality control systems can direct substrates for lysosomal degradation; all current studies only observe the localization of aberrant protein from the Golgi to lysosomes through activity of undefined system(s) [42,44]. There is no clear example of proteasomal degradation that is facilitated by localized systems at the mammalian Golgi, but this is likely a byproduct of the fact that degradative quality control at the Golgi as a whole is not well defined [19,42,44,46]. Multiple studies observe proteasome association with the mammalian Golgi membrane, suggesting the possibility of undefined protein quality system(s) involved in mammalian Golgi-localized proteasomal degradation [47].

Outside of facilitating degradation, Golgi quality control systems also function by returning misfolded or mislocalized proteins to the ER (Figure 1.1D). These Golgi-localized systems can engage with mislocalized substrates by recognizing specific ER-retention sequences on a protein, such as the C-terminal Lys-Asp-Glu-Leu (KDEL) sequence encoded on the chaperone GRP78/BiP and other native ER proteins. The KDEL retention signal is recognized by the appropriately termed KDEL receptor and packaged in COPI coated vesicles, which form at Golgi membranes for retrograde trafficking of proteins between cisternae and also for return to the ER [20,28,42,48]. Loss of GRP78/BiP retrieval to the ER lumen is implicated in several disease models, including lethal cardiomyopathy in mouse models or neurodegenerative disease progression [49,50]. Other Golgi-localized retrieval receptors recognize specific features associated with improperly assembled complex components [19,20]. One example of this is mammalian Rer1 recognition and return of improperly folded rhodopsin or unassembled acetylcholine receptor complex components to the ER in COPI, which hold implications in ocular or musculoskeletal development respectively [51,52]. Once returned to the ER, these misfolded proteins can be recognized by ER quality control systems and either be corrected by chaperone activity or degraded by ERAD [19,20,51–54].

Proteins not degraded or returned to the ER by Golgi quality control systems can be distributed into the secretory pathway. These proteins are then subjected to quality control systems that localize to the plasma membrane and/or endo-lysosomal system, depending on the trafficking pathway. Proteins trafficked in secretory vesicles localize to the plasma membrane where they can be exocytosed, which is also a quality control response that can relieve cellular protein burden

(Figure 1.1E) [1,19,28,46]. Some misfolded substrates that successfully traffic to the plasma membrane, effectively evading ER and Golgi quality control, are recognized and degraded by local, but poorly characterized, systems (Figure 1.1F) [55,56]. Based on domains and features of plasma membrane-associated proteins, there are a number of candidates that are proposed to be involved with the degradation of mutant proteins, which is further supported by their malfunction being associated with diverse human diseases [55]. One clear example of a plasma membrane degradative quality control system involves the interplay of cytosolic chaperones Hsc70 and Hsp90 with the soluble chaperone-associated ubiquitin ligase CHIP, which were found to direct lysosomal degradation of misfolded CFTR, a protein associated with the development of cystic fibrosis, from the plasma membrane [57]. Similar to Golgi-localized degradative quality control systems, there is no clear example of proteasomal degradation occurring at the mammalian plasma membrane though several studies observe proteasomes associate with this organelle [47,55,56].

Substrates of mammalian Golgi and plasma membrane quality control systems can be sorted into the endo-lysosomal system for lysosomal degradation through ubiquitin-independent and -dependent mechanisms discussed in Section 1.3 and Section 1.4, respectively [19,42–44,55]. These proteins are packaged into endosomal vesicles from the Golgi or the plasma membrane for entry into the endo-lysosomal pathway and are fated for degradation upon vesicle fusion with the lysosome. However, proteins that enter the endo-lysosomal system are not always degraded in the lysosome; proteins are packaged into endosomal vesicles for function, such as endosome-localized SNARE proteins required for vesicle fusion events, or for localization, including the trafficking of critical lysosomal hydrolytic enzymes [1,28]. As such, protein quality control systems also operate within the endo-lysosomal system, which can recognize and degrade misfolded proteins that localize to these organelles (Figure 1.1G) [20,43]. A comprehensive understanding of the specific proteins and associated mechanisms of mammalian endo-lysosomal quality control is still unclear, though impairment of these processes have been implicated in a number of human diseases [43].

Quality control of proteins that leave the ER and enter the secretory pathway frequently are discussed in the context of human health and disease, as indicated by examples given and reviews cited in this section. Notably, current experimental evidence in this field does not clearly define specific mechanisms or endogenous targets of mammalian quality control systems that operate in organelles beyond the ER. Understanding how eukaryotic protein quality control systems recognize and degrade substrates is critical for their development as future potential

therapeutic targets; identification of specific components in systems that function at organelles beyond the ER is an obvious important first step in this process [19,20,42]. These systems rely on both ubiquitin-independent and ubiquitin-dependent mechanisms to maintain cellular proteostasis, which are reviewed next.

1.3 Ubiquitin-independent protein quality control

Eukaryotic protein quality control systems are interconnected and can often involve activity from multiple systems to alleviate or prevent cell stress caused by disrupted proteostasis. A critical first step in protein quality control is the recognition of a target protein, however the resulting response is dependent on the engaged system. Some protein quality control systems center on the activity of a ubiquitin ligase to 'mark' substrates for degradation by conjugating a ubiquitin molecule, as detailed next in Section 1.4. However, many membrane and secretory protein quality control systems do not involve the activity of a ubiquitin ligase and therefore are considered ubiquitin-independent systems. These systems not only can direct substrates for degradation using ubiquitin-independent mechanisms, but are equally important for their functions in correcting or distributing aberrant proteins to restore proteostasis [19,20,58].

1.3.1 Chaperone-mediated protein quality control

Chaperones engage with nascent or misfolded proteins based on specific characteristics, such hydrophobic regions or specific sequence motifs [24,59,60]. As previously discussed, ER-localized chaperones can respond to misfolded protein by refolding and correcting conformation to achieve their proper folded state. Conversely, terminally misfolded ER proteins and even protein aggregates within the ER lumen can be targeted for autophagy by chaperones. During ER-autophagy, chaperones sequester protein aggregates with autophagy factors on the ER membrane, allowing autophagosome formation and encapsulation of aggregates and ER membrane. ER autophagy functions to reduce lumenal ER protein burden to restore proteostasis in eukaryotes.[19,32,61]. Though the work presented in this thesis focuses on organelles within the secretory pathway, it would be remiss not to mention the role of chaperones in the mitochondrial lumen, which share the many ubiquitin-independent functions of lumenal ER chaperones to regulate mitochondrial protein burden and maintain cellular proteostasis [62,63].

Chaperone-mediated quality control isn't limited to the ER or mitochondrial lumen. Soluble chaperones that localize to the cytosol can direct lysosomal degradation of membrane proteins from eukaryotic organelles by recognizing specific cytosolic-facing motifs or features [60,61,64–67]. These cytosolic chaperones can also direct selective autophagy of soluble/cytosolic proteins, macroautophagy of larger macromolecules, and even autophagy of entire organelles within the secretory pathway [60,64–67]. Chaperones are a large subset of ubiquitin-independent quality control, however it should be noted that chaperones can also coordinate ubiquitin-dependent degradation of misfolded protein, as noted in the earlier example of mutant CFTR protein quality control at the plasma membrane. CFTR is ubiquitinated by the ubiquitin ligase CHIP and directed for lysosomal degradation, but CHIP-CFTR interaction is dependent on activity from the soluble/cytosolic chaperones Hsc70 and Hsp90 [57]. CFTR ubiquitination initiates its entry into the endo-lysosomal pathway for degradation [57], however receptor proteins represent a large subset of ubiquitin-independent systems that can direct proteins for lysosomal degradation and are discussed next.

1.3.2 Receptor-mediated protein quality control

Receptor proteins are present on the surface of all eukaryotic organelles to recognize and engage specific substrates or signaling molecules. The result(s) of these interactions are vital to basic cellular functions, many of which are relevant to maintaining cellular proteostasis. The field of receptor-mediated biology is extensive [68], so this section only focuses on several processes directly involved in quality control responses, specifically receptor-mediated trafficking and degradation of proteins. Previous discussion of post-ER quality control systems included the trafficking of proteins in the secretory pathway to the ER for re-folding or to the lysosome for degradation. These processes are all mediated by receptor proteins, like the previously mentioned KDEL receptor which recognizes mislocalized ER-resident proteins and interacts with COPI components for COPI-mediated return to the ER [69].

Receptor proteins can also facilitate degradation of substrates; this process has already been discussed indirectly in the context of autophagy. As mentioned, lumenal chaperones can help mediate association of protein aggregates with autophagy receptors in or near the ER membrane, which induces autophagosome formation, recruits lysosomes to the ER membrane, and facilitates eventual lysosomal fusion with budded autophagosomes. Autophagy receptors can also associate

with non-chaperone proteins to trigger ER-phagy [33,61,65,66]. Another receptor-mediated lysosomal degradation pathway is exemplified by ALG-2-interacting protein X (ALIX) engagement with the Endosomal Sorting Complexes Required for Transport (ESCRT) system in cells, which fates proteins for degradation in the endo-lysosomal pathway in a ubiquitin-independent manner [70,71]. ALIX can bind tetraspanin membrane protein at the plasma membrane to initiate sequestration and budding into endosomal compartments at this organelle. Entry into the endo-lysosomal system is facilitated by engagement with ESCRT-III subunits, leading to the formation of multivesicular bodies (MVBs), eventually leading to delivery to lysosomes for degradation [70]. The mechanics of ESCRT and MVB formation will be detailed in Section 1.4, as ESCRT is most frequently considered part of ubiquitin-dependent lysosomal degradation systems. It remains, however, that receptor-mediated protein quality control systems target substrates for entry into autophagy or lysosomal degradation pathways without requiring the activity of a ubiquitin ligase.

Receptor proteins can also direct the degradation of proteins in the lysosome by simply trafficking proteins through the endo-lysosomal system. There are several known trafficking pathways that function at the Golgi to deliver proteins to the lysosome, which are used by hydrolytic enzymes for localization to the lysosomal lumen where they can function and degrade macromolecules [72]. For example, mannose 6-phosphate receptors (M6PR) and sortilin are among several receptors that cycle through the Golgi and late endosomes [72]. M6PRs recognize soluble proteins containing mannose 6-phosphate modifications, a characteristic of lysosomal proteases, for capture into endosomal vesicles, where they are internalized into MVBs and delivered to the lysosome for activation upon fusion [72,73]. Similarly, sortilin in mammalian systems is implicated in the endo-lysosomal trafficking of several lysosomal proteases, such as sphingolipid activator proteins [72,74]. The exact mechanisms of the sortilin remain to be well-characterized, however studies have found that it is required for regulating several cellular metabolic processes and is thought to associate with protein aggregates in the Golgi, which could indicate a role in Golgi-localized autophagy [19,75–77].

Receptors that function at the Golgi also associate to clathrin to sequester proteins for sorting in clathrin-coated vesicles. Clathrin adaptor proteins include GGA (Golgi-localizing, gamma-adaptin ear homology domain, ARF-binding) proteins and adaptor protein (AP) complexes, which recognize substrates based on various motifs or characteristics and are also involved with the trafficking of M6PRs and cargo [72,78,79]. GGA proteins function at the Golgi while

different AP complexes also function at several other organelles, including the plasma membrane, in mammalian systems for delivery of substrates to the endo-lysosomal system [72]. The AP complex AP-3 has also been implicated in ubiquitin-independent ESCRT-mediated lysosomal degradation of the endosomal protein protease-activated receptor-1 (Par1), by facilitating Par1 interaction with ESCRT adaptor ALIX, mentioned previously [71]. This section's brief review of receptor-mediated protein quality control in mammalian systems is certainly not exhaustive [72], however highlights several mechanisms that target proteins to the lysosomal lumen in a ubiquitin-independent manner, where they can be degraded. These mechanisms rely on trafficking pathways, while protein degradation by the soluble/cytosolic proteasome is thought to occur at any organellar membrane [47]. As will be discussed in Section 1.4, the ubiquitin-proteasome system is a cornerstone function in eukaryotic protein quality control, however ubiquitin-independent recognition and degradation of proteins by the proteasome will be briefly summarized next.

1.3.3 Ubiquitin-independent proteasomal degradation

A core concept of protein quality control is the recognition of substrates based on specific motifs or characteristics of a protein that allows recognition by quality control systems. These so-called degradation signals, or 'degrons,' can be recognized by quality control systems that facilitate protein degradation, such as the function of ubiquitin ligase systems that tag protein with ubiquitin for degradation by the 26S proteasome. A degron can also be directly recognized by the proteasome, which is the basic mechanism of ubiquitin-independent proteasomal degradation. Substrates of ubiquitin-independent proteasomal degradation are generally extremely unstable proteins, though proteins with certain features such as high oxidation are also found to directly interact with proteasomal subunits [80,81]. Currently characterized substrates of ubiquitin-independent degradation in eukaryotic systems are restricted to soluble/cytosolic or soluble/nuclear proteins, as these are the only proteins with direct access to proteasomal subunits, and therefore not directly relevant to the work discussed in this thesis. However, discoveries in this field [80,82,83] certainly reveal interesting capabilities of the proteasome outside of our understanding of the ubiquitin-proteasome system. For example, the 19S cap is traditionally recognized for its role as a regulatory particle to activate the 20S enzymatic core responsible for degradation processes, which together compose the 26S proteasome complex [29]. However, several non-ubiquitinated proteins can be degraded directly by the 20S proteasome core without the 19S

cap, inviting further investigation into 20S subunit function [84]. The 19S cap also plays a critical role as a ubiquitin adaptor for the degradation of ubiquitinated proteins [29], therefore this subunit is important for proteasome participation in ubiquitin-dependent protein quality control pathways, discussed next.

1.4 Ubiquitin-dependent protein quality control

Ubiquitin-dependent protein degradation is facilitated by protein quality control systems that first recognize specific degrons on target proteins and then conjugate a ubiquitin moiety that marks the protein for recognition by lysosomal or proteasomal degradation systems [85]. Ubiquitin and the process of ubiquitination is highly conserved across eukaryotes and is involved with many cell functions and processes [85] (Figure 1.2). It is important to note that a ubiquitin-conjugated protein is not always targeted for degradation and instead might alter protein activity or localization, among other effects. Work presented in this thesis focuses on a ubiquitin ligase in the *S. cerevisiae* secretory pathway that marks substrates for degradation via the proteasome and the vacuole (the yeast lysosome). Therefore, this section will focus on the process of ubiquitination and resulting mechanisms that facilitate ubiquitin-dependent protein degradation.

1.4.1 Ubiquitin ligases

In the ubiquitination cascade, a soluble and cytosolic ubiquitin molecule is first captured by a ubiquitin activating (Uba) enzyme in an ATP-dependent reaction to form a thioester bond between the C-terminus of the free ubiquitin and the side chain of a Uba enzyme's active-site cysteine (Figure 1.2A) [86,87]. Uba1 is the only known Uba enzyme in yeast, though at least two are identified in mammalian systems [88]. A 'ubiquitin-charged' Uba then interacts with a ubiquitin conjugating (Ubc) enzyme to transfer the ubiquitin onto the Ubc enzyme's active site cysteine (Figure 1.2A) [86,87]. Twelve Ubc enzymes are currently identified in yeast, while at least forty are identified in mammalian systems [89,90]. The specific Ubc enzyme a ubiquitin is conjugated to begins to specify the fated target and configuration of the moiety; each charged Ubc enzyme will only interact with certain ubiquitin ligases to produce specific types of ubiquitination. Ubiquitin ligases complete the next and the terminal step of the ubiquitination cascade by transferring the ubiquitin onto a target protein, most commonly on a lysine residue (Figure 1.2A) [86,87,89]. Existing as both

integral membrane and soluble/cytosolic proteins, over eighty ubiquitin ligases are defined in yeast and at least six hundred ubiquitin ligases are defined in mammalian systems [86,87,90,91].

Ubiquitin ligases are primarily classified by their mechanism of ubiquitin transfer (Figure 1.2B). Over 93% of known ubiquitin ligases in humans ubiquitinate substrates in a singular step, during which the ubiquitin ligase mediates the ubiquitin transfer from the charged Ubc enzyme directly onto the target protein (Figure 1.2B) [87]. Most of these mediating ubiquitin ligases are collectively referred to as RING (Really Interesting New Gene)-type ubiquitin ligases, which are classified further by specific domains and subunits composing the ubiquitin ligase system [86,87,89,91]. RING-type ubiquitin ligases interact with both substrates and a charged Ubc enzyme to bring each component into proximity and allow the transfer of ubiquitin directly onto the substrate from the Ubc enzyme [86,87,89,91]. These proteins generally contain the namesake RING domain, composed of two zinc finger folds with eight zinc-coordinating residues that are critical to function. Specifically, this cross-brace motif within the RING domain coordinates two Zn^{2+} ions and is required to recruit and interact with a charged Ubc enzyme [86,87,89,91]. RING-type ubiquitin ligases can function as monomers or homodimers, with the latter requiring at least two dimerized copies of the ubiquitin ligase to function, or as heterodimers, which require the interaction of two different RING-type ubiquitin ligases for function [87,89,91].

Many well-characterized, large, oligomeric ubiquitin ligase complexes belong to this class of RING-type ubiquitin ligases, including the distinct subclass of cullin-RING ubiquitin ligases (CRLs). CRLs center on cullin proteins and scaffold other components, including substrate receptors and adaptor proteins to facilitate substrate binding, and RING-box proteins for charged Ubc enzyme interaction, together coordinating ubiquitination of a target protein [86,87,89]. Similarly, U-box ubiquitin ligases are often grouped with RING-type ubiquitin ligases as they share the same basic mechanism of mediating the transfer of ubiquitin onto target proteins without directly accepting the ubiquitin from the Ubc enzymes (Figure 1.2B). U-box ubiquitin ligases have similar folds to RING-domains but are unique because they lack the RING's characteristic zinc-fingers [86,87,92]. The CHIP ubiquitin ligase, mentioned in previous sections for its role in degrading integral membrane proteins at the plasma membrane, is an example of a U-box ligase with a distinct feature of requiring chaperone interaction for activity [57,93].

The other classification of ubiquitin ligases, although far less abundant, ubiquitinate substrates in a two-step process by first accepting ubiquitin from a charged Ubc enzyme before

directly transferring the moiety onto a target protein (Figure 1.2B) [86,87,94]. HECT (Homologous to the E6AP Carboxyl Terminus)-type ubiquitin ligases compose the majority of known proteins in this class [87]. The N-terminus of a HECT-ubiquitin ligases interacts with the charged Ubc enzyme which transfers ubiquitin onto an internal active-cysteine, a function allowed by the flexible linker between these two domains. In a second step, the ubiquitin is then transferred from the active site HECT-type ligase onto the target protein. The C-terminus is conserved across HECT ubiquitin ligase enzymes, while variation of the N-terminus allows for interaction with diverse types of substrates. There are several sub-types of HECT ligases that share specific N-terminal motifs, such as the NEDD4 family of HECT ligases (Rsp5 in yeast) which contain a collection of WW motifs in its N-terminal domain for specific substrate or adaptor protein interactions [86,87,94–96].

Though RBR(RING-between-RING)-type ubiquitin ligases carry the namesake of RING-type ubiquitin ligases, their mechanism of two-step substrate ubiquitination is more similar to HECT ubiquitin ligases (Figure 1.2B). RBRs contain two RING domains, with a catalytically active Ubc enzyme-recruiting RING1 and a catalytic but noncanonical RING2 domain with an activated cysteine, bridged by an IBR (in-between-RING) domain. A charged Ubc enzyme interacts with RING1 on the RBR ligase, to allow transfer of ubiquitin to the activated cysteine in RING2. RING2 then transfers the moiety onto the targeted substrate [86,87,94]. The twelve known RBR-ubiquitin ligases in human systems possess unique domains specific to each enzyme and associated substrate(s) [87,97].

Regardless of the exact mechanism of substrate ubiquitination, whether one- or two-step processes, the activity of ubiquitin ligases can be regulated by post-translational modification. Such modifications might induce conformational changes to allow the ubiquitin ligase to engage with substrates and/or other protein components required for substrate ubiquitination, among other possible activities [94,98]. Phosphorylation is one of many examples of post-translational modifications that has been associated with the activation of both RING [99,100] and HECT [101,102] ubiquitin ligases in mammalian systems to allow substrate ubiquitination [94]. A few ubiquitin ligases can also 'autoubiquitinate,' meaning they are themselves ubiquitinated, or conjugated with ubiquitin-like protein(s), to regulate activity [94,98]. One example of this regulation is the Hrd1 ERAD ubiquitin ligase in *S. cerevisiae*, which requires autoubiquitination to form a channel by which lumenal substrates can retrotranslocate across the ER membrane into the cytosol for ubiquitination and degradation by the 26S proteasome [103].

A ‘resetting’ step in the ubiquitination cascade prevents unwanted degradation of autoubiquitinated ubiquitin ligases, carried out by activity from deubiquitinating enzymes (DUBs) (Figure 1.2A) [90]. *S. cerevisiae* Hrd1 deubiquitination by the DUB Ubp1 maintains Hrd1 stability at the ER membrane, and equally plays a regulatory role by resetting the retrotranslocon to attenuate lumenal substrate degradation [104]. Yeast encode twenty three DUBs, while humans encode at least one hundred [90,104]. DUBs are most recognized for their important role in maintaining levels of free-ubiquitin in a cell by deubiquitinating substrates before degradation by the proteasome or lysosomal systems, which might also play a role in regulating substrate degradation [85,90,105,106]. The resulting free-ubiquitin is recycled back into the system for activation by a Uba enzyme and subsequent reentry into the ubiquitination cascade (Figure 1.2A) [90]. DUB activity is important to many regulatory mechanisms and signaling pathways within a cell, with emerging insights on the various types of DUBs and specific DUBs implicated in disease and human health contexts [90,105,107]. Each DUB recognizes specific types of ubiquitin attachments, further highlighting their role in many ubiquitin-dependent pathways given that the different types of ubiquitin attachments on a target protein direct their fate or function [90,104].

1.4.2 Types of ubiquitin modifications

Types of ubiquitin modifications are commonly characterized by first by their length and then by their chain linkage-type (Figure 1.2C). Ubiquitin can be added as a monomer by forming an isopeptide bond from its C-terminal Gly-76 (Figure 1.2D) with the side chain of various cytosolic-facing amino acids, most commonly a lysine, on the target protein, as coordinated by the involved ubiquitin ligase. A protein that only contains one monomeric ubiquitin modification is termed ‘monoubiquitinated,’ while a protein conjugated with multiple monoubiquitin modifications at different residues are considered ‘multiubiquitinated’ (Figures 1.2C) [85,108]. Certain ubiquitin ligases can further build ubiquitin chains from initially monomeric ubiquitinated sites on substrates by cyclic repetition of the ubiquitination cascade in a process called polyubiquitination [85,108]. It is also proposed that some Ubc enzymes can pre-build polyubiquitin chains for transfer ‘en bloc’ to substrates [109].

There are many different types of linkages made between ubiquitin moieties when building polyubiquitin chains on a target protein [85,86,108,110] (Figure 1.2C). As mentioned, ubiquitin is conjugated to a target protein on its C-terminus (Figure 1.2D). Ubiquitin chains are built by

forming an isopeptide bond between a new ubiquitin and one of the seven lysine residues within the already-conjugated ubiquitin molecule: K6, K11, K27, K29, K33, K48, K63, or sometimes at the M1 amino group of the ubiquitin N-terminus (Figures 1.2C & 1.2D) [85,108]. Polyubiquitinated chains can be linear (homogenous polyubiquitin linkages) or branched (heterogenous polyubiquitin linkages) (Figure 1.2C).

Different types of ubiquitin conjugations are facilitated by the interactions of a ubiquitin ligase and are associated with different protein fates or cellular processes (Figure 1.2D). Monoubiquitination and multiubiquitination of substrates are generally associated with altering protein localization or interactions with other proteins, but are also associated with marking substrates for degradation through proteasomal and lysosomal pathways [111–113]. Generalizable functions of most types of ubiquitin linkages remain unclear outside of specific observations in specific pathways, which will be briefly summarized beginning with the six 'atypical' ubiquitin linkages (M1, K6, K11, K27, K29, and K33) [85,86,114]. M1 linkages, which are the only form of linear chains, are required for NF-κB activation and activation of other inflammation and immune response pathways [85,86,115,116]. K6 linkages are proposed to play a mostly non-degradative role, perhaps more involved with regulating quality control systems like mitophagy and has been associated with DNA damage repair responses. K11 linkages have been associated with proteasomal degradation for cell cycle regulation or innate immune responses. K27 linkages are also associated with DNA damage repair and innate immune responses, as well as protein secretion. K29 chains are associated with proteasomal degradation and implicated in innate immune response. K33 chains are also thought to play a role in innate immune responses through trafficking [85,86,114]. The variety of observed functions associated with these atypical ubiquitin chains highlight the necessity of ubiquitination in general cell processes outside of substrate degradation pathways.

The two remaining ubiquitin linkage types that are not considered 'atypical' are K48 and K63 linkages, which have been proposed to account for 80% of all types of ubiquitin linkages present in mammalian cells [85,86,117]. Though several of the other mentioned ubiquitin linkages are associated with marking substrates for degradation by the 26S proteasome (Figure 1.2D), K48 linkages are most clearly involved in marking proteins for proteasomal degradation and also the most abundant linkage type in eukaryotes [85,94,108,117,118]. There is some evidence that K48 linkages mark proteins for lysosomal degradation by interaction with ESCRT components [119], but it is

proposed that K48 engagement with the proteasome outcompetes engagement with lysosomal systems, therefore biasing proteins containing K48 polyubiquitin chains for proteasomal degradation [120,121]. Rather, lysosomal degradation and engagement in ESCRT is most strongly associated with K63 linkages, the second most abundant linkage type in eukaryotes, though it should be noted that K63 linkages are also often associated with immune signaling [117,119–121]. K63 linkages can associate with the 26S proteasome, but substrate degradation by this system is proposed to be prevented by specific K63-affinity binding of a ubiquitin-binding protein, such as ESCRT-0 components [120,121]. The addition of K48 and/or K63 linkages in a polyubiquitin chain do not always mark proteins for degradation, for example if built in chains containing other types of atypical ubiquitin linkages. Specifically, K63/M1 linkages direct protein involvement to intracellular signaling pathways and not for engagement with lysosomal degradation pathways [85]. As a whole, the field of types of ubiquitin linkages and the 'lynchpin' factor(s)/associated mechanisms that direct different types of polyubiquitinated protein fate requires further investigation [85,94,117,119–121].

The specific interactions of ubiquitin ligases with target proteins and the engaged Ubc enzyme dictates the type of ubiquitin linkage. Among its functions, ubiquitin ligases can dictate the residue by which a protein is ubiquitinated, whether a target protein can be mono- or polyubiquitinated, and certain types can facilitate the type of linkage(s) as well as the length of linkages allowed; longer K48 and K63 linkages are found to better interact with degradation machinery [119,122]. The work presented in this thesis focuses on dissecting a ubiquitin ligase system that directs substrates for degradation through either proteasomal or lysosomal pathways, therefore known mechanisms associated with each degradative pathway is detailed next.

1.4.3 Ubiquitin-dependent lysosomal and proteasomal degradation

Substrates ubiquitinated by ubiquitin ligases can be degraded by both lysosomal and proteasomal pathways (Figure 1.3). Lysosomal degradation of ubiquitinated substrates is coordinated by components in the ESCRT pathway, briefly mentioned for its role in ALIX-mediated ubiquitin-independent degradation of plasma membrane substrates in Section 1.3. The ESCRT pathway, which is conserved in yeast and mammals, can be broken down into four complexes with distinct functions: ESCRT-0, ESCRT-I, ESCRT-II, and ESCRT-III (Figure 1.3A). ESCRT-0 begins by recognition of ubiquitinated cargo and sequestration of proteins on the surface

of endosomes. ESCRT-I continues recruitment of factors and ultimately allows binding of ESCRT-II components, which begins to deform membrane for internal budding. ESCRT-III associates with these factors and DUBs remove ubiquitin from substrates for recycling back into the system. Release of ESCRT-III components at the enclosing bud-sites result in invagination, which is catalyzed AAA-ATPase Vps4. The budding of vesicles into endosomal compartments leads to the creation of MVBs, which eventually fuse with lysosomes for cargo degradation [1,28]. Ubiquitination of substrates by ubiquitin ligases is necessary for substrate engagement with ESCRT-0 and lysosomal degradation, though discovery of ESCRT-III-associating receptors such as ALIX include ubiquitin-independent mechanisms that allow entry of membrane and secretory proteins into the endo-lysosomal degradation system.

Ubiquitin-dependent lysosomal degradation relies on trafficking of vesicles from organelles for fusion with lysosomes (Figure 1.3A). Degradation of membrane and secretory substrates through the ubiquitin-proteasome system occurs from the membrane of the eukaryotic ER and mitochondria, and at the Golgi in budding yeast [19,32,62]. The eukaryotic ubiquitin-proteasome system requires two steps for degradation of membrane and secretory proteins (Figure 1.3B), beginning with extraction of ubiquitinated protein from the organellar membrane for engagement with the soluble/cytosolic 26S proteasome. If a substrate is soluble/lumenal, it must first undergo the process of retrotranslocation to move the substrate across the organellar membrane into the cytosol for exposure to the cytosolic ubiquitination machinery. Ubiquitinated substrates in the organellar membrane interact with AAA-ATPase complexes for retrotranslocation and ultimately extraction from the membrane (Figure 1.3B). The AAA-ATPases p97/Cdc48 in mammalian/yeast systems, respectively, are most often associated with this step though the 26S proteasome itself is also thought to be independently capable of this extraction function as it contains AAA-ATPases in its multi-enzymatic complex [123,124].

As previously mentioned, the 26S proteasome is composed of a 20S proteasome core and 19S regulatory particles. Ubiquitin receptors in the 19S subunit engage ubiquitinated substrates, ultimately leading to substrate deubiquitination by proteasome-associated DUBs, substrate unfolding, and finally substrate internalization into the 20S core for proteolysis [124]. The exact steps and components coordinating 26S proteasome function remains to be clearly defined, though insights on the contribution(s) of subunits within the multi-enzymatic complex are associated with various steps in this process [124,125]. There is also evidence that the 20S proteasome core alone can

recognize and subsequently degrade ubiquitinated, highly disordered substrates without the 19S cap, somewhat reflective of substrates associated with 20S ubiquitin-independent degradation [126].

In summary, ubiquitin-dependent degradation of proteins in eukaryotic systems is carried out by either trafficking substrates into the lysosomal lumen or by proteasomal degradation of substrates from organellar membranes (Figure 1.3). While substrates and protein quality control systems associated with the latter of these degradation pathways are only defined in mammalian systems the eukaryotic ER and mitochondria, it is predicted that the ubiquitin-proteasome system operates at other organelles in the mammalian secretory pathway, though the engaged systems let alone substrates are unknown [20,47]. This prediction is also supported by the fact that the ubiquitin-proteasome system engages at the Golgi in *S. cerevisiae*, directed by a Golgi-localized integral membrane RING-type ubiquitin ligase system [127] which is the focus of the work presented in this thesis. Quality control of membrane and secretory proteins in yeast are generally quite homologous to mammalian systems [19,42,43], though shifting focus to protein quality control in yeast requires a change of terminology as we move from lysosomal degradation in mammalian lysosomes to lysosomal degradation in the yeast vacuole in the next section.

1.5 Secretory and membrane quality control in yeast

Beginning with quality control at the yeast ER, three ERAD systems are characterized in *S. cerevisiae*, each of which are, conceptually, centered on a RING-type ubiquitin ligase. Polyubiquitinated ERAD substrates are extracted by the AAA-ATPase complex Cdc48/Ufd1/Npl4 followed by degradation by the cytosolic 26S proteasome [128]. Each currently known ERAD ubiquitin ligase engages in specific substrate degradation based on localization and ability to recognize specific degrons. The Doa10 system recognizes and degrades integral membrane substrates that contain degrons in their cytoplasmic domain ('ERAD-C'). The Asi complex localizes to the inner nuclear membrane (INM) where it recognizes and degrades ERAD-INM substrates, a function also carried out by Doa10. The Hrd1 complex recognizes and degrades ERAD-M substrates and 'ERAD-L' substrates – integral membrane or soluble proteins with ER-lumenal degrons [128].

It is likely that ERAD substrates can be recognized and degraded by multiple quality control systems in yeast [20]. Like in mammalian cells, protein quality systems function in all organelles that receive secretory and membrane proteins from the ER and can respond to

malfunctions that occur after a protein enters the secretory pathway. Again, like in mammals, these 'post-ER' systems in yeast can either correct mistakes in protein composition or localization, or can simply degrade these proteins [19,20]. Furthermore, it is likely that some systems can compensate for ERAD malfunction [20]. Aside from the consequences of specific environmental perturbations or other intrinsic factors like ERAD saturation, which allow proteins to leak from the ER into the secretory pathway as first described in mammalian system in Section 1.2, certain characteristics encoded into a protein also enable substrates to evade degradation and leave the ER. This is because ERAD is only an effective system when it can recognize a substrate. The presence of a functional ER-exit signal or the inability of ERAD to recognize a mutant protein due to a 'buried' degron in the protein's structure are some of traits associated with ERAD-evading mutant proteins in yeast [38–41]. More often, however, mutant proteins are simply not a substrate of ERAD, allowing for ER export [19,20,42]. These proteins can instead be substrates of distinct systems that operate in organelles that receive protein from the ER in the secretory pathway which facilitate their degradation [129,130].

Like in mammalian systems, the Golgi is the next organelle 'checkpoint' for secretory and membrane proteins after synthesis in the ER. Protein quality control systems that exist at the yeast Golgi can recognize aberrant proteins and prevent their cellular distribution, however the exact mechanisms of these systems and their substrates are generally unknown. There are several conserved systems that operate in yeast and mammalian systems. Beginning with yeast ubiquitin-independent protein quality control systems, Rer1, homologous to mammalian Rer1, is a ubiquitin-independent retrieval system that localizes to the Golgi where it can recognize mis-localized ER-integral membrane proteins and reroute them back to the ER in COPI vesicles [19,20,131].

Receptor-mediated trafficking from the Golgi in yeast is carried out by several different, but somewhat conserved, pathways. Two distinct examples are the clathrin adaptor protein 3 (AP-3) complex pathway or the endosomal vacuolar protein sorting (VPS) pathway, though certainly several other conserved pathways exist using similar mechanisms [68]. Either pathway engages with its own set of receptors to mediate transfer of proteins from the Golgi to the vacuole, with the AP-3 pathway trafficking proteins directly from the Golgi to the vacuole without the formation of MVBs, while VPS pathway traffics proteins to the vacuole via MVBs [132]. AP-3 (also described previously mammalian systems) is required for alkaline phosphatase delivery to the vacuolar membrane [133]. Vps10 (homologous to mammalian sortilin) is a receptor required for trafficking

several soluble vacuolar proteases in yeast, including carboxypeptidase Y (CPY), proteinase A (PrA), and Kex2, to the lysosomal lumen for function [19,134,135].

Importantly, Vps10 trafficking has also been implicated in directing mutant secretory proteins from the Golgi to the vacuolar lumen for degradation by the internal proteases in a ubiquitin-independent manner [40,136,137]. The ERAD-L substrate CPY*, a mutated, misfolding form of the vacuolar protease CPY, is one likely candidate of this system; saturation of Hrd1 can cause the soluble CPY* to exit the ER and be degraded in the vacuole from the Golgi, likely by engaging with its endogenous trafficking pathway [138]. While the specific mechanisms or sequences by which Vps10 recognizes substrates is not clearly defined, loss of Vps10 in these systems led to secretion of substrates, solidifying Vps10's role as a ubiquitin-independent quality control system that traffics misfolded proteins for vacuolar degradation.

Ubiquitin-dependent protein quality control also functions at the yeast Golgi in the form of two different ubiquitin ligases. The cytosolic HECT-ubiquitin ligase Rsp5 marks integral membrane substrates at the Golgi for degradation, as well as at other eukaryotic organelles. Given its soluble cytosolic nature, Rsp5 was characterized for mostly recognizing cytosolic substrates [96], however, can use integral membrane adaptor proteins that localize to the Golgi to recognize integral membrane substrates [130,139]; interaction with these adaptor proteins facilitate Rsp5 to ubiquitinate these proteins for ESCRT-mediated delivery to the vacuole [19,42,130]. Beyond the Golgi, the Rsp5 HECT-ubiquitin ligase was found to associated with the plasma membrane and the vacuole to degrade integral membrane substrates, again through activity of adaptor proteins [139,140]. Rsp5 is not the only known soluble ubiquitin ligase that can localize to the vacuole; the soluble RING-type ubiquitin ligase Pib1 functions at the vacuole for ubiquitin-dependent lysosomal substrate degradation in yeast [43,141].

The only integral membrane ubiquitin ligase that is known to localize to the Golgi and vacuole is the RING-type ubiquitin ligase Tul1 (Transmembrane ubiquitin ligase 1) [42–44]. Golgi-localized Tul1 can recognize and ubiquitinate integral membrane substrates for ESCRT-mediated delivery to the vacuole for lysosomal degradation [129,130,142]. One interesting feature unique to Golgi-localized Tul1 is that individual targets are degraded in different ways. Some integral membrane substrates are degraded via ESCRT in the vacuole, others are degraded via the 26S proteasome [127]. As such, Tul1 is the only known system in eukaryotes to engage in the ubiquitin-proteasome system at the Golgi membrane [44]. Furthermore, a protein quality control system with

different degradative fates for specific targets appears to be unique to this system compared to other integral membrane ubiquitin ligase systems [19,42,44]. Golgi-localized Tul1 selective degradation capabilities is unique even from its own differently-localized subcomplex; vacuole-localized Tul1 complexes can only degrade integral membranes substrates in the vacuole [127,132]. Our limited understanding of the differences between Golgi- and vacuole-localized Tul1 complexes, including the component that dictates subcomplex localization, and Golgi-localized Tul1 engagement in the ubiquitin-proteasome system are further explored in the next section.

1.6 The Tul1 complex

Tul1 was first identified for its ability to degrade a mutant form of Pep12, a yeast syntaxin-like t-SNARE protein involved in endosomal trafficking to the vacuole and is normally associated with late endosomal compartments [12,13]. When an aspartic acid mutation was introduced into the third residue of Pep12's transmembrane domain, it was ubiquitinated and localized to the vacuole for degradation [14]. Inhibiting Pep12(D) ubiquitination impaired its vacuolar localization, which indicated that its degradation required the activity of a ubiquitin ligase [15]. A screen of putative *S. cerevisiae* ubiquitin ligases revealed that an integral membrane RING-domain containing protein, now known as Tul1, was responsible for Pep12(D) ESCRT-mediated vacuolar degradation. Further characterization of Tul1 found that its RING domain was required for Pep12(D) ubiquitination, certifying it as a true RING-type ubiquitin ligase which interacts with the ubiquitin conjugating enzymes Ubc4 and Ubc5 [15]. Tul1 was the first, and currently still, the only characterized integral membrane ubiquitin ligase that localizes to the Golgi membrane in yeast. Shortly after Tul1's discovery in *S. cerevisiae*, a homologue and its associated complex, the Dsc1 (Defective for SREBP cleavage 1) complex, was identified in fission yeast for its role in a hypoxia-sensing pathway [143]. Insights gained from *S. pombe* Dsc1 has contributed heavily to our current understanding of the Tul1 complex.

1.6.1 The S. pombe *Dsc1 complex*

As its name suggests, the Dsc1 complex is required for activation of sterol regulatory binding proteins (SREBPs) in fission yeast (Figure 1.4A). [129,144,145] In both mammals and *S. pombe*, SREBPs serve as a transcription factor that localize to ER membranes as integral membrane proteins. Upon physiologically-induced stimulation, these proteins traffic to the Golgi apparatus

where the cytosolic N-terminus is proteolyzed from the transmembrane segments and transported into the nucleus to induce transcription of specific genes. In mammalian systems, two isoforms of SREBPs, aptly named SREBP-1 and SREBP-2, are trafficked to the Golgi for subsequent N-terminal cleavage in response to low cellular levels of cholesterol and fatty acids to stimulate sterol biosynthesis. Mammalian SREBP function and regulation has been extensively reviewed and is a focus of many studies as this process relates to many metabolic human diseases [146–148]. Two SREBP homologues function in *S. pombe*, Sre1 and Sre2, however Sre1/2 differ from mammalian SREBPs because their main function is to act as oxygen sensors [149]. Under normal oxygen levels, Sre1/2 localizes to the ER where they are inactive. Under hypoxia, Sre1/2 is activated and localizes to the Golgi where it undergoes proteolytic cleavage of the N-terminal transcription factor, which then localizes to the nucleus where it acts as a transcription factor for oxidative genes [143–145,150–152]. This cleavage event requires the activity of the Golgi-localized complex containing five complex components that centers on an integral membrane RING-type ubiquitin ligase, Dsc1.

Dsc1 was discovered in complex with Dsc2, Dsc3, Dsc4, and Dsc5. All components of the Dsc1 complex are required for complete complex formation, for proper localization to the Golgi, and for proper Sre1/2 cleavage. Dsc1 complexes are built at the ER before transport to the Golgi and failure to interacts with all complex components traps the complex to the ER membrane, where it is not able to function [150–152]. The necessity of the complex to be constructed has made it difficult to determine the specific contributions of each complex component outside of those implied by predicted domains (Figure 1.4A). Briefly, Dsc2 contains a 'ubiquitin-associated' (UBA) domain, Dsc3 contains a 'ubiquitin-like' (UBL), and Dsc4 has no characterizable domains [144]. The functional importance of these domains will be discussed later in the context of Tul1 complex components. Dsc5, which contains a 'ubiquitin regulatory X' (UBX) domain was confirmed to be required for Dsc1 complex interaction with the AAA-ATPase Cdc48, which is required for complex function [1–3]. Generally, AAA-ATPases are thought to provide mechanical force, which can be used to extract substrates from an organelle membrane for degradation by the cytosolic proteasome, like Cdc48 in Hrd1 ERAD [153,154]. AAA-ATPases are also a part of ESCRT pathways; ATP hydrolysis of Vps4 provides the force for ESCRT-III membrane scission and complete the invagination of substrates in MVBs fated for vacuolar degradation [154–156]. The activity of the Dsc1 complex results in proteolytic cleavage of its substrate, therefore the exact role of Cdc48 in this

system is unknown [150,151]. Furthermore, it is unclear if substrate ubiquitination is even required for this cleavage step [157].

The Dsc1 complex in *S. pombe* only seems to function as a regulator in the SREBP pathway; no other Dsc1 substrates have been identified. Regardless, the study of the Dsc1 complex led to many Tul1 complex insights in *S. cerevisiae*; the discovery of the Dsc1 complex suggested that there was likely a homologous Tul1 complex in *S. cerevisiae* which led efficient identification of Tul1 complex components that bear homology to their Dsc1 counterparts (Figures 1.4B & 1.4C) [144,145,150–152]. It should be noted that SREBPs and the associated pathway are not found in *S. cerevisiae*, therefore Dsc1 and Tul1 are not known to share substrates nor functions [143,158]. Furthermore, Dsc1's only known function is to proteolytically cleave substrates; Tul1 ubiquitinates substrates for selective degradation via ESCRT-mediated delivery to the vacuole or the ubiquitin-proteasome system. As such, many structural insights on Tul1 complex construction were gained from Dsc1 study [158], however it is difficult to directly infer possible mechanisms that allow Tul1 the ability to degrade substrates using either degradation pathway.

1.6.2 Golgi-Tul1 selective substrate degradation

As previously mentioned, Tul1 ubiquitinates the mutant SNARE Pep12(D) for ESCRT-mediated degradation from the Golgi and endosomes (Figure 1.4B). Tul1 was found to recognize and ubiquitinate other polar integral membrane proteins for degradation in the vacuole but, unlike Pep12(D), these substrates are not exclusive to degradation by the Tul1 system [129]. Further characterization of mutant SNAREs in the yeast secretory pathway determined that Tul1 was also specifically required for ESCRT-mediated vacuolar degradation of a mutant version of the t-SNARE Tlg1, involved in fusion of late Golgi and early endosomal compartments in the VPS pathway [159,160]. Tlg1(LL) contains a di-leucine motif in its cytosolic-facing transmembrane domain that prevents protein palmitoylation, resulting in ubiquitination and degradation by Tul1 [130]. Pep12(D) and Tlg1(LL) are constitutively targeted and degraded by Tul1 if expressed in *S. cerevisiae*, however a more dramatically modified, synthetic Tul1 substrate is degraded in response to environmental cues. Yif1 is a Golgi-localized transmembrane protein required for COPII vesicle fusion [161]. If Yif1 is fused with a green fluorescent protein on its N-terminus (GFP-Yif1), it becomes a Tul1 vacuolar substrate when cells are starved. It is important to note that untagged Yif1 is not a Tul1 substrate under any cellular or environmental conditions [142].

Recently, Tul1 was found to ubiquitinate a non-protein substrate, phosphatidylethanolamine (PE), at endosomal compartments and the vacuole under starvation conditions. This function is suggested to stimulate ESCRT recruitment and MVB formation at these organelles as part of a starvation-based cellular stress response [162]. The DUB Doa4 was found to remove ubiquitin from PE in a reconstituted system [162], in agreement with previous findings of Doa4-Tul1 genetic interactions [158].

In addition to being able to direct substrates for degradation in the vacuole, Golgi-Tul1 can also degrade at least one substrate via the 26S cytosolic proteasome, an integral membrane protein called Orm2 [127] (Figure 1.4B). Orm2 is an ER membrane protein that assembles in complex with SPT (Lcb1/2 and Tsc3), Sac1, and its paralogue, Orm1, to form the SPOTS complex. The SPOTS complex regulates sphingolipid biosynthesis by inhibiting SPT activation of the first step of sphingolipid biosynthesis when localized to the ER [163]. This lipid biosynthesis pathway is largely conserved in mammalian systems, with three Orm proteins encoded in humans (ORMDL1/2/3), and ORMDL3 playing the primary role in inhibiting mammalian SPT complex activation, though the exact mechanism(s) of this regulation is not well understood [163–165]. Mutations in ORMDL3 have been associated with numerous diseases [164,165].

When sphingolipid levels are low in *S. cerevisiae*, Orm2 is phosphorylated, leaves the ER, and localizes to the Golgi. At the Golgi, Orm2 is ubiquitinated by Tul1 and degraded by the 26S proteasome. It is important to note that Orm2 phosphorylation does not seem to be required for Tul1 recognition of Orm2, but rather for export of Orm2 to the Golgi. Despite a high level of homology, Orm1 does not appear to be a Tul1 substrate [127]. As such, Orm2 is the only currently defined Tul1 substrate that is degraded by the proteasome, however published quantitative proteomic data suggests that other proteasomal substrates exist but remain to be validated [127].

Our current understanding of Tul1 degradation mechanics suggests that vacuolar and proteasomal degradation are not interchangeable among substrates (Figure 1.4B). Impairing the proteasome does not lead to degradation of proteasomal substrates in the vacuole, and vice versa [127,129,142,166]. However, the mechanisms defining the degradation pathway remain unknown. How, or even if, Tul1 proteasomal substrates are extracted and degraded from the Golgi membrane is not clear. It is hard to disregard the often noted [86,127,144,145,151,158,166,167] similarities between *S. pombe* Dsc1, *S. cerevisiae* Tul1, and *S. cerevisiae* Hrd1 ERAD complex components (Figures

1.4B-1.4D). As such, a brief summary of Hrd1 ERAD substrate degradation is helpful before further exploring Tul1 complex components and their potential functions.

1.6.3 Hrd1 ERAD in S. cerevisiae

Different components of the *S. cerevisiae* Hrd1 complex play specific roles in ERAD-L or ERAD-M pathways (Figure 1.4D). The core components of the Hrd1 complex, Hrd1, Hrd3, and Usa1, are involved in both pathways [168]. Hrd1 is a RING-type ubiquitin ligase integrated into the ER membrane [169,170] and ubiquitinates substrates along with a variety of additional roles, described below. Hrd1 interacts with the integral membrane protein Hrd3, which is required for complex stability [171], and the scaffolding protein Usa1 promotes complex oligomerization [172,173]. A UBX-domain containing protein, Ubx2, also associates to the core complex to coordinate the AAA-ATPase Cdc48 interaction with the complex, to provide mechanical force for protein extraction from the membrane for degradation by the proteasome [168]. Some functions of these and other components play other critical roles in the ERAD-L pathway, which are dispensable in the ERAD-M pathway and vice versa [168].

This is likely due to the fact that ERAD-L requires coordination by multiple mechanisms to reach the cytosol for engagement with the ubiquitin-proteasome system [168]. ERAD-L substrates must first be recognized in the ER lumen by soluble lumenal adaptors (Yos9, Kar2, Scj1) that also interact with Hrd3 [168,171] and carry ERAD-L substrates to the Hrd1 complex. Upon arrival to the complex, ERAD-L substrates move across the ER lipid bilayer to the cytosol in a process called retrotranslocation, through a retrotranslocon channel formed by a Hrd1 heterodimer with the rhomboid pseudoprotease Der1, or potentially a Hrd1/Hrd1 homodimer [103,168,172]. Usa1 serves as a stabilizing linker for Hrd1/Der1 interaction [172,173] and contains a ubiquitin-like domain that counters DUB regulation of Hrd1 function, mentioned earlier in Section 1.4.1 [104]. Once exposed to the cytosol, ERAD-L substrates can be ubiquitinated by Hrd1's cytosolic RING domain for degradation by the 26S proteasome [103,168,172].

In contrast, ERAD-M substrates localize to the ER membrane by nature, therefore recruitment by adaptors for association with Hrd1 is not required; ERAD-M substrates can likely be recognized directly by Hrd1 in the ER membrane [168,174]. ERAD-M requires the Hrd1 core components (Hrd1, Hrd3, and Usa1) and a different rhomboid pseudoprotease, Dfm1 (Figure 1.4D). After substrate recognition and ubiquitination by Hrd1, ERAD-M substrates are extracted

from the membrane for degradation by the proteasome via the AAA-ATPase Cdc48, and possibly aided by Dfm1[128,168]. In vivo, Hrd1 can play a role in extracting ERAD-M substrates from the ER membrane [174], however this function remains to be tested in a reconstituted system.

Overexpression of Hrd1 in vivo [172,174,175] and in experiments in vitro [103,176] can compensate for the loss of all other complex components in ERAD-M and ERAD-L pathways, which suggests that Hrd1 is independently capable of recognizing and degrading both types of substrates. However, cytosolic regions within the Hrd1 ubiquitin ligase itself were recently identified to be critical to ERAD-L, but not ERAD-M function [177]. These regions specifically correlated in function to dysregulation of Hrd1 autoubiquitination, required for forming a channel by which ERAD-L substrates retrotranslocate [103,104], and to ERAD-L substrate interaction [177]. Characterization of mutations within Hrd1 that are critical to ERAD-M, but not ERAD-L, function is in progress (unpublished work from our group). To conclude, it is well established that Hrd1 ERAD recognizes and degrades lumenal and membrane proteins using specific mechanisms unique to each type of substrate [168], which has recently been shown be directed by specific regions within the integral membrane RING-type ubiquitin ligase Hrd1 [177].

1.6.4 Features of Tul1 complex components

The integral membrane RING-type ubiquitin ligase Tul1 is in complex with four other membrane proteins in *S. cerevisiae*: Dsc2, Dsc3, Ubx3, and a localization signal Gld1 or Vld1 [132,158]. Evidence indicates that the Tu1l complex is constructed at the ER membrane and must be fully assembled for localization to the Golgi/endosomal or vacuolar membrane and for function [127,132,166]. The functions of each component within the system are unknown, aside from the Gld1/Vld1-directed localization and inferences made from domains each of these components possess (Figures 1.4B & 1.4C). Beginning with the rhomboid pseudoprotease Dsc2, other proteins that share this characteristic fold are found in the Hrd1 ERAD system and might play a role in membrane thinning [178] to better facilitate substrate extraction. Dsc2 also contains a UBA (ubiquitin-associated) domain which, as the name suggests, can interact with ubiquitin and assist or manipulate in the orientation and attachment to substrates [179]. Dsc3, which was found to mediate Tul1 binding to the remaining complex components, contains a UBL (ubiquitin-like) domain, which has previously been associated with stabilizing protein interactions, recruitment and regulation of deubiquitinating enzymes, and even catalyzing degradation of substrates [179–181]. The

Tul1 complex also interacts with the AAA-ATPase Cdc48 for substrate degradation, thought to be mediated by Ubx3's UBX domain.[127,166]. As mentioned earlier, Cdc48 plays a role in extracting substrates from the ER membrane in Hrd1-ERAD systems, mediated by interaction with a UBX-domain containing protein [168], which is likely the role of Cdc48 in the Tul1 complex, though the mechanism of Tul1 proteasomal substrate extraction remains unclear.

Gld1-containing Tul1 complexes localize to the Golgi/endosome through the VPS pathway while Vld1-containing complexes localize directly to the vacuole from the Golgi through the AP-3 pathway, described briefly in Section 1.5 (Figures 1.4C & 1.4D) [132,158]. Gld1-Tu11 complexes are proposed to cycle between Golgi and endosomes via retromer activity while vacuole-Tul1 complexes are thought to remain on the vacuolar membrane after arrival [132]. The discovery of two Tul1 complex localization signals was the first indication that the Tul1 complex functions differently depending on its localization, which is directed by its associated factor. Specifically, it was proposed that Gld1-Tul1 complexes do not degrade the same substrates as Vld1-Tul1 complexes, and vice versa [127,132].

Outside of its core complex components and the ability to degrade substrate using two degradative systems, the mechanics of the entire Tul1 complex are poorly understood. All components of the Golgi-localized complex (Tul1, Dsc2, Dsc3, Ubx3, Gld1, and Cdc48) are required for degradation of Tul1 substrates via their respective pathways [127,132,158]. Overexpression of Tul1 partially compensated for the loss of other complex components to deliver vacuolar substrates to the MVB pathway (this work was conducted prior to the discovery of the proteasomal substrate and the localization factors Gld1/Vld1) [166]. This suggests that Tul1 is independently capable of direct substrate recognition and ubiquitination of at least vacuolar substrates. Whether Tul1 can independently degrade its proteasomal substrate Orm2, which would suggest that it also plays a critical part in extraction of Orm2 proteasomal degradation, is unknown.

1.7 Summary and Overview of Dissertation

As highlighted throughout this review, there are several outstanding questions in the field of eukaryotic secretory and membrane protein quality control that are interesting to study in the context of the yeast Golgi-localized Tul1 complex function. First, understanding this system will highlight a novel observed mechanism for how an integral membrane ubiquitin ligase system can selectively target a substrate for degradation through the proteasome versus the vacuole. Activity

of the ubiquitin ligase itself, perhaps by specific interactions with ubiquitin conjugating enzymes, might play a role in directing substrates to proteasomal or vacuolar systems. This could lend further understandings of how and why proteins are ubiquitinated with different linkages in eukaryotic systems. Second, the specific functions of Tul1 complex components remain poorly characterized, outside of predicted domains and their associated function(s). Interrogation of Tul1 complex components could reveal other ubiquitin-independent mechanisms by which an integral membrane ubiquitin ligase system can selectively direct substrates for degradation.

In this dissertation, we attempt to answer the question of how the Golgi-localized Tul1 ubiquitin ligase complex in *S. cerevisiae* selects proteins for degradation by the proteasome versus the vacuole. Chapter Two describes a deep mutational scanning approach that provides a glimpse into this question and allows us to propose new models for Tul1 function that are thoroughly discussed in Chapter 3.

1.8 Figures

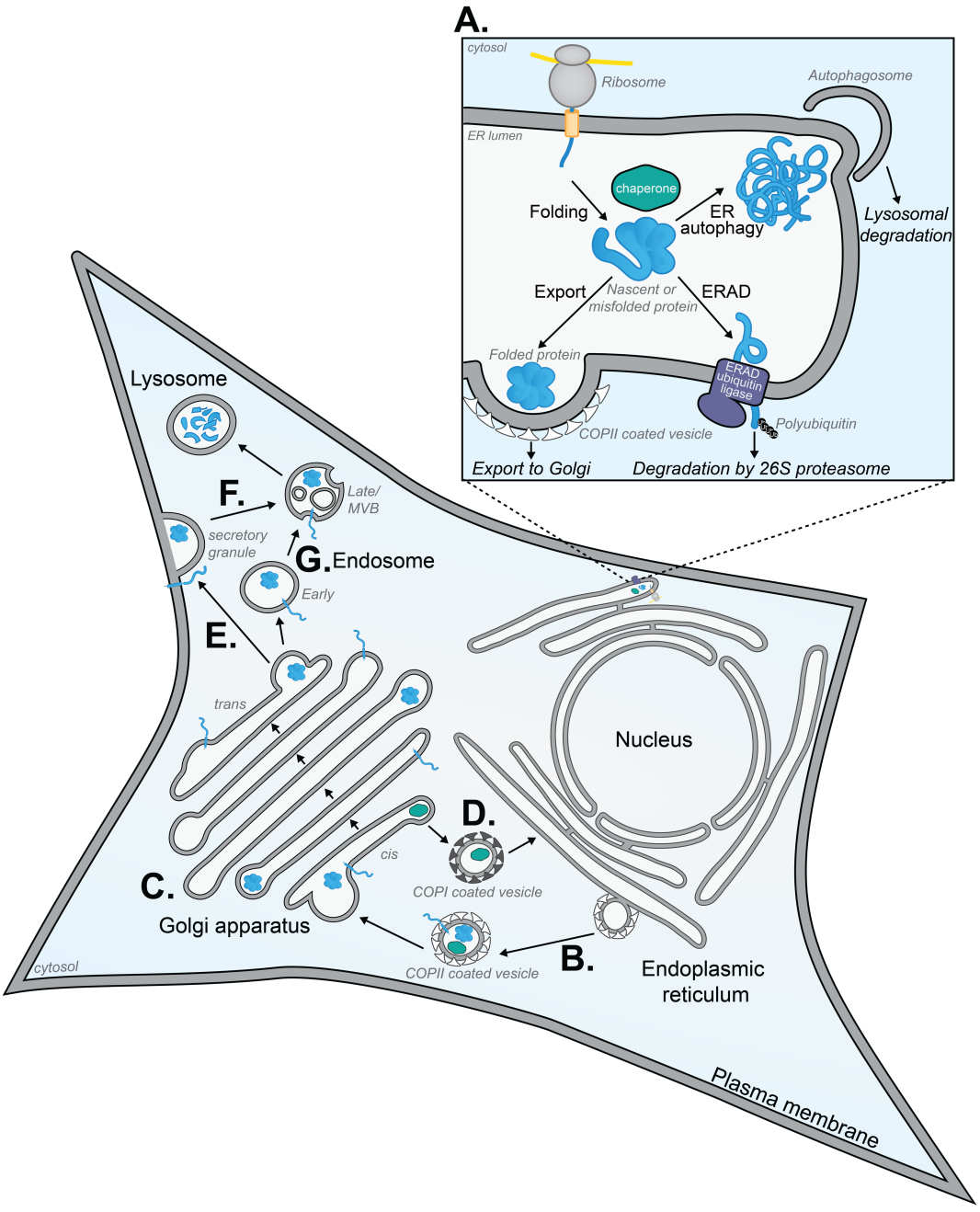

Figure 1.1: Secretory pathway protein quality control in mammalian systems.

Figure 1.1: Secretory pathway protein quality control in mammalian systems.

A) Summary of quality control systems and their responses that operate at the ER, including protein folding by lumenal chaperons, degradation (ERAD and ER-autophagy), and protein export in COPII coated vesicles.
B) Summary of quality control systems that operate in organelles that receive proteins from the ER in the secretory pathway. Golgi quality control systems can return proteins to the ER in COPI coated vesicles for re-localization, refolding, or degradation. Other proteins can enter endosomes for trafficking to the plasma membrane in secretory granules or for entry into the endo-lysosomal pathway for degradation. Proteins from the plasma membrane can endocytose and enter the endo-lysosomal system for degradation.

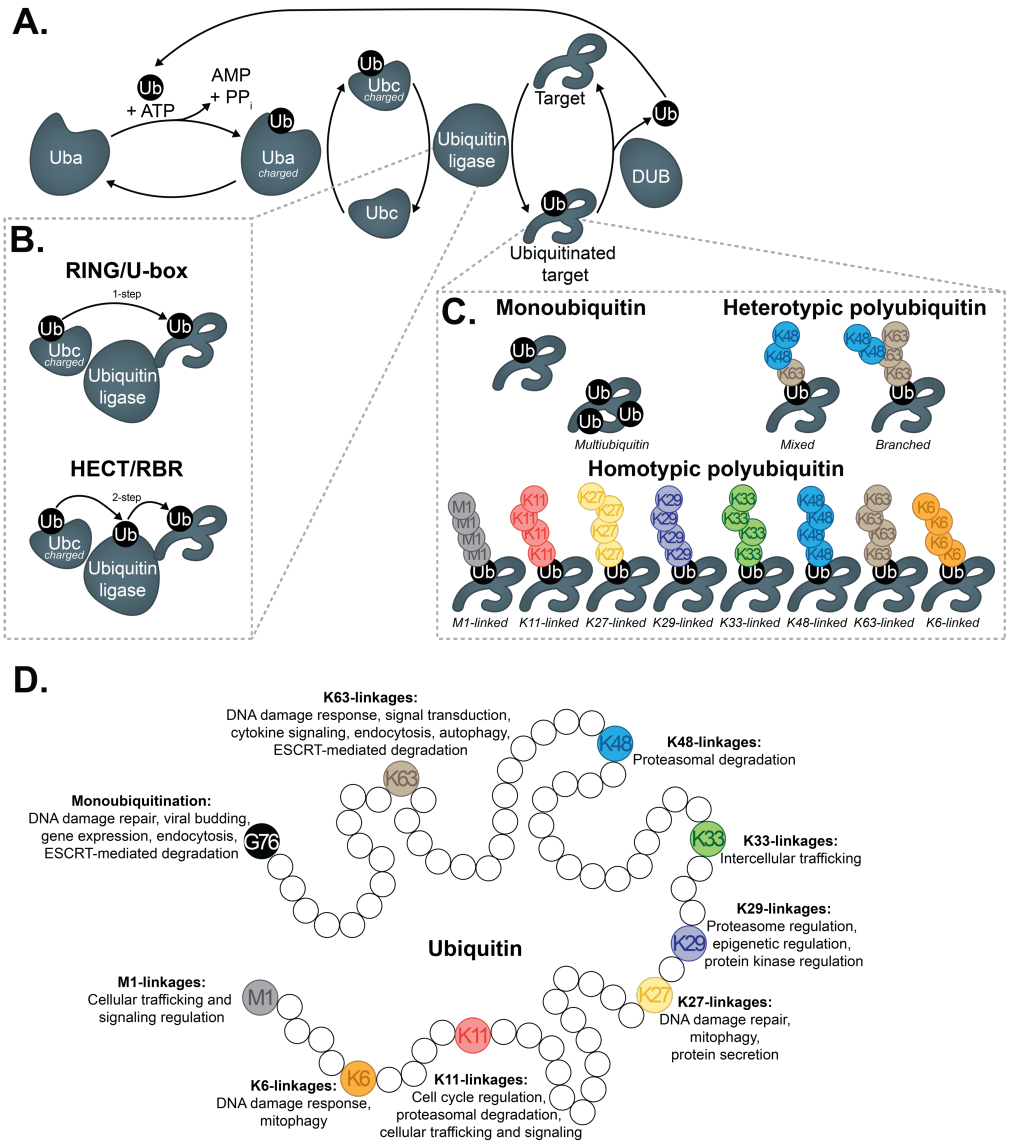

Figure 1.2: Different types of ubiquitin ligases conjugate specific types of ubiquitin linkages on substrates which can modulate fate.

Figure 1.2: Different types of ubiquitin ligases conjugate specific types of ubiquitin linkages on substrates which can modulate fate.

A) The ubiquitination cascade, beginning with ATP-dependent conjugation of free ubiquitin onto a ubiquitin activating (Uba) enzyme. The Uba enzyme then transfers the ubiquitin onto a ubiquitin conjugating (Ubc) enzyme. The Ubc enzyme then transfers ubiquitin onto a ubiquitin ligase, to complete the final step in the ubiquitination cascade and conjugate ubiquitin onto a target protein. Deubiquitinating (DUB) enzymes reset the system by removing ubiquitin from the target protein, which can then be recycled and re-enter the ubiquitination cascade.
B) Two types of mechanisms by which a ubiquitin ligase conjugate ubiquitin onto a target protein from a charged Ubc enzyme. RING/U-box ubiquitin ligases mediate the one-step transfer of the ubiquitin onto the substrate by interacting with both the charged Ubc enzyme and the targeted protein to facilitate transfer of ubiquitin directly from the Ubc enzyme onto the target. HECT/RBR ubiquitin ligases mediate a two-step transfer of ubiquitin by first accepting the ubiquitin from a charged Ubc enzyme, then transferring the moiety directly onto a target protein.
C) Different types of ubiquitin chains can be built from the ubiquitination cascade. Mono- or multiubiquitin conjugations are just one moiety attached to an amino acid on a target substrate, most often a lysine. Polyubiquitination results from processive additions of ubiquitin onto one site of a target protein, building ubiquitin chains. These chains can be heterotypic, meaning consisting of mixed types of linkages built between the moieties and can sometimes result in branched chains, or homotypic, meaning built with only one type of linkage between moieties.
D) Different cellular activities are correlated with different ubiquitin conjugations built during polyubiquitin chains. Most of these details are mostly from observations of cellular processes where these linkages are found/important and the field is still quite murky in terms of specific functions, outside of K48- and K63 linkages. There is still no clear picture on how or what exactly can cause the functional consequences of these linkages.

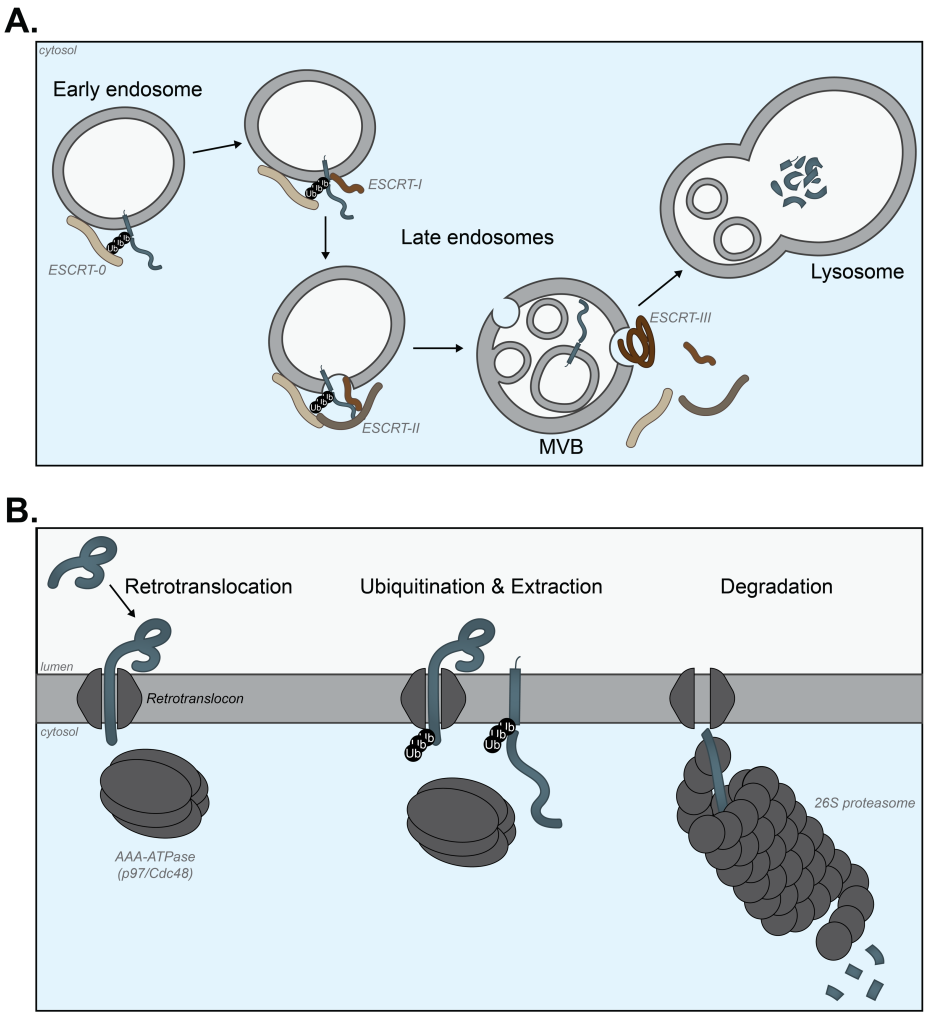

Figure 1.3: Ubiquitin-dependent degradation of secretory and membrane proteins.

Figure 1.3: Ubiquitin-dependent degradation of secretory and membrane proteins.

A) ESCRT-mediated lysosomal degradation of proteins generally is initiated when ESCRT-0 complexes engage ubiquitinated protein in endosomal compartments. This initiates a cascade of complexes that are then recruited, beginning with ESCRT-I and ESCRT-II complexes, which bind the ubiquitinated protein as well as each other. At this point, the endosomal membrane begins to bud inward, however the completed budding of intralumenal vesicles into the endosomal lumen is not completed until ESCRT-II recruits ESCRT-III. ESCRT-III complexes include the AAA-ATPase Vps4, which is required to provide force for ESCRT-III membrane scission and budding inward of these vesicles, after substrates are deubiquitinated by local DUBS, to complete the formation of late endosomal multivesicular bodies (MVBs). These MVBs then fuse with the lysosome (or the vacuole in yeast) to degrade the cargo proteins. Failure of ESCRT to engage substrates or properly form MVBs results in proteins accumulating in aberrant 'Class E compartments' which are late endosomal compartments that do not fuse with lysosomes, leading to stabilized protein.

B) Degradation of secretory and membrane proteins by the ubiquitin-proteasome system requires a series of coordinated steps. If the substrate of the ubiquitin-proteasome system is soluble/lumenal, it must first be retrotranslocated across the ER membrane through a retrotranslocon where it can be exposed to the cytosol. The mechanical force for this is provided by the activity of a AAA-ATPase, for which p97/Cdc48 is most often referenced. Once exposed to the cytosol, soluble/lumenal proteins and integral membrane proteins alike are ubiquitinated by a ubiquitin ligase (not included in this depiction). The ubiquitinated proteins are recognized by the 19S cap of the 26S proteasome complex, which localizes the multi-enzymatic complex to the organellar membrane. These ubiquitinated proteins are then extracted from the membrane, again through AAA-ATPase activity provided by p97/Cdc48 or sometimes AAA-ATPases that compose the 26S proteasome. Once extracted from the organelle membrane, proteins are deubiquitinated and linearized by enzymes that compose the 26S proteasome, leading to their degradation in the 20S core.

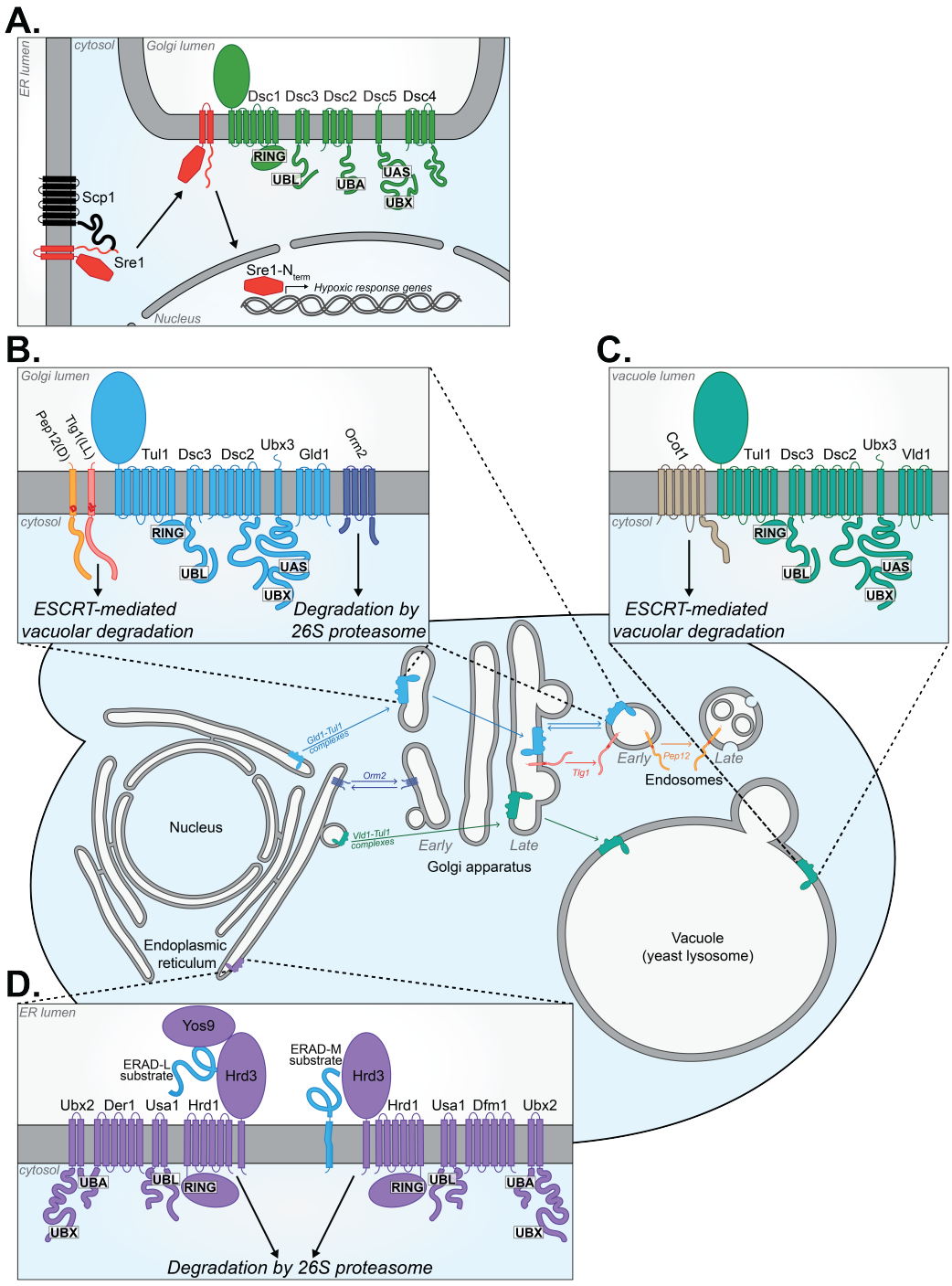

Figure 1.4: Dsc1, Hrd1, and Tul1 ubiquitin ligase complexes in yeast.

Figure 1.4: Dsc1, Hrd1, and Tul1 ubiquitin ligase complexes in yeast.

A) The *S. pombe* Dsc1 complex and its conserved domains. Dsc1 is involved with the SREBP pathway in *S. pombe*, during which Sre1 disassociates from Scp1 at the ER membrane, where it then localizes to the Golgi membrane. Sre1 is recognized by the Dsc1 complex at the Golgi, which cleaves the N-terminal transcription factor of Sre1 through protease activity, which then localizes to the nucleus for upregulation of hypoxic response genes. RING = RING domain on the ubiquitin ligase, UBL = ubiquitin-like domain, UBA = ubiquitin-associated domain, UAS = member of the thioredoxin-like protein superfamily, UBX = ubiquitin regulatory X domain.
B) The Golgi-localized Tul1 complex in *S. cerevisiae* and its conserved domains. Golgi-localized Tul1 complexes recognize substrates at the Golgi membrane for degradation by both vacuolar and proteasomal systems.
C) The vacuole-localized Tul1 complex in *S. cerevisiae* and conserved domains. Vacuole-localized Tul1 complexes only degrades substrates in the vacuole and differs in construction from the Golgi-localized Tul1 complex if assembled with the localization signal Vld1.
D) The Hrd1 complex in *S. cerevisiae* with conserved domains. Hrd1 localizes to the ER membrane and can degrade two different types of substrates, ERAD-L (containing a lumenal mutation) and ERAD-M (containing a mutation within its membrane domain), using similar, but different complex components.

1.9 References

1. *Campbell Biology (UC Berkeley Edition)*. (Benjamin Cummings / Pearson, Boston, 2011).
2. Gregersen, N., Bross, P., Vang, S. & Christensen, J. H. Protein Misfolding and Human Disease. *Annu. Rev. Genomics Hum. Genet.* **7**, 103–124 (2006).
3. Hipp, M. S., Park, S.-H. & Hartl, F. U. Proteostasis impairment in protein-misfolding and -aggregation diseases. *Trends Cell Biol.* **24**, 506–514 (2014).
4. Labbadia, J. & Morimoto, R. I. The Biology of Proteostasis in Aging and Disease. *Annu. Rev. Biochem.* **84**, 435–464 (2015).
5. Mogk, A., Huber, D. & Bukau, B. Integrating protein homeostasis strategies in prokaryotes. *Cold Spring Harb. Perspect. Biol.* **3**, a004366 (2011).
6. Yerbury, J. J., Stewart, E. M., Wyatt, A. R. & Wilson, M. R. Quality control of protein folding in extracellular space. *EMBO Rep.* **6**, 1131–1136 (2005).
7. Mogk, A., Schmidt, R. & Bukau, B. The N-end rule pathway for regulated proteolysis: prokaryotic and eukaryotic strategies. *Trends Cell Biol.* **17**, 165–172 (2007).
8. Anagnostou, M. E. *et al.* Transcription errors in aging and disease. *Transl. Med. Aging* **5**, 31–38 (2021).
9. Pereira, M. *et al.* Impact of tRNA Modifications and tRNA-Modifying Enzymes on Proteostasis and Human Disease. *Int. J. Mol. Sci.* **19**, 3738 (2018).
10. Needham, P. G., Guerriero, C. J. & Brodsky, J. L. Chaperoning Endoplasmic Reticulum-Associated Degradation (ERAD) and Protein Conformational Diseases. *Cold Spring Harb. Perspect. Biol.* **11**, a033928 (2019).
11. Moreno-Gonzalez, I. & Soto, C. Misfolded protein aggregates: mechanisms, structures and potential for disease transmission. *Semin. Cell Dev. Biol.* **22**, 482–487 (2011).
12. Höhn, A., Tramutola, A. & Cascella, R. Proteostasis Failure in Neurodegenerative Diseases: Focus on Oxidative Stress. *Oxid. Med. Cell. Longev.* **2020**, 5497046 (2020).
13. Devi, S. *et al.* Proteotoxicity: A Fatal Consequence of Environmental Pollutants-Induced Impairments in Protein Clearance Machinery. *J. Pers. Med.* **11**, 69 (2021).
14. Louros, N., Schymkowitz, J. & Rousseau, F. Mechanisms and pathology of protein misfolding and aggregation. *Nat. Rev. Mol. Cell Biol.* (2023) doi:10.1038/s41580-023-00647-2.
15. Tartaglia, G. G., Pechmann, S., Dobson, C. M. & Vendruscolo, M. Life on the edge: a link between gene expression levels and aggregation rates of human proteins. *Trends Biochem. Sci.* **32**, 204–206 (2007).
16. Winklhofer, K. F., Tatzelt, J. & Haass, C. The two faces of protein misfolding: gain- and loss-of-function in neurodegenerative diseases. *EMBO J.* **27**, 336–349 (2008).
17. Hodish, I. *et al.* Misfolded Proinsulin Affects Bystander Proinsulin in Neonatal Diabetes. *J. Biol. Chem.* **285**, 685–694 (2010).
18. Xu, J. *et al.* Gain of function of mutant p53 by coaggregation with multiple tumor suppressors. *Nat. Chem. Biol.* **7**, 285–295 (2011).
19. Sun, Z. & Brodsky, J. L. Protein quality control in the secretory pathway. *J. Cell Biol.* **218**, 3171–3187 (2019).
20. Arvan, P., Zhao, X., Ramos-Castaneda, J. & Chang, A. Secretory Pathway Quality Control Operating in Golgi, Plasmalemmal, and Endosomal Systems: Post-ER Quality Control Pathways. *Traffic* **3**, 771–780 (2002).
21. Hartl, F. U. Protein Misfolding Diseases. *Annu. Rev. Biochem.* **86**, 21–26 (2017).

22. Hemagirri, M. *et al.* Crosstalk between protein misfolding and endoplasmic reticulum stress during ageing and their role in age-related disorders. *Biochimie* S0300908423002900 (2023) doi:10.1016/j.biochi.2023.10.019.
23. Chen, B., Retzlaff, M., Roos, T. & Frydman, J. Cellular strategies of protein quality control. *Cold Spring Harb. Perspect. Biol.* **3**, a004374 (2011).
24. Wankhede, N. L. *et al.* Involvement of molecular chaperone in protein-misfolding brain diseases. *Biomed. Pharmacother.* **147**, 112647 (2022).
25. Li, H. & Sun, S. Protein Aggregation in the ER: Calm behind the Storm. *Cells* **10**, 3337 (2021).
26. Braakman, I. & Hebert, D. N. Protein folding in the endoplasmic reticulum. *Cold Spring Harb. Perspect. Biol.* **5**, a013201 (2013).
27. Hebert, D. N. & Molinari, M. In and Out of the ER: Protein Folding, Quality Control, Degradation, and Related Human Diseases. *Physiol. Rev.* **87**, 1377–1408 (2007).
28. Alberts, B. *Molecular Biology of the Cell*. (Garland Science, Taylor and Francis Group, New York, NY, 2015).
29. Tanaka, K. The proteasome: overview of structure and functions. *Proc. Jpn. Acad. Ser. B Phys. Biol. Sci.* **85**, 12–36 (2009).
30. Guerriero, C. J. & Brodsky, J. L. The delicate balance between secreted protein folding and endoplasmic reticulum-associated degradation in human physiology. *Physiol. Rev.* **92**, 537–576 (2012).
31. De Leonibus, C., Cinque, L. & Settembre, C. Emerging lysosomal pathways for quality control at the endoplasmic reticulum. *FEBS Lett.* **593**, 2319–2329 (2019).
32. Koenig, P.-A. & Ploegh, H. L. Protein quality control in the endoplasmic reticulum. *F1000prime Rep.* **6**, 49 (2014).
33. Knupp, J. *et al.* The ER transmembrane protein PGRMC1 recruits misfolded proteins for reticulophagic clearance. *Autophagy* **18**, 228–230 (2022).
34. Li, Y.-Y., Qin, Z.-H. & Sheng, R. The Multiple Roles of Autophagy in Neural Function and Diseases. *Neurosci. Bull.* (2023) doi:10.1007/s12264-023-01120-y.
35. Li, J. *et al.* The unfolded protein response regulator GRP78/BiP is required for endoplasmic reticulum integrity and stress-induced autophagy in mammalian cells. *Cell Death Differ.* **15**, 1460–1471 (2008).
36. Hetz, C., Zhang, K. & Kaufman, R. J. Mechanisms, regulation and functions of the unfolded protein response. *Nat. Rev. Mol. Cell Biol.* **21**, 421–438 (2020).
37. Ren, J., Bi, Y., Sowers, J. R., Hetz, C. & Zhang, Y. Endoplasmic reticulum stress and unfolded protein response in cardiovascular diseases. *Nat. Rev. Cardiol.* **18**, 499–521 (2021).
38. Kincaid, M. M. & Cooper, A. A. Misfolded Proteins Traffic from the Endoplasmic Reticulum (ER) Due to ER Export Signals. *Mol. Biol. Cell* **18**, 455–463 (2007).
39. Coughlan, C. M., Walker, J. L., Cochran, J. C., Wittrup, K. D. & Brodsky, J. L. Degradation of mutated bovine pancreatic trypsin inhibitor in the yeast vacuole suggests post-endoplasmic reticulum protein quality control. *J. Biol. Chem.* **279**, 15289–15297 (2004).
40. Wang, S. & Ng, D. T. W. Evasion of Endoplasmic Reticulum Surveillance Makes Wsc1p an Obligate Substrate of Golgi Quality Control. *Mol. Biol. Cell* **21**, 1153–1165 (2010).
41. Suyama, K., Hori, M., Gomi, K. & Shintani, T. Fusion of an intact secretory protein permits a misfolded protein to exit from the endoplasmic reticulum in yeast. *Biosci. Biotechnol. Biochem.* **78**, 49–59 (2014).

42. Schwabl, S. & Teis, D. Protein quality control at the Golgi. *Curr. Opin. Cell Biol.* **75**, 102074 (2022).
43. Sardana, R. & Emr, S. D. Membrane Protein Quality Control Mechanisms in the Endo-Lysosome System. *Trends Cell Biol.* **31**, 269–283 (2021).
44. Buzuk, L. & Hellerschmied, D. Ubiquitin-mediated degradation at the Golgi apparatus. *Front. Mol. Biosci.* **10**, 1197921 (2023).
45. Ashok, A. & Hegde, R. S. Selective Processing and Metabolism of Disease-Causing Mutant Prion Proteins. *PLoS Pathog.* **5**, e1000479 (2009).
46. Arvan, P., Zhao, X., Ramos-Castaneda, J. & Chang, A. Secretory pathway quality control operating in Golgi, plasmalemmal, and endosomal systems. *Traffic Cph. Den.* **3**, 771–780 (2002).
47. Guo, X. Localized Proteasomal Degradation: From the Nucleus to Cell Periphery. *Biomolecules* **12**, 229 (2022).
48. Jin, H., Komita, M. & Aoe, T. The Role of BiP Retrieval by the KDEL Receptor in the Early Secretory Pathway and its Effect on Protein Quality Control and Neurodegeneration. *Front. Mol. Neurosci.* **10**, 222 (2017).
49. Hamada, H. *et al.* Dilated cardiomyopathy caused by aberrant endoplasmic reticulum quality control in mutant KDEL receptor transgenic mice. *Mol. Cell. Biol.* **24**, 8007–8017 (2004).
50. Jin, H., Komita, M. & Aoe, T. The Role of BiP Retrieval by the KDEL Receptor in the Early Secretory Pathway and its Effect on Protein Quality Control and Neurodegeneration. *Front. Mol. Neurosci.* **10**, 222 (2017).
51. Yamasaki, A. *et al.* Rer1p regulates the ER retention of immature rhodopsin and modulates its intracellular trafficking. *Sci. Rep.* **4**, 5973 (2014).
52. Valkova, C. *et al.* Sorting receptor Rer1 controls surface expression of muscle acetylcholine receptors by ER retention of unassembled α-subunits. *Proc. Natl. Acad. Sci.* **108**, 621–625 (2011).
53. Park, H.-J., Ryu, D., Parmar, M., Giasson, B. I. & McFarland, N. R. The ER retention protein RER1 promotes alpha-synuclein degradation via the proteasome. *PLOS ONE* **12**, e0184262 (2017).
54. Hara, T. *et al.* Rer1 and calnexin regulate endoplasmic reticulum retention of a peripheral myelin protein 22 mutant that causes type 1A Charcot-Marie-Tooth disease. *Sci. Rep.* **4**, 6992 (2014).
55. Okiyoneda, T., Apaja, P. M. & Lukacs, G. L. Protein quality control at the plasma membrane. *Curr. Opin. Cell Biol.* **23**, 483–491 (2011).
56. Babst, M. Quality control: quality control at the plasma membrane: one mechanism does not fit all. *J. Cell Biol.* **205**, 11–20 (2014).
57. Okiyoneda, T. *et al.* Peripheral protein quality control removes unfolded CFTR from the plasma membrane. *Science* **329**, 805–810 (2010).
58. Chen, B., Retzlaff, M., Roos, T. & Frydman, J. Cellular Strategies of Protein Quality Control. *Cold Spring Harb. Perspect. Biol.* **3**, a004374–a004374 (2011).
59. Bose, D. & Chakrabarti, A. Substrate specificity in the context of molecular chaperones. *IUBMB Life* **69**, 647–659 (2017).
60. Hartl, F. U. & Hayer-Hartl, M. Molecular Chaperones in the Cytosol: from Nascent Chain to Folded Protein. *Science* **295**, 1852–1858 (2002).

61. Yang, M. *et al.* ER-Phagy: A New Regulator of ER Homeostasis. *Front. Cell Dev. Biol.* **9**, 684526 (2021).
62. Ng, M. Y. W., Wai, T. & Simonsen, A. Quality control of the mitochondrion. *Dev. Cell* **56**, 881–905 (2021).
63. Onishi, M., Yamano, K., Sato, M., Matsuda, N. & Okamoto, K. Molecular mechanisms and physiological functions of mitophagy. *EMBO J.* **40**, e104705 (2021).
64. Tekirdag, K. & Cuervo, A. M. Chaperone-mediated autophagy and endosomal microautophagy: Jointed by a chaperone. *J. Biol. Chem.* **293**, 5414–5424 (2018).
65. Gubas, A. & Dikic, I. A guide to the regulation of selective autophagy receptors. *FEBS J.* **289**, 75–89 (2022).
66. Zaffagnini, G. & Martens, S. Mechanisms of Selective Autophagy. *J. Mol. Biol.* **428**, 1714–1724 (2016).
67. Kaushik, S. & Cuervo, A. M. The coming of age of chaperone-mediated autophagy. *Nat. Rev. Mol. Cell Biol.* **19**, 365–381 (2018).
68. Heldin, C.-H., Lu, B., Evans, R. & Gutkind, J. S. Signals and Receptors. *Cold Spring Harb. Perspect. Biol.* **8**, a005900 (2016).
69. Yamamoto, K. The KDEL receptor mediates a retrieval mechanism that contributes to quality control at the endoplasmic reticulum. *EMBO J.* **20**, 3082–3091 (2001).
70. Larios, J., Mercier, V., Roux, A. & Gruenberg, J. ALIX- and ESCRT-III–dependent sorting of tetraspanins to exosomes. *J. Cell Biol.* **219**, (2020).
71. Dores, M. R. *et al.* AP-3 regulates PAR1 ubiquitin-independent MVB/lysosomal sorting via an ALIX-mediated pathway. *Mol. Biol. Cell* **23**, 3612–3623 (2012).
72. Braulke, T. & Bonifacino, J. S. Sorting of lysosomal proteins. *Biochim. Biophys. Acta BBA - Mol. Cell Res.* **1793**, 605–614 (2009).
73. Brown, W. J., Goodhouse, J. & Farquhar, M. G. Mannose-6-phosphate receptors for lysosomal enzymes cycle between the Golgi complex and endosomes. *J. Cell Biol.* **103**, 1235–1247 (1986).
74. Lefrancois, S. The lysosomal trafficking of sphingolipid activator proteins (SAPs) is mediated by sortilin. *EMBO J.* **22**, 6430–6437 (2003).
75. Venkat, S. & Linstedt, A. D. Manganese-induced trafficking and turnover of GPP130 is mediated by sortilin. *Mol. Biol. Cell* **28**, 2569–2578 (2017).
76. Nielsen, M. S., Jacobsen, C., Olivecrona, G., Gliemann, J. & Petersen, C. M. Sortilin/Neurotensin Receptor-3 Binds and Mediates Degradation of Lipoprotein Lipase. *J. Biol. Chem.* **274**, 8832–8836 (1999).
77. Amengual, J. *et al.* Autophagy Is Required for Sortilin-Mediated Degradation of Apolipoprotein B100. *Circ. Res.* **122**, 568–582 (2018).
78. Ghosh, P., Dahms, N. M. & Kornfeld, S. Mannose 6-phosphate receptors: new twists in the tale. *Nat. Rev. Mol. Cell Biol.* **4**, 202–213 (2003).
79. Le Borgne, R., Alconada, A., Bauer, U. & Hoflack, B. The mammalian AP-3 adaptor-like complex mediates the intracellular transport of lysosomal membrane glycoproteins. *J. Biol. Chem.* **273**, 29451–29461 (1998).
80. Erales, J. & Coffino, P. Ubiquitin-independent proteasomal degradation. *Biochim. Biophys. Acta BBA - Mol. Cell Res.* **1843**, 216–221 (2014).
81. Shringarpure, R., Grune, T., Mehlhase, J. & Davies, K. J. A. Ubiquitin Conjugation Is Not Required for the Degradation of Oxidized Proteins by Proteasome. *J. Biol. Chem.* **278**, 311–318 (2003).

82. Hsiao, J. C. *et al.* A ubiquitin-independent proteasome pathway controls activation of the CARD8 inflammasome. *J. Biol. Chem.* **298**, 102032 (2022).
83. Makaros, Y. *et al.* Ubiquitin-independent proteasomal degradation driven by C-degron pathways. *Mol. Cell* **83**, 1921-1935.e7 (2023).
84. Ben-Nissan, G. & Sharon, M. Regulating the 20S proteasome ubiquitin-independent degradation pathway. *Biomolecules* **4**, 862–884 (2014).
85. Swatek, K. N. & Komander, D. Ubiquitin modifications. *Cell Res.* **26**, 399–422 (2016).
86. Yang, Q., Zhao, J., Chen, D. & Wang, Y. E3 ubiquitin ligases: styles, structures and functions. *Mol. Biomed.* **2**, 23 (2021).
87. Morreale, F. E. & Walden, H. Types of Ubiquitin Ligases. *Cell* **165**, 248-248.e1 (2016).
88. Schulman, B. A. & Harper, J. W. Ubiquitin-like protein activation by E1 enzymes: the apex for downstream signalling pathways. *Nat. Rev. Mol. Cell Biol.* **10**, 319–331 (2009).
89. Metzger, M. B., Pruneda, J. N., Klevit, R. E. & Weissman, A. M. RING-type E3 ligases: Master manipulators of E2 ubiquitin-conjugating enzymes and ubiquitination. *Biochim. Biophys. Acta BBA - Mol. Cell Res.* **1843**, 47–60 (2014).
90. Snyder, N. A. & Silva, G. M. Deubiquitinating enzymes (DUBs): Regulation, homeostasis, and oxidative stress response. *J. Biol. Chem.* **297**, 101077 (2021).
91. Deshaies, R. J. & Joazeiro, C. A. P. RING Domain E3 Ubiquitin Ligases. *Annu. Rev. Biochem.* **78**, 399–434 (2009).
92. Hatakeyama, S. & Nakayama, K. I. U-box proteins as a new family of ubiquitin ligases. *Biochem. Biophys. Res. Commun.* **302**, 635–645 (2003).
93. Murata, S., Minami, Y., Minami, M., Chiba, T. & Tanaka, K. CHIP is a chaperone-dependent E3 ligase that ubiquitylates unfolded protein. *EMBO Rep.* **2**, 1133–1138 (2001).
94. Zheng, N. & Shabek, N. Ubiquitin Ligases: Structure, Function, and Regulation. *Annu. Rev. Biochem.* **86**, 129–157 (2017).
95. Wang, Y., Argiles-Castillo, D., Kane, E. I., Zhou, A. & Spratt, D. E. HECT E3 ubiquitin ligases – emerging insights into their biological roles and disease relevance. *J. Cell Sci.* **133**, jcs228072 (2020).
96. Fang, N. N. *et al.* Rsp5/Nedd4 is the main ubiquitin ligase that targets cytosolic misfolded proteins following heat stress. *Nat. Cell Biol.* **16**, 1227–1237 (2014).
97. Smit, J. J. & Sixma, T. K. RBR E3-ligases at work. *EMBO Rep.* **15**, 142–154 (2014).
98. Hunter, T. The Age of Crosstalk: Phosphorylation, Ubiquitination, and Beyond. *Mol. Cell* **28**, 730–738 (2007).
99. Khosravi, R. *et al.* Rapid ATM-dependent phosphorylation of MDM2 precedes p53 accumulation in response to DNA damage. *Proc. Natl. Acad. Sci.* **96**, 14973–14977 (1999).
100. Dou, H. *et al.* Structural basis for autoinhibition and phosphorylation-dependent activation of c-Cbl. *Nat. Struct. Mol. Biol.* **19**, 184–192 (2012).
101. Debonneville, C. Phosphorylation of Nedd4-2 by Sgk1 regulates epithelial Na+ channel cell surface expression. *EMBO J.* **20**, 7052–7059 (2001).
102. Gallagher, E., Gao, M., Liu, Y.-C. & Karin, M. Activation of the E3 ubiquitin ligase Itch through a phosphorylation-induced conformational change. *Proc. Natl. Acad. Sci.* **103**, 1717–1722 (2006).
103. Baldridge, R. D. & Rapoport, T. A. Autoubiquitination of the Hrd1 Ligase Triggers Protein Retrotranslocation in ERAD. *Cell* **166**, 394–407 (2016).

104. Peterson, B. G., Glaser, M. L., Rapoport, T. A. & Baldridge, R. D. Cycles of autoubiquitination and deubiquitination regulate the ERAD ubiquitin ligase Hrd1. *eLife* **8**, e50903 (2019).
105. Clague, M. J., Urbé, S. & Komander, D. Breaking the chains: deubiquitylating enzyme specificity begets function. *Nat. Rev. Mol. Cell Biol.* **20**, 338–352 (2019).
106. Schaefer, J. B. & Morgan, D. O. Protein-linked ubiquitin chain structure restricts activity of deubiquitinating enzymes. *J. Biol. Chem.* **286**, 45186–45196 (2011).
107. Singhal, S., Taylor, M. C. & Baker, R. T. Deubiquitylating enzymes and disease. *BMC Biochem.* **9 Suppl 1**, S3 (2008).
108. Komander, D. & Rape, M. The Ubiquitin Code. *Annu. Rev. Biochem.* **81**, 203–229 (2012).
109. Deol, K. K., Lorenz, S. & Strieter, E. R. Enzymatic Logic of Ubiquitin Chain Assembly. *Front. Physiol.* **10**, 835 (2019).
110. Dittmar, G. & Winklhofer, K. F. Linear Ubiquitin Chains: Cellular Functions and Strategies for Detection and Quantification. *Front. Chem.* **7**, 915 (2019).
111. Chen, Y. *et al.* Monoubiquitination in Homeostasis and Cancer. *Int. J. Mol. Sci.* **23**, 5925 (2022).
112. Braten, O. *et al.* Numerous proteins with unique characteristics are degraded by the 26S proteasome following monoubiquitination. *Proc. Natl. Acad. Sci. U. S. A.* **113**, E4639-4647 (2016).
113. Haglund, K. Distinct monoubiquitin signals in receptor endocytosis. *Trends Biochem. Sci.* **28**, 598–604 (2003).
114. Tracz, M. & Bialek, W. Beyond K48 and K63: non-canonical protein ubiquitination. *Cell. Mol. Biol. Lett.* **26**, 1 (2021).
115. Rahighi, S. *et al.* Specific recognition of linear ubiquitin chains by NEMO is important for NF-kappaB activation. *Cell* **136**, 1098–1109 (2009).
116. Gerlach, B. *et al.* Linear ubiquitination prevents inflammation and regulates immune signalling. *Nature* **471**, 591–596 (2011).
117. Zhao, L., Zhao, J., Zhong, K., Tong, A. & Jia, D. Targeted protein degradation: mechanisms, strategies and application. *Signal Transduct. Target. Ther.* **7**, 113 (2022).
118. Xu, P. *et al.* Quantitative Proteomics Reveals the Function of Unconventional Ubiquitin Chains in Proteasomal Degradation. *Cell* **137**, 133–145 (2009).
119. Ren, X. & Hurley, J. H. VHS domains of ESCRT-0 cooperate in high-avidity binding to polyubiquitinated cargo. *EMBO J.* **29**, 1045–1054 (2010).
120. Grice, G. L. & Nathan, J. A. The recognition of ubiquitinated proteins by the proteasome. *Cell. Mol. Life Sci.* **73**, 3497–3506 (2016).
121. Nathan, J. A., Tae Kim, H., Ting, L., Gygi, S. P. & Goldberg, A. L. Why do cellular proteins linked to K63-polyubiquitin chains not associate with proteasomes? *EMBO J.* **32**, 552–565 (2013).
122. Thrower, J. S. Recognition of the polyubiquitin proteolytic signal. *EMBO J.* **19**, 94–102 (2000).
123. Brodsky, J. L. & Wojcikiewicz, R. J. H. Substrate-specific mediators of ER associated degradation (ERAD). *Curr. Opin. Cell Biol.* **21**, 516–521 (2009).
124. Sahu, I. & Glickman, M. H. Proteasome in action: substrate degradation by the 26S proteasome. *Biochem. Soc. Trans.* **49**, 629–644 (2021).
125. Bard, J. A. M. *et al.* Structure and Function of the 26S Proteasome. *Annu. Rev. Biochem.* **87**, 697–724 (2018).

126. Sahu, I. *et al.* The 20S as a stand-alone proteasome in cells can degrade the ubiquitin tag. *Nat. Commun.* **12**, 6173 (2021).
127. Schmidt, O. *et al.* Endosome and Golgi-associated degradation (EGAD) of membrane proteins regulates sphingolipid metabolism. *EMBO J.* **38**, (2019).
128. Mehrtash, A. B. & Hochstrasser, M. Ubiquitin-dependent protein degradation at the endoplasmic reticulum and nuclear envelope. *Semin. Cell Dev. Biol.* **93**, 111–124 (2019).
129. Reggiori, F. & Pelham, H. R. B. A transmembrane ubiquitin ligase required to sort membrane proteins into multivesicular bodies. *Nat. Cell Biol.* **4**, 117–123 (2002).
130. Valdez-Taubas, J. & Pelham, H. Swf1-dependent palmitoylation of the SNARE Tlg1 prevents its ubiquitination and degradation. *EMBO J.* **24**, 2524–2532 (2005).
131. Sato, K., Sato, M. & Nakano, A. Rer1p, a retrieval receptor for ER membrane proteins, recognizes transmembrane domains in multiple modes. *Mol. Biol. Cell* **14**, 3605–3616 (2003).
132. Yang, X., Arines, F. M., Zhang, W. & Li, M. Sorting of a multi-subunit ubiquitin ligase complex in the endolysosome system. *eLife* **7**, e33116 (2018).
133. Stepp, J. D., Huang, K. & Lemmon, S. K. The yeast adaptor protein complex, AP-3, is essential for the efficient delivery of alkaline phosphatase by the alternate pathway to the vacuole. *J. Cell Biol.* **139**, 1761–1774 (1997).
134. Bowers, K. & Stevens, T. H. Protein transport from the late Golgi to the vacuole in the yeast Saccharomyces cerevisiae. *Biochim. Biophys. Acta BBA - Mol. Cell Res.* **1744**, 438–454 (2005).
135. Hecht, K. A., O'Donnell, A. F. & Brodsky, J. L. The proteolytic landscape of the yeast vacuole. *Cell. Logist.* **4**, e28023 (2014).
136. Hong, E., Davidson, A. R. & Kaiser, C. A. A pathway for targeting soluble misfolded proteins to the yeast vacuole. *J. Cell Biol.* **135**, 623–633 (1996).
137. Holkeri, H. & Makarow, M. Different degradation pathways for heterologous glycoproteins in yeast. *FEBS Lett.* **429**, 162–166 (1998).
138. Spear, E. D. & Ng, D. T. W. Stress Tolerance of Misfolded Carboxypeptidase Y Requires Maintenance of Protein Trafficking and Degradative Pathways. *Mol. Biol. Cell* **14**, 2756–2767 (2003).
139. Belgareh-Touzé, N. *et al.* Versatile role of the yeast ubiquitin ligase Rsp5p in intracellular trafficking. *Biochem. Soc. Trans.* **36**, 791–796 (2008).
140. Shiga, T. *et al.* Quality control of plasma membrane proteins by Saccharomyces cerevisiae Nedd4-like ubiquitin ligase Rsp5p under environmental stress conditions. *Eukaryot. Cell* **13**, 1191–1199 (2014).
141. Shin, M. E., Ogburn, K. D., Varban, O. A., Gilbert, P. M. & Burd, C. G. FYVE Domain Targets Pib1p Ubiquitin Ligase to Endosome and Vacuolar Membranes. *J. Biol. Chem.* **276**, 41388–41393 (2001).
142. Dobzinski, N., Chuartzman, S. G., Kama, R., Schuldiner, M. & Gerst, J. E. Starvation-Dependent Regulation of Golgi Quality Control Links the TOR Signaling and Vacuolar Protein Sorting Pathways. *Cell Rep.* **12**, 1876–1886 (2015).
143. Hughes, A. L., Todd, B. L. & Espenshade, P. J. SREBP Pathway Responds to Sterols and Functions as an Oxygen Sensor in Fission Yeast. *Cell* **120**, 831–842 (2005).
144. Stewart, E. V. *et al.* Yeast SREBP Cleavage Activation Requires the Golgi Dsc E3 Ligase Complex. *Mol. Cell* **42**, 160–171 (2011).

145. Stewart, E. V. *et al.* Yeast Sterol Regulatory Element-binding Protein (SREBP) Cleavage Requires Cdc48 and Dsc5, a Ubiquitin Regulatory X Domain-containing Subunit of the Golgi Dsc E3 Ligase. *J. Biol. Chem.* **287**, 672–681 (2012).
146. Brown, M. S. & Goldstein, J. L. The SREBP Pathway: Regulation of Cholesterol Metabolism by Proteolysis of a Membrane-Bound Transcription Factor. *Cell* **89**, 331–340 (1997).
147. Shimano, H. & Sato, R. SREBP-regulated lipid metabolism: convergent physiology — divergent pathophysiology. *Nat. Rev. Endocrinol.* **13**, 710–730 (2017).
148. Eberlé, D., Hegarty, B., Bossard, P., Ferré, P. & Foufelle, F. SREBP transcription factors: master regulators of lipid homeostasis. *Biochimie* **86**, 839–848 (2004).
149. Todd, B. L., Stewart, E. V., Burg, J. S., Hughes, A. L. & Espenshade, P. J. Sterol Regulatory Element Binding Protein Is a Principal Regulator of Anaerobic Gene Expression in Fission Yeast. *Mol. Cell. Biol.* **26**, 2817–2831 (2006).
150. Cheung, R. & Espenshade, P. J. Structural Requirements for Sterol Regulatory Element-binding Protein (SREBP) Cleavage in Fission Yeast. *J. Biol. Chem.* **288**, 20351–20360 (2013).
151. Lloyd, S. J.-A., Raychaudhuri, S. & Espenshade, P. J. Subunit Architecture of the Golgi Dsc E3 Ligase Required for Sterol Regulatory Element-binding Protein (SREBP) Cleavage in Fission Yeast. *J. Biol. Chem.* **288**, 21043–21054 (2013).
152. Raychaudhuri, S. & Espenshade, P. J. Endoplasmic Reticulum Exit of Golgi-resident Defective for SREBP Cleavage (Dsc) E3 Ligase Complex Requires Its Activity. *J. Biol. Chem.* **290**, 14430–14440 (2015).
153. Schuberth, C., Richly, H., Rumpf, S. & Buchberger, A. Shp1 and Ubx2 are adaptors of Cdc48 involved in ubiquitin-dependent protein degradation. *EMBO Rep.* **5**, 818–824 (2004).
154. Yedidi, R. S., Wendler, P. & Enenkel, C. AAA-ATPases in Protein Degradation. *Front. Mol. Biosci.* **4**, 42 (2017).
155. Babst, M. The Vps4p AAA ATPase regulates membrane association of a Vps protein complex required for normal endosome function. *EMBO J.* **17**, 2982–2993 (1998).
156. Schöneberg, J. *et al.* ATP-dependent force generation and membrane scission by ESCRT-III and Vps4. *Science* **362**, 1423–1428 (2018).
157. Hwang, J. *et al.* A Golgi rhomboid protease Rbd2 recruits Cdc48 to cleave yeast SREBP. *EMBO J.* **35**, 2332–2349 (2016).
158. Tong, Z., Kim, M.-S., Pandey, A. & Espenshade, P. J. Identification of Candidate Substrates for the Golgi Tul1 E3 Ligase Using Quantitative diGly Proteomics in Yeast. *Mol. Cell. Proteomics* **13**, 2871–2882 (2014).
159. Coe, J. G., Lim, A. C., Xu, J. & Hong, W. A role for Tlg1p in the transport of proteins within the Golgi apparatus of Saccharomyces cerevisiae. *Mol. Biol. Cell* **10**, 2407–2423 (1999).
160. Siniossoglou, S. & Pelham, H. R. B. Vps51p Links the VFT Complex to the SNARE Tlg1p. *J. Biol. Chem.* **277**, 48318–48324 (2002).
161. Barrowman, J., Wang, W., Zhang, Y. & Ferro-Novick, S. The Yip1p.Yif1p complex is required for the fusion competence of endoplasmic reticulum-derived vesicles. *J. Biol. Chem.* **278**, 19878–19884 (2003).
162. Sakamaki, J.-I. *et al.* Ubiquitination of phosphatidylethanolamine in organellar membranes. *Mol. Cell* **82**, 3677-3692.e11 (2022).
163. Schäfer, J.-H. *et al.* Structure of the ceramide-bound SPOTS complex. *Nat. Commun.* **14**, 6196 (2023).

164. Breslow, D. K. *et al.* Orm family proteins mediate sphingolipid homeostasis. *Nature* **463**, 1048–1053 (2010).
165. Xie, T. *et al.* Ceramide sensing by human SPT-ORMDL complex for establishing sphingolipid homeostasis. *Nat. Commun.* **14**, 3475 (2023).
166. Li, M., Koshi, T. & Emr, S. D. Membrane-anchored ubiquitin ligase complex is required for the turnover of lysosomal membrane proteins. *J. Cell Biol.* **211**, 639–652 (2015).
167. Burr, R. *et al.* Dsc E3 ligase localization to the Golgi requires the ATPase Cdc48 and cofactor Ufd1 for activation of sterol regulatory element-binding protein in fission yeast. *J. Biol. Chem.* **292**, 16333–16350 (2017).
168. Wu, X. & Rapoport, T. A. Mechanistic insights into ER-associated protein degradation. *Curr. Opin. Cell Biol.* **53**, 22–28 (2018).
169. Deak, P. M. & Wolf, D. H. Membrane Topology and Function of Der3/Hrd1p as a Ubiquitin-Protein Ligase (E3) Involved in Endoplasmic Reticulum Degradation. *J. Biol. Chem.* **276**, 10663–10669 (2001).
170. Bays, N. W., Gardner, R. G., Seelig, L. P., Joazeiro, C. A. & Hampton, R. Y. Hrd1p/Der3p is a membrane-anchored ubiquitin ligase required for ER-associated degradation. *Nat. Cell Biol.* **3**, 24–29 (2001).
171. Vashistha, N., Neal, S. E., Singh, A., Carroll, S. M. & Hampton, R. Y. Direct and essential function for Hrd3 in ER-associated degradation. *Proc. Natl. Acad. Sci.* **113**, 5934–5939 (2016).
172. Carvalho, P., Stanley, A. M. & Rapoport, T. A. Retrotranslocation of a Misfolded Luminal ER Protein by the Ubiquitin-Ligase Hrd1p. *Cell* **143**, 579–591 (2010).
173. Horn, S. C. *et al.* Usa1 Functions as a Scaffold of the HRD-Ubiquitin Ligase. *Mol. Cell* **36**, 782–793 (2009).
174. Gardner, R. G. *et al.* Endoplasmic Reticulum Degradation Requires Lumen to Cytosol Signaling. *J. Cell Biol.* **151**, 69–82 (2000).
175. Plemper, R. K. *et al.* Genetic interactions of Hrd3p and Der3p/Hrd1p with Sec61p suggest a retro-translocation complex mediating protein transport for ER degradation. *J. Cell Sci.* **112**, 4123–4134 (1999).
176. Stein, A., Ruggiano, A., Carvalho, P. & Rapoport, T. A. Key Steps in ERAD of Luminal ER Proteins Reconstituted with Purified Components. *Cell* **158**, 1375–1388 (2014).
177. Peterson, B. G. *et al.* Deep mutational scanning highlights a role for cytosolic regions in Hrd1 function. *Cell Rep.* **42**, 113451 (2023).
178. Nejatfard, A. *et al.* Derlin rhomboid pseudoproteases employ substrate engagement and lipid distortion to enable the retrotranslocation of ERAD membrane substrates. *Cell Rep.* **37**, 109840 (2021).
179. Su, V. & Lau, A. F. Ubiquitin-like and ubiquitin-associated domain proteins: significance in proteasomal degradation. *Cell. Mol. Life Sci. CMLS* **66**, 2819–2833 (2009).
180. Kim, H. T. & Goldberg, A. L. UBL domain of Usp14 and other proteins stimulates proteasome activities and protein degradation in cells. *Proc. Natl. Acad. Sci.* **115**, (2018).
181. Foster, B. M. *et al.* Critical Role of the UBL Domain in Stimulating the E3 Ubiquitin Ligase Activity of UHRF1 toward Chromatin. *Mol. Cell* **72**, 739-752.e9 (2018).

Chapter 2
The Golgi-localized Tul1 Ubiquitin Ligase Plays a Central Role in Directing Substrate Degradation

2.1 Abstract

Cellular protein quality control consists of multiple, networked systems that survey and maintain a healthy proteome within eukaryotic organelles. The Tul1 (transmembrane ubiquitin ligase 1) complex is an integral membrane protein quality control system that functions within the Golgi-endosomal system in *S. cerevisiae*. Golgi-localized Tul1 complexes recognize and ubiquitinate proteins for degradation by either the cytosolic proteasome or the vacuole. To understand how the Tul1 complex recognizes and degrades its substrates, we developed high-throughput functional assays for a deep mutational scanning analysis of the Tul1 ubiquitin ligase. This deep mutational scan identified mutations that disrupted Tul1 interaction with its complex and other mutations that altered the substrate specificity of the complex. This work demonstrates that Tul1 plays an important role in directing specific substrate degradation of the complex and provides tools for future dissection of the entire Tul1 complex.

2.2 Introduction

Secretory and integral membrane proteins comprise one third of the eukaryotic proteome and are folded within the endoplasmic reticulum (ER). Genetic mutations or errors during and after ER-localized protein synthesis can create misfolded proteins and result in their distribution or toxic accumulation within cellular organelles [1,2]. Disruption of organellar protein homeostasis induces cellular stress responses that begin at the ER with the unfolded protein response [3]. Continued disruption of organellar proteostasis can impair cell function and cause cell death; consequences of which are linked to many pathologies [4,5]. Protein quality control systems function in all eukaryotic organelles to maintain proteostasis by either correcting misfolded conformational and localization abnormalities, or by degrading these proteins [1,2].

The ER is considered the first checkpoint for newly synthesized membrane and secretory proteins [1,2]. Substrates can evade ER protein quality control systems and enter the secretory pathway if they contain specific traits embedded in the protein sequence, like a strong ER-exit signal or simply because they are not recognized by systems that function at the ER [2,6–9]. Substrates of ER quality control systems as well as ER-resident proteins can also erroneously exit the ER, which is often a byproduct of prolonged ER stress and/or elevated protein export as part of the UPR response [1,2]. The Golgi apparatus is the next organellar checkpoint with quality control systems that recognize secretory and membrane proteins that leave the ER and can prevent their continued distribution in the secretory pathway. Substrates recognized by Golgi quality control systems can be 1) returned to the ER in COPI for refolding or degradation [10,11], 2) routed to the vacuole through pathways including the VPS or AP3 pathways [12], or 3) degraded by a local quality control system [1,13–16].

In *S. cerevisiae*, the Tul1 (Transmembrane ubiquitin ligase 1) complex is an integral membrane ubiquitin ligase system that functions at the Golgi [15]. Tul1 was initially characterized for its role in recognizing and ubiquitinating the mutant SNARE proteins Pep12(D) and Tlg1(LL) for lysosomal degradation via ESCRT-mediated transport to the yeast vacuole [13,16]. Most of the identified Golgi-Tul1 substrates are degraded in the vacuole [17,18]. However, a separate class of Tul1 substrates are degraded by the proteasome, with the prototype being the ER-localized integral membrane protein Orm2. When sphingolipid levels are low, Orm2 is phosphorylated and transported to the Golgi, where it is recognized and ubiquitinated by Tul1 [14]. In this case, instead of being delivered to the vacuole like other Tul1 substrates, Orm2 is extracted from the membrane and degraded by the cytosolic proteasome. Orm2 degradation plays a critical, albeit nonessential, role modulating cellular sphingolipid levels in *S. cerevisiae* [19]; genetic deletion of Tul1 stabilizes Orm2 and is reported to attenuate cellular ceramide levels [14]. Tul1 substrate degradation-fates seem to be fixed and specific to each protein. Inhibition of the proteasome does not result in degradation of Orm2 in the vacuole, while impairing ESCRT or vacuole function stabilizes vacuolar Tul1 substrates in class E compartments rather than redirecting for degradation by proteasome [13,14,17,18]. The mechanisms by which Tul1 recognizes and specifically degrades its substrates through either pathway is unknown.

The current understanding of *S. cerevisiae* Tul1 is derived from insights gained studying the homologous Dsc1 (Defective for SREBP cleavage 1) integral membrane ubiquitin ligase found

in *S. pombe* [20–24]. In *S. pombe*, Dsc1 forms a complex with other integral membrane proteins, Dsc2, Dsc3, Dsc4, and Dsc5, to activate proteolytic cleavage and transcriptional activity of a sterol regulatory binding protein (SREBP) homolog called Sre1 [20,21]. This Dsc1 endogenous function is not shared with Tul1 because Sre1 is absent in *S. cerevisiae* [25]. In fission yeast, Dsc1 activity appears to be limited to facilitating proteolytic cleavage of substrate and therefore does not provide a framework for understanding how Tul1 participates in vacuolar and proteasomal degradation [24]. Furthermore, it is unclear if Dsc1 substrates require ubiquitination for engagement with proteases [24,25]. Regardless, insights derived from *S. pombe* Dsc1 studies prompted further investigation in *S. cerevisiae* to establish the current understanding of Tul1 and its associated complex components [25].

The Tul1 ubiquitin ligase is assembled into a complex at the ER with four other integral membrane proteins: Dsc2, Dsc3, Ubx3, and either Gld1 or Vld1 [25,26]. Gld1 directs the complex to Golgi and endosomal compartments following the VPS pathway and likely is cycled by retromer, while Vld1 traffics the complex directly from the late Golgi to the vacuole via the AP3 pathway [26]. While these Golgi-Tul1 and vacuole-Tul1 complexes form by competitive binding of Gld1 or Vld1 to otherwise identical components, each complex appears distinct in substrate specificity [26]. Both complexes degrade substrates via the vacuole, however vacuole-Tul1 does not appear to have any proteasomal substrates [14,26]. As such, we focused our attention on dissecting the mechanics of the Golgi-localized Tul1 complex because of its ability to degrade substrates through both pathways [14,26]. Previous studies indicated that genetic deletion of any Golgi-Tul1 complex component resulted in stabilization of both proteasomal and vacuolar Tul1 substrates, likely due to the necessity of the complex to be constructed at the ER prior to localization, and presumably function, at the Golgi [14,26]. The specific interaction interface(s) and role(s) of each component within the Golgi-Tul1 complex remain largely untested, including whether any specific component is responsible for sending a substrate to the proteasome versus the vacuole [14,18,25,26].

In this study, we explored the enigmatic mechanism(s) responsible for Golgi-Tul1 complex function, beginning with a residue-level interrogation of a central enzymatic component to the system, the Tul1 ubiquitin ligase. We established a high-throughput dual-reporter assay that allowed us to concurrently monitor the degradation of proteasomal and vacuolar Golgi-Tul1 substrates. We incorporated this assay into a deep mutational scanning pipeline to profile the function of Tul1 variants. We identified mutations in the Tul1 lumenal domain that impaired

protein stability and complex construction. We also identified Tul1 variants in the RING-finger domain that maintained complex binding, but altered complex substrate specificity and were in proximity to the predicted E2 ubiquitin conjugating enzyme and ubiquitin interaction interfaces. This work establishes an adaptable, high-throughput deep mutational scanning pipeline for comprehensive analysis of the Golgi-Tul1 complex, which we used to identify residues that play a role in substrate degradation selectivity.

2.3 Results

2.3.1 Establishing a high-throughput method to test Golgi-Tul1 function

To enable systematic analyses of Tul1 complex function, we designed a high-throughput fluorescence-based assay to follow the degradation of proteasomal and vacuolar substrates (Figure 2.1A). As a proteasomal Tul1 substrate, we used a phosphomimetic variant of Orm2 (called Orm2(DDD)) that is constitutively degraded independent of cellular lipid composition [14]. We confirmed that cells expressing Orm2(DDD) with a C-terminal mScarlet-I showed a shift in fluorescence intensity after a 2-hour cycloheximide chase in wild-type (WT) but not *tul1*Δ cells (hereafter called Orm2*-RFP, Figure 2.1B). To track Tul1-dependent vacuolar substrate degradation, we added an N-terminal super-ecliptic pHluorin to the Tul1 substrates Pep12(D) (called Pep12*) and Tlg1(LL) (called Tlg1*)[13,16]. Super-ecliptic pHluorin is a pH sensitive GFP with fluorescence that is prevented in acidic environments such as the vacuole (hereafter referred to as GFP) [27]. Correspondingly, we observed a decrease in fluorescence intensity of the GFP-tagged vacuolar substrates in wild-type, but not *tul1*Δ, cells after a 2-hour cycloheximide chase (see GFP-Pep12* and GFP-Tlg1*, Figures 2.1C & 2.1D). Using spectrally-distinct fluorophores on proteasomal and vacuolar Tul1 substrates, we were able to simultaneously monitor degradation for both classes of Tul1 substrates with flow cytometry.

All vacuolar and proteasomal substrates required Tul1 for degradation; we tested whether substrate degradation could be complemented in *tul1*Δ cells when *TUL1* was integrated at an exogenous locus. Tul1 expressed from its endogenous promoter at the *his3* locus was insufficient to complement a *tul1*Δ strain, however, Tul1 expressed from the *ADH1* promoter at this exogenous locus complemented substrate degradation in a *tul1*Δ strain (Figures 2.1E-2.1G & S2.1A-S2.1C). We observed a moderate overexpression of Tul1 under the *ADH1* promoter but no increase in the

expression of other Tul1 complex components (Figure S2.1D). We reasoned that the requirement for assembly of Tul1 complexes at the ER prior to vesicular trafficking and Golgi localization, acted as a limiting factor for Tul1 complex activity, as observed previously [20,26]. In alignment with this reasoning, we found that overexpressing Tul1 in wild-type cells did not drastically alter substrate degradation profiles (Figures S2.1E-S2.1G). Our ability to complement Tul1 function at an exogenous locus allowed us to develop screening strains that we could use for a high-throughput functional analysis of the Tul1 ubiquitin ligase.

As a final control for the sensitivity of the fluorescent reporter substrates, we tested whether the ubiquitin ligase activity of Tul1 was required by disrupting the Tul1 RING-finger cross-brace motif (Tul1(C699A)). We hypothesized this mutation would break Tul1 function based on the analogous Dsc1(Cys634Ala) substitution in *S. pombe*, which was reported to be nonfunctional (Figure S2.1H) [23]. We confirmed that Tul1(C699A) was nonfunctional using our fluorescent reporter assays and either a 2-hour cycloheximide treatment or in cells grown to saturation (Figures 2.1H-2.1J & S2.1I-S2.1K). We confirmed that the reporter substrates behaved similarly with smaller epitope tags compared to the fluorophore by following their degradation using cycloheximide chases and immunoblotting. The proteasomal Tul1 substrate Orm2 containing a C-terminal 3xHA epitope tag (Orm2-HA) was stable in *tul1*Δ cells and cells expressing Tul1(C699A) but was degraded with Tul1 expressing cells (Figure 2.1K). This was consistent with previous findings that Orm2-3xFLAG was degraded in wild-type but not *tul1*Δ cells (Figure S2.1L) [14]. Similarly, N-terminal 3xHA epitope tagged Tul1 vacuolar substrates, HA-Pep12* and HA-Tlg1*, were not degraded in *tul1*Δ cells except when complemented with Tul1 (Figures 2.1L & 2.1M). Altogether, these reporter substrates could be used to monitor function of the Tul1 ubiquitin ligase.

2.3.2 Tul1 complex assembly is not required for Tul1-substrate interaction

Currently, it is unclear how the Tul1 complex interacts with its substrates, aside from studies that suggest interactions with Dsc3 bridge Tul1 with the rest of its complex [13,14,16,17,25]. To enable Tul1 complex co-immunoprecipitation, we inserted a 3xV5 epitope tag after the Tul1 signal sequence and confirmed that V5-Tul1 complemented substrate degradation in *tul1*Δ cells similarly to unmodified Tul1 (Figures 2.2A-2.2C). We immunoprecipitated V5-Tul1 and probed for co-immunoprecipitation of the Tul1 complex components (Figure 2.2D) [25,26]. To follow Gld1 and Vld1 interaction, we integrated 3xHA tags at the endogenous C-termini of both Gld1 and Vld1

and verified the HA-tagged proteins functioned similarly to untagged protein (Figures S2.2A-S2.2C). We reasoned that using the same epitope tag would allow comparison of relative amounts of Tul1-Gld1 and Tul1-Vld1 containing complexes. We confirmed Gld1-HA and Vld1-HA co-immunoprecipitated with V5-Tul1 and observed a slight preference for Gld1 with wild-type Tul1 (Figure S2.2D).

Next, we confirmed previous observations that Tul1 interaction with its complex requires each component; V5-Tul1 expressed in *dsc2*Δ, *dsc3*Δ, *ubx3*Δ, and *gld1*Δ*vld1*Δ failed to co-immunoprecipitate any other complex components (Figure 2.2E). To test whether Tul1 could directly interact with its substrates, we immunoprecipitated each of our model HA-tagged substrates and followed co-immunoprecipitation of V5-Tul1. We observed interactions of V5-Tul1 with each of the HA-tagged substrates (Figures 2.2F-2.2H). To understand the mechanics of recognition, we performed the same co-immunoprecipitations from strains lacking each of the complex components. We found that loss of any individual complex components did not impair Tul1 interaction with any of the substrates (Figures 2.2F-2.2H), which suggests Tul1 could interact with substrates independent from its known complex (Figure 2.2E), either directly or indirectly through another currently unidentified interacting protein.

Without every complex component assembled, Tul1 is unable to exit the ER, which suggests that the Tul1 complex is nonfunctional at the ER despite its ability to interact with substrates [17,25,26]. We tested whether our Tul1 model substrates were degraded in the absence of individual components of the Tul1 complex. In agreement with previous studies [14], we confirmed that each component of the Tul1 complex (Dsc2, Dsc3, Ubx3, and Gld1), but not Vld1, was required to degrade the proteasomal substrate Orm2*-RFP (Figure 2.2I). The necessity of each complex component was not known for the vacuolar model substrates Pep12* and Tlg1* [13,16]. Therefore, we tested whether each complex component was required for GFP-Pep12* degradation and found that Pep12* degradation was independent of Vld1 but required Dsc2, Dsc3, Ubx3 (Figure 2.2J). Surprisingly, we observed some degradation of this substrate in *gld1*Δ cells (Figure 2.2J). We observed similar trends in the degradation of the second vacuolar Tul1 substrate, GFP-Tlg1* (Figure 2.2K). Genetic deletion of both Gld1 and Vld1 (*gld1*Δ*vld1*Δ) completely stabilized both GFP-Pep12* and GFP-Tlg1* (Figures 2.2J & 2.2K). Together these data supported that vacuole-Tul1 complexes can inefficiently degrade Tlg1* in the absence of Gld1, and to some extent Pep12*, but both vacuolar substrates were primarily degraded by Golgi-Tul1 complexes

(Figures 2.2J & 2.2K) and required Tul1 ubiquitin ligase activity (Figures S2.2E-S2.2G). We concluded that our functional reporters were suitable to test Golgi-Tul1 function and provided sufficient dynamic range to detect functional, nonfunctional, and hypomorphic phenotypes.

2.3.3 Deep mutational scanning of the Tul1 E3 ubiquitin ligase

To systematically identify residues required for Tul1 function, we adapted a tiling primer mutagenesis strategy to comprehensively generate Tul1 variant libraries to test in our functional assays (Figure S2.3A) [28–30]. We divided Tul1 into eight variant sub-libraries (~96 amino acids each, Figure 2.3A) compatible with Illumina sequencing. To ensure stable expression of the Tul1 variant libraries without the 'on/off' expression states observed using centromeric plasmids [31,32], we used a genomic integration strategy. We cloned our variant libraries into integrating plasmids that target the genomic *his3* locus (Figure S2.3B) [31,33]. A limitation of yeast genomic integration strategies is difficulty achieving the required transformation and integration efficiencies for library-scale experiments. We engineered a *tul1*Δ strain to include two I-*SceI* restriction sites [34] flanking a selection marker at the *his3* locus (Figure S2.3B). During transformations with this engineered strain, we achieved transformation efficiencies in >10-fold excess of our library diversity, avoiding a diversity bottleneck at this step.

Following transformation, we grew the yeast containing the Tul1 variant libraries in liquid selection media and allowed these cultures to saturate, which allowed us to follow reporter substrate degradation without exposing cells to cytotoxic chemicals to stop translation (Figures S2.1I-S2.1K). We used fluorescence-activated cell sorting (FACS) to collect cells that fell into four populations correlating to four distinct degradation profiles. We predicted the first section would contain Tul1 variants unable to degrade proteasomal substrates (in Quadrant 1, P1), the second section would contain nonfunctional Tul1 variants (in P2), the third section would contain the wildtype-like Tul1 variants (in P3), and in the fourth section would be Tul1 variants unable to degrade vacuolar substrates (in P4) (Figure S2.3C).

Sequencing of the input populations demonstrated that 96% of all possible Tul1 single-residue substitutions were sampled (Figure 2.3A). Every individual position contained single-residue substitutions to at least 10 other amino acids and most positions had >90% of the possible substitutions included (Figure 2.3A). We collected cells that fell into functional (P3) and nonfunctional (P2) populations from each sub-library (Figures 2.3B & S2.3C). We recovered the

cells and confirmed the degradation phenotypes of each FACS-sorted population in flow cytometry prior to DNA extraction, amplification, and sequencing (Figure S2.3C). In most sub-libraries, we saw small percentages of cells that fell into the populations predicted to have altered substrate specificity (Figure 2.3B & see P1/P4 in Figure S2.3C), however these sorted cells either failed to grow or failed in the phenotype confirmation step. Therefore, we assumed these cells were false positives. We successfully recovered and confirmed cells that were defective in degradation of the proteasomal substrate Orm2*-RFP (from P1, Figure S2.3C) from Library 8, spanning positions 673-758, which covered the cytosolic Tul1 RING domain (Figure 2.3B).

We used Enrich2, a statistical framework for analyzing sequencing enrichment datasets [35], to analyze amino acid enrichment scores at each position from the sequencing results (Figures 2.3C & 2.3D). In the nonfunctional populations we observed an enrichment of stop codons, demonstrating success of experimental setup because premature stop codons would result in protein truncation and would disrupt the C-terminal Tul1 RING domain essential for Tul1 function (Figures 2.3C & 2.3D). This observation was a simple validation of the approach by showing our experiments accurately selected for mutations expected to lie within the nonfunctional populations.

2.3.4 Single-residue substitutions in the Tul1 lumenal domain impair complex formation

Broadly, we observed several regions within the Tul1 lumenal domain that were enriched for multiple variants in nonfunctional population and depleted from the functional population (Figures 2.3C & 2.4A). To identify substitutions in the Tul1 lumenal domain that restricted function, we returned to the sequencing data and selected five resides with higher variant counts in the nonfunctional population from sorting and sequencing experiments. We introduced the highest represented mutation at each of these residues into a V5-Tul1 construct and tested for function using the reporter substrates. The FACS-based experiments were performed with only GFP-Tlg1* so we tested whether substitutions had similar phenotypes with both GFP-Tlg1* and GFP-Pep12*. Four of the five variants were nonfunctional and unable to degrade either class of substrate (Figures 2.4B & 2.4C). However, one variant (Tul1(E346V)) was unable to degrade Orm2*-RFP and GFP-Pep12* but partially able to degrade GFP-Tlg1* (Figures 2.4B & 2.4C). This variant was somewhat reminiscent of the phenotype observed with the *gld1*Δ strain (Figures 2.2I-2.2K) but, unlike the *gld1*Δ, was unable to degrade GFP-Pep12*; we concluded the phenotype was unable to be explained only by a simple disruption in Gld1 interaction.

We found that each of the substitutions within the Tul1 lumenal domain partially destabilized Tul1, including the Tul1(E346V) substitution (Figure 2.4D). Tul1(E346V) displayed reduced steady state levels but appeared to have a longer half-life compared to wild-type Tul1. The destabilization of the lumenal mutants was likely responsible for the nonfunctional phenotypes. However, we also wondered whether the Tul1 variants interacted with the rest of its complex because previous studies suggested the Tul1 complex must be fully assembled for ER exit and subsequent function [25,26]. We found that each of the nonfunctional Tul1 lumenal variants were unable to co-immunoprecipitate with additional component of the Tul1 complex, with the exception of Tul1(E364V) (Figure 2.4E). Tul1(E346V) was able to interact with other complex components, albeit weakly, and had a change in preference for Vld1 over Gld1 (Figure 2.4E). Together, we concluded that the Tul1 lumenal domain is critical for Tul1 interaction with its complex, overall stability, and substrate selection.

2.3.5 The Tul1 RING domain influences substrate specificity

Outside of the lumenal domain, we observed residues with several amino acid depletions from the wildtype-like Tul1 sorted population, which fell within TM1, the TM3-TM4 cytosolic loop, and the cytosolic Tul1 RING domain (Figures 2.5A & 2.5B). The most dramatic disenrichment profiles were found in the RING domain, and analysis of the sequencing data confirmed that substitutions of these RING-residues were overrepresented in the nonfunctional population compared to functional population. Residues in TM1 and the TM3-TM4 cytosolic loop were not enriched within the nonfunctional population, therefore we focused our attention on confirming residues of interest in the RING domain (Figure 2.5B).

We created single-position variant libraries to cover all twenty amino acid substitutions for residues of interest in the RING domain and tested their phenotypes after both a 2-hour cycloheximide treatment and in saturated cells using flow cytometry. Within these mini-libraries, single-residue substitutions resulted in mixed functional and nonfunctional populations across all three substrates (Figure S2.4A). Two of the positions (Ala700 and His731, see ~ residues in Figure S2.4A) were also identified in off-axis populations collected in our FACS screen as unable to degrade the proteasomal substrate Orm2*-RFP (P1 in Figure S2.3C), and these libraries did show more impaired Orm2* degradation phenotypes than Pep12* or Tlg1* (Figure S2.4A). In total, we identified ten residues that exhibited noticeable profile shifts from their single-position libraries

and returned to our sequencing data to identify the highest represented substitutions from the nonfunctional or proteasomal-defective populations (Figure S2.4A).

We tested these ten V5-Tul1 RING mutants for degradation of the proteasomal substrate Orm2* and vacuolar substrates Pep12* and Tlg1*. From the results, we grouped these mutants into three different phenotypic classes. In the first grouping, we found that six of these variants were generally nonfunctional, meaning they were broadly unable to degrade substrates (Figures 2.5C & 2.5D). We found that most of these variants were similar in stability to wild-type Tul1, except for Tul1(C748V) which seemed to be less stable (Figure 2.5E). Despite this difference in stability, we confirmed that all five nonfunctional mutants were able to successfully interact with Tul1 complex components by co-immunoprecipitation experiments (see ⊗ in Figure S2.4B). This also suggested that, in contrast to the lumenal nonfunctional mutants (Figures 2.4B-2.4E & Figure S2.4B), unstable Tul1 RING variants could still interact with other complex components (C748V in Figure S2.4B), thus Tul1 destabilization likely resulted from different underlying mechanics.

In the second grouping were three Tul1 RING variants that were hypomorphic in degrading all three substrates, although to varying degrees (Figures 2.5F & 2.5G). Steady-state levels of each variant were similar to wild-type Tul1, however Tul1(C729R) and Tul1(C751S) were less stable with shorter half-lives (Figure 2.5H). Each variant was able to co-immunoprecipitate other Tul1 complex components, similarly to wild-type Tul1 (see ∅ Figure S2.4D).

The third grouping comprised two RING domain variants (A700D and H731S) that were present in proteasomal-nonfunctional off-axis population (P1 in Figure 2.3C). We found that each variant was unable to degrade Orm2*-RFP (and GFP-Pep12*), but were able to degrade GFP-Tlg1*, although inefficiently (Figures 2.5I & 2.5J). The Tul1(A700D) variant steady state levels and stability were considerably reduced compared to wild-type Tul1 (Figure 2.5K) while the Tul1(H731S) steady state was comparable to wild-type Tul1. The overall stabilities of each variant were unable to account for their differences in function (compare Figures 2.5C-2.5K). Importantly, each of these variants were able to interact with the other Tul1 complex components (see ∪ Figure S2.4B). In summary, we identified several Tul1 RING mutants that had a spectrum of impaired function, from nonfunctional, hypomorphic, and selectively unable to degrade proteasomal substrates.

2.3.6 Tul1 variants require Gld1 for function

Several of the variants with altered substrate specificity were reminiscent of *gld1*Δ cells (Figures 2.2I-2.2K) so we tested whether the variants had altered Gld1/Vld1 interaction profiles. Co-immunoprecipitation of the nonfunctional RING domain variants (Figure S2.4B) highlighted a preference for Vld1 over Gld1 (Figure 2.6A). To test whether competition between Gld1 and Vld1 could explain the reduction in substrate degradation, we tested the variants in strains lacking Gld1, Vld1, or both Gld1 and Vld1. We found that loss of either Gld1 or Vld1 had no effect on substrate degradation (Figure 2.6B).

Next, we tested the Tul1 hypomorphic mutants (M703S, C729R, C751S) for alterations in the Gld1 and Vld1 binding profiles (Figure 2.5F). We found that the hypomorphs exhibited decreased Gld1 binding compared to wild-type Tul1, but no apparent preference for Gld1 or Vld1 (Figure 2.6C). In the absence of Gld1 (*gld1*Δ cells), these variants were unable to degrade Orm2*, Pep12*, or Tlg1* whereas in the absence of Vld1, these substrates were degraded slightly more efficiently (Figure 2.6D).

Finally, we tested the Tul1 variants that had altered substrate specificity (A700D, H731S, Figure 2.5I). Similarly to the hypomorphs (Figure 2.6C) these variants had reduced preference for Gld1 over Vld1 compared to wild-type Tul1 (Figure 2.6E). In strains lacking Gld1 and/or Vld1, we observed a requirement for Gld1, but not Vld1, in the degradation of GFP-Tlg1* (Figure 2.6F). Together, these experiments demonstrate that the disparate phenotypes are unable to be attributed solely to changing Gld1/Vld1 preferences.

2.4 Discussion

In this work, we used a deep mutational scanning approach to dissect the function of the Tul1 ubiquitin ligase. We developed high-throughput fluorescence-based reporters to assay degradation of proteasomal and vacuolar Tul1 substrates (Figure 2.1). We found that Tul1 interacts with substrates in the absence of other complex components, but confirmed proper Tul1 complex formation is required for degradative function (Figure 2.2). We generated variant libraries covering nearly all possible single-residue substitutions spanning Tul1, which we separated into functional, nonfunctional or proteasomal-nonfunctional populations (Figure 2.3). Tul1 was relatively tolerant of many single-residue substitutions, but we identified several mutations in the N-terminal lumenal and C-terminal RING domains that altered the activity of Tul1 to varying degrees and toward different substrates (Figures 2.3-2.5). Profiling of these variants identified the Tul1 lumenal

domain as critical for association with the complex components and the resulting protein stability (Figure 2.4). Mutations in the RING domain were able to alter Tul1 complex specificity by completely preventing the degradation of proteasomally-degraded substrates, but did not completely separate the function between the proteasome and vacuolar substrate degradation pathways (Figures 2.5 & 2.6). Therefore, we conclude that Tul1 plays a central role, but requires additional factors to determine the ultimate fate of its substrates.

Our assays simultaneously monitored degradation of Tul1 substrates through both the proteasome and vacuole. This allowed us to identify mutations within the Tul1 RING domain that specifically impaired degradation of proteasomal substrate (Figures 2.5I & 2.5J). These mutants were largely hypomorphic for degradation of vacuolar substrates (Figures 2.5I & 2.5J), which was somewhat reminiscent of substrate degradation in the *gld1*Δ strain (Figures 2.2I-2.2K). Vacuolar degradation in these mutants was somewhat improved when Vld1 was removed from the system, presumably improving the Tul1 interaction with Gld1 [26], emphasizing the importance of the Golgi-localization signal for both proteasomal and vacuole substrate degradation of these model substrates (Figure 2.6F) [14,26]. Proteasomal substrates remained stable in *vld1*Δ expressing these mutants (Figure 2.6F). Importantly, Gld1 was not required for Tul1 interaction with either class of substrates, as Tul1 co-immunoprecipitated with all substrates in *gld1*Δ cells (Figures 2.2F-2.2H). Altogether, this indicated that Tul1 mutants with selectively impaired proteasomal degradation were not exclusively caused by altered Gld1/Vld1 interactions.

Many of the substitutions causing the nonfunctional phenotypes comprise the zinc coordinating residues within the Tul1 RING domain. These substitutions likely disrupt the fold and destabilize zinc interactions (Figure 2.7). Zinc coordination is required for the RING fold to enable recruitment of a ubiquitin-charged E2 conjugating enzyme, which mediates the transfer of ubiquitin onto substrate [36,37]. We modeled the Tul1 RING domain with Ubc4 (E2) [13,38] and ubiquitin using AlphaFold Multimer (Figures 2.7B & 2.7C) [39,40]. The RING-domain positions resulting in nonfunctional Tul1 that were identified in our screen (Figures 2.5C & 2.5D) were predicted to cluster within the Ubc4 interaction interface (grey residues within Figure 2.7). Visualizing the positions where substitutions were able to create Tul1 hypomorphs (white residues in Figure 2.7), or Tul1 with altered specificity (pink residues in Figure 2.7), also fell near the E2 interaction interface, but were not in direct contact within this (static) model (Figures 2.7B & 2.7C). These other RING substitutions likely retain function if they can engage the E2 properly

and allow substrate ubiquitination. However, substrate polyubiquitination might be less efficient, be more prone to certain types of ubiquitin chain linkages catalyzed by Ubc4, have an altered preference for an alternate E2, or perhaps alter the dynamics of the RING/E2/ubiquitin with the substrate binding domain encompassed in the other parts of Tul1 or the Tul1 complex. In addition, it is possible that the protein substrates themselves may not be the most important ubiquitination targets for degradation of vacuole targeted substrates and a lipid target may still be ubiquitinated [38].

RING-type ubiquitin ligases do not directly accept the ubiquitin moiety that is conjugated to substrates, rather they coordinate the attachment of the ubiquitin onto substrates by promoting the closed conformation of the E2-Ub [36,37]. Consistent with this idea, substitutions of the arginine residue critical for RING-type E3s to promote the closed conformation that is required for ubiquitin transfer (Arg752) are nonfunctional in degradation of both classes of substrates (Figures 2.5C & 2.5D)[37,41,42]. It is possible that the other RING mutations we have identified as hypomorphic across all substrates alter the conformational dynamics and, therefore, reduce the rate of substrate ubiquitination producing these phenotypes (Figures 2.5F and 2.5G) [37,41,42]. Extension of the ubiquitin chain could be disrupted, and it is possible that Orm2 requires a higher degree of ubiquitination for degradation using the proteasome [42–45], compared to the ESCRT-targeted substrates (Pep12* and Tlg1*). Perhaps these mutants fail to build polyubiquitin chains that are sufficient to engage the proteasome. Or slower ubiquitination elongation causes Orm2 to be prone to premature de-ubiquitination, which could impede its ability to engage proteasomal degradation machinery [46].

Tul1 participation in proteasomal versus vacuolar pathways might rely on a new role for Tul1 in directing specific types of ubiquitin linkages on substrates. RING-type ubiquitin ligases are not thought to dictate the ubiquitin linkages attached to substrate, but with E2's that produce multiple types of linkages, like Ubc4 [47], Tul1 could influence the type of ubiquitin conjugated onto a substrate by interacting with and positioning both a ubiquitin-charged E2 and substrate. How a ubiquitin ligase interacts with an E2 and a substrate, including what E2 is recruited, can determine if mono- or poly-ubiquitin are conjugated, and directs the type of ubiquitin added (e.g. K48 versus K63) [36,37,41,42,48]. The type of polyubiquitin chain conjugated on proteins determines the fate of a protein, including the degradation pathways it engages with [42,43,45,49]. Along this model, it is possible that Tul1 interacts with proteasomal and vacuolar substrates differently, which could

uniquely orient substrates for different polyubiquitin chain conjugation from the same E2 thus explaining the whether a substrate is degraded at the proteasome (K48-linked) or vacuole (K63-linked) [36,37,41]. Lastly, it is also possible that proteasomal and vacuolar substrates are targeted by different E2 enzymes interacting with Tul1 and our mutants have altered the E2 interactions [36,37,41]. Tul1 is reported to use both Ubc4 and Ubc5 [13,38], along with other potential ubiquitin conjugating enzymes [50]. However, Ubc4 and Ubc5 are paralogs [51] and Ubc5 is primarily expressed under stress conditions [13,52] so is unlikely to explain these results.

Outside of Tul1's role in the substrate ubiquitination cascade, the various impaired substrate degradation phenotypes of Tul1 RING variants could also be related to important RING-domain features not directly tested here. While we did observe destabilization of several mutants, stability alone was unable to account for the resulting phenotypes. However, stability could have impacted some of the degradation capacity of nonfunctional or hypomorphic mutants such as Tul1(C748V), Tul1(C729R), or Tul1 (C751S). Perhaps, like other known integral membrane RING-type ubiquitin ligases [36,37,53–55], Tul1 dimerization is important to function and these mutants could fail to dimerize, contributing to degradation failures. Tul1 was recently reported to ubiquitinate phosphatidylethanolamine (PE) at endosomal compartments and the vacuole, which could assist with facilitating internalization of vacuolar substrates into multivesicular bodies as part of ESCRT-mediated degradation [38]. We only tested Tul1 for its ability to degrade protein substrates, but perhaps these mutants fail to ubiquitinate PE, contributing to their associated phenotypes. In summary, the phenotypes caused by mutations in the Tul1 RING domain could disrupt many ubiquitin ligase functions, which will require further investigation and can be conducted by adapting tools introduced in this study.

However, substitutions we tested in the Tul1 RING domain did not disrupt interactions with known complex components (Figure S2.4B). In contrast, nonfunctional mutations in the Tul1 lumenal domain (Figures 2.4B & 2.4C) impaired the ability to interact with known complex components (Figure 2.4E) and these mutants were also destabilized (Figure 2.4D). The lumenal mutant Tul1(E346V) also had altered substrate specificity (Figures 2.4B & 2.4C) and could still interact with Tul1 complex components (Figure 2.4E). Thus, we concluded that the Tul1 lumenal domain was critical for interaction with complex components and that the correlated destabilization could be caused by orphaned Tul1 degradation. As such, we propose that the Tul1 lumenal domain is required for interaction with complex components, allowing for ER-exit and

localization to the Golgi membrane, where it can ubiquitinate substrates for degradation. Tul1 can directly recognize substrate (Figures 2.2F-2.2H) and the Tul1(E364V) variant data support the lumenal domain as an important part of this function. However, the lumenal domain is also important for interaction with complex components (Figure 2.5) and we could be missing additional proteins, so future studies will be needed to separate these functions.

We identified Tul1 variants with altered substrate specificity, which led us to conclude that Tul1 plays an important role in substrate selection, although we suspect additional factors to play equally-important roles. We did not identify any Tul1 mutants that were completely separation of function capable of proteasome-targeted substrates but not vacuole-targeted substrates. However, it is possible that single residue substitution within Tul1 were not disruptive enough to uncover these phenotypes, which future experiments using this deep mutational scanning pipeline will uncover. It is also possible that the mild Tul1 overexpression in this screen could have obscured these, or other subtle, phenotypes. This screening pipeline can also be applied towards functional dissection of the remaining known complex components [25,26]. Despite the insights gleaned from the *S. pombe* Dsc1 complex analysis, the roles for other complex components remain to be defined. Dsc3 is thought to bridge Tul1 to a subcomplex of Dsc2, Ubx3, and Gld1, however the function of its predicted ubiquitin-like (UBL) domain remains to be explored [25,26] which could play an important role in regulating other components of the ubiquitination system [56]. Dsc2 belongs to the rhomboid-liked superfamily, but its role is unknown [14,25]. Ubx3 contains predicted UAS and UBX domains, the latter likely interacting with the AAA-ATPase Cdc48 which has been suggested to be required for both vacuolar and proteasomal substrate degradation; again, the specific contributions to complex function are unclear [14,17,25]. The Gld1 and Vld1 are localization-determining proteins, but lack any previously-characterized domains. They have been proposed to be functionally-homologous to the *S. pombe* Dsc4 [26], but do not share sequence homology. In addition, only 23% sequence homology is shared between Gld1 and Vld1 further mystifying the mechanistic roles of these proteins [57–59]. One function of these factors in the Tul1 complex is clear: Vld1 localizes the Tul1 complex to the yeast vacuole while Gld1 localizes Tul1 complexes within the Golgi and endosomal system [26].

Our findings suggest that Gld1 could play an additional role, designating substrate for proteasomal degradation (Figures 2.2I-2.2K). Previous studies characterizing Gld1-Tul1 and Vld1-Tul1 did not include Pep12* or Tlg1* in experiments, which led to the proposal that these

subcomplexes did not share substrates [14,26]. Our observation that these vacuolar substrates are primarily degraded by Gld1-Tul1 but in the absence of Gld1 are somewhat degraded by Vld1-Tul1 (Figures 2.2J & 2.2K), is the first indication that these subcomplexes could have overlapping substrates. Importantly, Golgi-localized Tul1 (Gld1-Tul1) appears to be the only complex that can also degrade substrates through the proteasome (Figure 2.2I). This result suggests that Gld1 could play a central role in degrading substrates by the proteasome, an idea we can now explore using our established screening pipeline.

Altogether, we developed a high-throughput functional screen for an E3 ubiquitin ligase complex that degrades substrates through either the proteasome or the vacuole. Our deep mutational scanning results show that the Tul1 RING domain is involved with substrate specificity because we characterized RING mutants that were unable to degrade proteasomal substrate but degraded vacuolar substrates. Our results also suggest that Tul1 alone does not make the primary decision in a substrate's degradation fate and other complex components (or unidentified factors) are also involved in this decision. Continued dissection of the Tul1 complex mechanics are enabled by our Tul1 reporter substrates and deep mutational scanning pipeline.

2.5 Methods

2.5.1 Strains and plasmids

Plasmids were generated using either HiFi DNA assembly (New England Biolabs) or standard restriction cloning and propagated in DH5α *E. coli*. Plasmids were confirmed by restriction digestion and sequencing. See Table 2.1.

Wild type BY4742 (*MATα his3Δ1 leu2Δ0 lys2Δ0 ura3Δ0*) and *tul1*Δ BY4742 (*MATα his3Δ1 leu2Δ0 lys2Δ0 ura3Δ0 tul1::kanR*) were purchased from GE Dharmacon. Additional deletion strains were sporulated from the heterozygous knockout collection purchased from Horizon Discovery Ltd and were derivatives of BY4743 (*MATa/ his3Δ1/his3Δ1 leu2Δ0/leu2Δ0 LYS2/lys2Δ0 met15Δ0/MET15 ura3Δ0/ura3Δ0*) background (see Table 2.2). Genetic deletions were confirmed by immunoblotting using antibodies against Tul1, Dsc2, Dsc3, and Ubx3, generated in [25] (see Table 2.3). The *gld1*Δ*vld1*Δ strain was created by crossing *gld1*Δ and *vld1*Δ strains, sporulation of the resulting diploid, and confirmed via PCR. Other multiple-deletion yeast strains (*tul1*Δ*dsc2*Δ*, tul1*Δ*dsc3*Δ, *tul1*Δ*ubx3*Δ, *tul1*Δ*gld1*Δ, *tul1*Δ*vld1*Δ, *tul1*Δ*gld1*Δ*vld1*Δ*)* were created by transforming *dsc2*Δ, *dsc3*Δ, *ubx3*Δ, *gld1*Δ, *vld1*Δ, and *gld1*Δ*vld1*Δ with PCR-generated cassette containing an antibiotic resistance selection [60] marker with ~60bp of genomic homology to target and replace *TUL1* (see Tables 2.1 & 2.4) [60]. For the 3xHA tags on Gld1 and Vld1, PCR-amplified cassettes (see Tables 2.1 & 2.4) with antibiotic resistance selection markers were transformed and inserted at the endogenous 3' end of Gld1 and Vld1, sequentially, and verified by immunoblotting. For maximum-efficiency integration of *HIS3* integrating plasmids, we engineered the *his3* locus to contain two I-SceI sites flanking a cassette containing the *Ashbya gossypii TEF* promoter, hygromycin B phosphotransferase (hph) resistance gene and the *S. cerevisiae TDH1* terminator (together hphNT3) in a *tul1*Δ strain.

Yeast were transformed into yeast using PEG/LiAc methods[61] and grown on selective dropout media (0.17 % (w/v) yeast nitrogen base(Becton, Dickinson and Company), 0.5 % (w/v) ammonium sulfate (Fisher), ~0.1 % (w/v) drop-out powder (Teknova and Sigma), 2 % (w/v) glucose (Sigma)); drop-out powder for synthetic complete media are at the following concentration: adenine sulfate (20 mg/L), uracil (20 mg/L), L-tryptophan (20 mg/L), L-histidine (20 mg/L), L-arginine (20 mg/L), L-methionine (20 mg/L), L-tyrosine (30 mg/L), L-leucine (60 mg/L), L-isoleucine (30 mg/L), L-lysine (30 mg/L), L- phenylalanine (50 mg/L), L-glutamic Acid

(100 mg/L), L-aspartic Acid (100 mg/L), L-valine (150 mg/L), L-threonine (200 mg/L), and L-serine (400 mg/L)).

2.5.2 Flow cytometry-based degradation assays

Flow cytometry experiments were performed on either the ZE5 Cell Analyzer (Bio-Rad) or MACSQuant® VYB Flow Cytometer (Miltenyi Biotec). Cells from PEG/LiAc transformations were either directly added to selection media or single colonies were selected from plates and grown in selection media. For substrate degradation using saturated chases and flow cytometry, cells were grown in selection media in 96-well plates for 40 hours at 30˚C, shaking at 1000RPM. For cycloheximide treated cells, cultures were grown overnight and were sub-cultured and grown to log phase (OD_{600} = 0.4-1.0). Once in log phase, cells were treated with 50µg/mL of cycloheximide (or ethanol only as a control) and grown for 2 hours at 30˚C, shaking at 1000RPM. Cells were pelleted at 2,000 x g, washed once in PBS, resuspended in cold PBS + 0.05% glucose containing 1µM Sytox Blue (Invitrogen), and were kept on ice or at 4˚C during flow cytometry analysis. Glucose was added to PBS to prevent cells from entering starvation, which causes cytosolic acidification[62] which preliminary optimization of these assays found to affect SEP fluorescence intensity after >30min, but was remedied by the addition 0.05% glucose (data not shown).

For flow cytometry analysis, yeast cells were selected using forward and side scatter gating (Bio-Rad Ze5 uses 488nm laser, Miltenyi MacsQuant VYB uses a 561nm laser). Viable cells were selected based on low Sytox Blue fluorescence using the 405nm laser (Ze5 using 509nm/22nm filter; MacsQuant VYB using 450nm/50nm filter). SEP was followed using the 488nm laser (Ze5 509nm/24nm filter; MacsQuant VYB 525nm/50nm). mScarlet-I was followed using the 561nm laser (Ze5 615nm/24nm filter; MacsQuant VYB 615nm/20nm filter). Flow cytometry data was analyzed in FlowJo V10.7.1 (FlowJo LLC), a minimum of 10^4 events were collected to characterize or quantify substrate degradation. For quantification, the median SEP or mScarlet-I values were quantified in FlowJo and normalized to fluorescence within a *tul1*Δ strain expressing either WT Tul1 (set to 0) or Tul1(C699A) (set to 1). For *tul1*Δ*gld1*Δ, *tul1*Δ*vld1*Δ, and *tul1*Δ*gld1*Δ*vld1*Δ strains, WT Tul1 in *tul1*Δ was set to "0" and Tul1(C699A) for the respective strain was set to "1". Values that were <0 or >1 Heatmaps were set to 0 and 1, respectively. Heatmaps were generated using GraphPad Prism (Dotmatics).

2.5.3 Immunoblotting

Single colonies were grown overnight in selection media, sub-cultured, and grown to log phase (OD_{600} = 0.4-1.0). Log phase cultures were adjusted to a final concentration of 2.0 OD_{600}/mL in selection media and incubated with 50µg/mL cycloheximide at 30˚C with agitation for 60-180 minutes, depending on the protein being studied. Samples were flash frozen at the appropriate time point. Cells were resuspended in SUME lysis buffer 10 mM 3-(N- morpholino)propanesulfonic acid (MOPS), pH 6.8, 1 % sodium dodecyl sulfate (SDS), 8 M urea, 10 mM ethylenediaminetetraacetic acid (EDTA), fresh protease inhibitors (1 mM phenylmethylsulfonyl fluoride (PMSF), 1.5 µM pepstatin A) to 20 OD_{600}/mL and lysed by vortexing with 0.1mm diameter glass beads for 2 minutes. 2xSUME loading buffer (125mM trisaminomethane (Tris), pH 6.8, 4 % SDS, 8 M urea, 10 % β-mercaptoethanol and bromophenol blue) was added to each sample for a final concentration of 10 OD_{600}/mL and heated for 5 minutes at 65˚C. Samples were separated by SDS-PAGE and transferred to either low fluorescence PVDF (Bio-Rad) or Nitrocellulose membranes (Bio-Rad). Membranes were blocked in 5% milk in TBST for 30 minutes-1 hour at room temperature, incubated with the appropriate primary[25] antibodies (see Table 2.3) for at least 2 hours-overnight, washed 3 x ≥5 minutes in TBST, incubated with the appropriate secondary antibodies (see Table 2.3) for ≥30 minutes, and washed 3 x ≥10 minutes in TBST. Blots were imaged on the ChemiDoc MP (Bio-Rad), either based on fluorescence of conjugated secondary antibodies or using chemiluminescence. If re-blotted, blots were stripped with OneMinute®Advance Western Blot Stripping Buffer (GM Biosciences Inc.) per instructions. Sample loading was detected by stain free imaging on the ChemiDoc MP (Bio-Rad). Blots were quantified using ImageJ and graphed using GraphPad Prism.

2.5.4 Tul1 complex and substrate coimmunoprecipitations

Log phase cells (OD = 0.4-1.0) were grown in selection media and 50 OD_{600} (for HA) or 100 OD_{600} (for V5) cells were collected for immunoprecipitation, respectively. Cells were pelleted, washed once in water, and resuspended in immunoprecipitation (IP) buffer (50mM HEPES pH= 7.4, 150mM KCl, fresh protease inhibitors 1 mM PMSF, 1.5 µM pepstatin A, 50µM bortezomib). Cells were flash frozen into yeast 'balls' and cryogenically lysed using freezer/mill (SPEX SamplePrep), with 2 minute precooling followed by 5x cycles of 2 minute run time, 2 minute cool

time, at 10 CPS. Protease inhibitors (1 mM PMSF, 1.5 µM pepstatin A, 50µM bortezomib) were immediately added to the thawed lysate and the lysate was centrifuged at 300 x g for 5 minutes to remove unbroken cells. The supernatant was collected and the microsomal fractions were isolated by centrifuging at 100,000 x g for 30 minutes – 1 hour at 4°C. The pelleted microsomes were resuspended in IP buffer containing fresh protease inhibitors and 1% digitonin (Calbiochem). The membranes were solubilized rotating end-over-end at 4°C for at least 1 hour. Insoluble proteins were removed by centrifugation at 21,130xg for 10 minutes at 4°C. The post centrifugation supernatant was used as the "Input" and diluted to 0.2% digitonin with IP buffer containing fresh protease inhibitors. For V5 immunoprecipitation, samples were incubated with 20µL (40µL slurry) of either V5-Trap Magnetic Agarose beads (ChromoTek) for experiments testing V5-Tul1 mutants in Figures 2.4-2.6, or Anti-V5 Agarose Affinity Gel antibody beads produced in mouse (Sigma) for experiments in *tul1*Δ and Tul1 complex component deletion strains in Figure 2.2, and gently rotated end-over-end for at least 2 hours at 4˚C. For HA immunoprecipitation in Figure 2.2, input samples were pre-cleared by rotating gently with 20µL (40µL slurry) Protein A/G Magnetic Agarose beads (Pierce) at 4˚C for at least 2 hours. The beads were removed before addition of 200ng Anti-HA High Affinity from rat IgG1 (Roche) antibody and 20µL of fresh Protein A/G Magnetic Agarose beads (40µL slurry), followed by overnight end-over-end rotation at 4˚C. The flow-through for all immunoprecipitations were collected. Following overnight incubations, the beads were washed once with IP buffer + fresh protease inhibitors + 0.2% digitonin, and then three times with IP buffer + protease inhibitors + 0.1% digitonin. Immunoprecipitated proteins were eluted in 10% SDS and heating to 65˚C for 5 minutes, and separated on SDS-PAGE gel followed by immunoblotting. All steps in these experiments until elution were either performed on ice or at 4˚C. Anti-V5 Agarose Affinity Gel antibody beads and Protein A/G Magnetic Agarose beads were blocked in 5% BSA for at least 1 hour, washed twice and incubated in IP buffer + 0.2% digitonin + fresh protease inhibitors before use.

2.5.5 Generation of tiling primer libraries

We used the CodonTilingPrimers script [29,30] to generate 759 primers that encoded "NNK" at each residue spanning the Tul1 coding sequence. Primers were synthesized by Integrated DNA Technologies (IDT) in 8 separate 96-well plates normalized to 20ng/µL in diH_2O. For screening, primers from each plate were pooled into 8 sub-libraries. For single-residue library construction,

individual NNK primers were pulled for each residue tested (Figure S2.4A). We modified a previously described method [28] to generate the Tul1 libraries.

We first created two dUTP-containing templates for use in future PCR steps by amplifying the following primer pairs and plasmids with Q5U Hot Start High-Fidelity DNA Polymerase (NEB), dUTPs (2mM dATP, 2mM dCTP, 2mM dGTP, 4mM dUTP), and 2% DMSO, beginning with an initial 3 minute 98˚ denaturation, followed by 35 x cycles of [98˚C for 10 seconds, 65˚C for 20 seconds, 72˚C for 2 minutes] and a final 5 minute 72˚C extension. Tul1_Template1 (for use in PCR#1 in Figure S2.3A) was created by amplifying phosphorylated prDD148 (pprDD148) and phosphorylated prDD203 (pprDD203) with 1ng pDD66, a plasmid encoding Tul1(WT) with its endogenous promoter expressed in a LEU2 integrating plasmid which would reduce any undigested Tul1_Template1 from being amplified in downstream amplification steps (i.e. PCR #4 in Figure S2.3A) and also would not be compatible with the final HiFi assembly step into a HIS3-integrating expression vector (Figure S2.3B). We created Tul1_Template2 (for use in PCR#3 in Figure S2.3A) by amplifying prDD202 and phosphorylated prDD203 (pprDD203) with 1ng pDD69, which encodes Tul1(WT) with an ADH1 promoter expressed on a HIS3 integration plasmid to create full-length Tul1 variants compatible with the final HiFi step (Figure S2.3B). Both reactions were run on a 1% agarose gel with Safe DNA Gel Stain (ApexBio), excised, and purified with the QIAquick Gel Extraction Kit (Qiagen). To make sense-Tul1_Template2 DNA, Tul1_Template2 PCR products were digested with 5U Lambda Exonuclease (NEB) at 37˚C for 30 minutes, then 10mm EDTA was added for 10 minutes at 75˚C to stop the reaction, which was purified following protocol for 1.8x AMPure XP SPRI Reagent (Beckman).

PCR#1 in our tiling primer protocol amplified 30ng of NNK-encoded primers/primer libraries were amplified against 9ng of Tul1_Template1 using Q5U, dTTPs (2mM dATP, 2mM dCTP, 2mM dGTP, 2mM dTTP), and 2% DMSO (PCR #1 in Figure S2.3A). For this reaction, an initial 3 minute denaturation at 98˚C was followed by 2 cycles of [98˚C for 10 seconds, 65˚C for 20 seconds, 72˚C for 2 minutes (sub-libraries 1 & 2) or 1.5 minutes (sub-libraries 3, 4, & 5) or 1 minute (sub-libraries 6, 7, & 8)], and a final extension of 72˚C for 5 minutes. dUTP-containing Tul1_Template1 was degraded by incubating PCR#1 products with 2U of USER (NEB) enzyme for 15 minutes at 37˚C to degrade the phosphorylated Tul1_Template1, and immediately purified using 1.8x AMPure XP beads. The resulting ‘forward megaprimers’ were amplified from their 3’ terminus with prDD203 using Q5 High-Fidelity DNA Polymerase (NEB), dTTPs, and 2% DMSO

for PCR#2 (Figure S2.3A), which followed an initial 3 minute 98˚C denaturation with 35 x cycles [98˚C for 10 seconds, 65˚C for 20 seconds, 72˚C for 2 minutes (for megaprimers from sub-libraries 1-4) or 1 minute (for megaprimers from sub-libraries 5-8)], and a final 72˚C 5 minute extension. These reactions were run on a 2% agarose gel to confirm products, which at this point we noted the bands for megaprimers from sub-library 4 were less intense than all other sub-libraries. We repeated PCR#2 on sub-library 4 and reduced the cycled extension time to 1.5 minutes, but still observed lower intensity bands in later PCR reactions, suggesting that PCR#1 for this sub-library was less efficient, and ultimately resulted in decreased representation of substitutions in input libraries for this region (Figure 2.3A). The 'reverse megaprimers' from PCR#2 were purified with 0.6x AMPure XP beads.

PCR#3 (Figure S2.3A) amplified the reverse megaprimers against 3ng of Tul1_Template2 using Q5U, dTTPs, and 2% DMSO following an initial 3-minute 98˚ denaturation, followed by 35 x cycles of [98˚C for 10 seconds, 65˚C for 20 seconds, 72˚C for 2 minutes] and a final 5 minute 72˚C extension, which is the cycles used for the rest of this protocol. 10X CutSmart buffer was added to these reactions along with 1.5U of USER (NEB) enzyme, which was incubated for 20 minutes at 37˚C and immediately purified using 0.6x AMPure XP beads to create full-length single stranded Tul1 variant libraires. dsDNA products were enriched in PCR#4 by amplifying these ssDNA products with prDD200 and prDD201 using Q5, dTTPs, and 2% DMSO. Products were purified using 0.6x AMPure XP and the resulting full length Tul1 variant dsDNA libraries were run on a 1% agarose gel and visualized with Safe DNA Gel Stain (ApexBio) to confirm products. These products were amplified with Q5, dTTPs, and 5%DMSO using primers to add the necessary barcodes (see Table 2.4) for Amplicon EZSeq (Azenta) to determine library diversities.

Tul1 dsDNA variant libraries contained 5' and 3' homologies to a linearized HIS3 integrating expression plasmid (pDD228, with ADH1prom and CYC1term) containing kanamycin resistance using NEBuilder HiFi DNA Assembly (NEB) using 1:2 vector:insert ratio and 1 hour 50˚C incubation (Figure S2.3B). These products were transformed into *E. cloni* 10G Chemically Competent Cells (Biosearch Technologies) following kit instructions. After 1 hour recovery outgrowth, cells were added to 50mL LB + 50µg/mL kanamycin, grown in 250mL baffled flasks at 37˚C with agitation overnight. Dilutions of 1 x 10^{-3} of each transformation was plated on LB-Kan(50µg/mL) plates before overnight growth to calculate transformation efficiency and confirmed that we achieved transformations >2 x 10^4 CFU, which would enable >10x the

theoretical diversity of transformants. Transformation of the HiFi negative control with only linearized empty expression vector from these reactions suggested that 1% - 10% of the *E. coli* libraries contained background empty vectors, which could explain the high number of cells in nonfunctional populations observed in FACS (Figure 2.3B) despite Tul1 variants seemingly mostly falling into functional populations (Figures 2.3-2.5). Plasmid libraries from 6mL of these cultures were purified using QIAprep Spin Miniprep Kit (Qiagen), while the remaining cultures were collected and stocked in LB + 33% glycerol at -80˚C. The resulting Tul1 variant plasmids were linearized by overnight incubation with PvuII-HF (NEB) enzyme and purified with QIAquick PCR Purification Kit (Qiagen) Amplicon sequencing of the final products from our tiling-primer pipeline (Figure S2.3A, PCR #4 products) confirmed that we achieved >10X the theoretical diversity (>$2.1x10^4$) for each of our mutant linear DNA libraries.

2.5.6 Isolation of Tul1 variants by fluorescence activated cell sorting (FACS)

For maximum-efficiency transformations, we used the *tul1*Δ strain containing *his3::I-SceI_hphNT3_I-SceI* (yRB508). To induce DNA damage and remove the HygB resistance cassette, we co-transformed a linear DNA fragment containing the *PGK1* promoter, *PGK1* terminator and either the I-SceI restriction endonuclease (pRB867) or Venus (as a control, pRB868) with the linearized Tul1 variant libraries in custom yeast vectors that target to the *his3* locus [33]. Co-transformation of the linearized Tul1 plasmids with the I-SceI containing DNA fragment increased integration efficiency >1,000 fold relative to the Venus DNA, presumably by allowing temporary expression of I-SceI to induce double-stranded breaks, thereby increasing the efficiency of homologous recombination. This modified strain was transformed with Orm2*-RFP and GFP-Tlg1* integrated at the URA3 locus, and then transformed with Tul1 variant libraries using a modified library-scale version of PEG/LiAc transformation adapted from published Yeastmaker Yeast Transformation System 2 (Clontech/Takara Bio) protocol. Briefly, 100mL of cells were grown to OD_{600} 0.4-0.5 in YPD, washed twice in sterile water, once in 1.5 mL 1.1xTE/LiAc (1.1mL 10X TE + 1.1mL 1M LiAC + 7.8mL diH_2O) and resuspended 600µL of 1.1x TE/LiAc. 200ng of PvuII-linearized library DNA (purified by QIAquick PCR Purification Kit) + 200ng of I-SceI (pRB827) were transformed into cells in 2.5mL of 40%PEG/1xLiAc/1xTE solution with 200µg ssDNA and incubated at 30˚C for 45 minutes, inverting at 15 minute intervals to mix. 160µL of DMSO was added to the mixture and incubated at 45˚C for 1 hour, inverting

every 10 minutes to mix. Cells were collected and grown in 50mL 2X selection media (0.34% (w/v) yeast nitrogen base(Becton, Dickinson and Company), 1% (w/v) ammonium sulfate (Fisher), ~0.2% (w/v) drop-out powder (Teknova and Sigma), 4% (w/v) glucose (Sigma), adenine sulfate (40 mg/L), L-tryptophan (40 mg/L), L-arginine (40 mg/L), L-methionine (40 mg/L), L-tyrosine (60 mg/L), L-leucine (120 mg/L), L-isoleucine (60 mg/L), L-lysine (60 mg/L), L- phenylalanine (100 mg/L), L-glutamic Acid (200 mg/L), L-aspartic Acid (200 mg/L), L-valine (300 mg/L), L-threonine (400 mg/L), and L-serine (800 mg/L)) in 250mL baffled flasks, with dilutions of 1×10^{-3} grown on -His-Ura selection plates to determine transformation efficiency $>2 \times 10^4$ CFU. FACS experiments were conducted using a Bigfoot Spectral Cell Sorter (Thermo Scientific (formally Propel Labs)) on transformed cells grown in 250mL baffled flasks containing 2X selection media that were grown at 30˚C for 40 hours with shaking to achieve saturation. 6 OD_{600} of unsorted cells were collected and washed once in diH_2O, then flash frozen for sequencing of 'input' populations. 6 OD_{600} cells were collected to be sorted, washed twice in PBS, and resuspended in cold PBS + 0.05% glucose + 1μM Sytox Blue (Invitrogen) at 3 OD_{600}/mL, and kept on ice or at 4˚C during FACS. 2X selection media was added immediately after sorting and cells were allowed to recover in 25mm glass tubes or 250mL baffled flasks containing 5mL or 100mL of 2X selection media, respectively, depending on the number of cells sorted in each bin. After recovery and saturation, cells were tested in flow cytometry using MACSQuant VYB (MACSQuantify software; Miltenyi Biotec) to confirm phenotype. Once confirmed, 6 OD of cells were collected and washed once in diH_2O, which would be used later for DNA extraction and Illumina sequencing. The remaining saturated cells were frozen and stocked in 33% glycerol + 2X selection media at -80˚C. Three replicates of these FACS experiments were performed, with sublibraries 1, 5, and 8 tested in the first replicate and all eight libraries tested in the second and third replicates.

2.5.7 Amplicon sequencing and analysis

Plasmid sub-library efficiencies from tiling primer mutagenesis (PCR #4 in Figure S2.3A) was determined by amplifying DNA from plasmid miniprep reactions (as described earlier) with primers to add partial adaptors (see Table 2.4) compatible with Genewiz (now Azenta Life Sciences) EZSeq services, which included sequencing analysis. To sequence FACS sorted populations, genomic DNA was collected from each population via colony PCR. Initial attempts to extract genomic DNA from FACS sorted populations using zymolase colony PCR [63] were

unsuccessful, likely because these cells were very saturated when collected which made efficient zymolase solubilization of cell membranes difficult. We followed published protocols using lithium acetate (LiOAc)-SDS DNA extraction followed by ethanol precipitation from 6 OD_{600} of FACS-sorted yeast populations [64]. Extracted genomic DNA was further purified by 1.8x AMPure XP SPRI Reagent (Beckman) to remove any EDTA traces in the reaction from the LiOAC-SDS DNA extraction protocol, which could impede polymerase activity. The extracted and purified genomic DNA of each population was amplified with primers specific to the regions tested in the associated sub-libraries, containing Illumina R1 and R2 adaptor sequences (see Table 2.4) using Q5 High-Fidelity DNA Polymerase (NEB) and dTTPs (2mM dATP, 2mM dCTP, 2mM dGTP, 2mM dTTP), with an initial 3 minute 98˚ denaturation, followed by 35 x cycles of [98˚C for 10 seconds, 60˚C for 20 seconds, 72˚C for 2 minutes] and a final 5 minute 72˚C extension. Genomic DNA from Sub-library 6 Replicate 2 nonfunctional populations failed to amplify during this step and was not included in our analysis. Each reaction was purified using 1.8x AMPure XP beads and subjected to another round of PCR, this time with only 12x cycles, to add i5 and i7 indexes using the Index Kit 2 for Illumina (Apexbio Technology LLC). These products were again purified by AMPure XP beads, normalized using Qubit dsDNA HS Assay Kit (ThermoFisher), and pooled for Illumina MiSeq 2x300 through the University of Michigan Sequencing Core.

The returned FASTQ files were first processed to trim adaptor sequences using cutadapt [65], followed by PANDAseq [66] to trim primer sequences and to align paired reads to Tul1. Sequencing data was then subjected to two methods of analysis, either by inputting the resulting FASTQ files into the ENRICH2 GUI [35] or translated and statistically analyzed in Excel (Microsoft Office). For the former, ENRICH2 produced heatmaps for each sub-library to visualize regions of interest based on enrichment of substitutions at each residue. For the latter, sequences were translated using SeqKit [67] 'translate' command and saved to tables in Excel using the 'rmdup' command to build a table of sequences that were counted at least twice in the sequencing data. We used this data to quantify represented Tul1 single-residue variants in each of the input or sorted populations (P1 = proteasomal nonfunctional, P2 = nonfunctional, P3 = functional), which we used to determine substitutions that had higher counts in nonfunctional versus functional populations. Enrichment of Tul1 substitutions at each residue were plotted using RStudio (version 2023.06.2 +561) and ggplot2 [68] to generate the diverging heatmaps, which is shown in Figures 2.3-2.5.

2.5.8 Tul1 RING-Ubc4-ubiquitin structure prediction

We folded the RING domain of Tul1 (YKL034W [59], His668-Lys758, the C-terminus [13,25]) with Ubc4 (YBR082C [59]) and Ubiquitin (YLL039C [59], residues 1-76) using Cosmic2 [39] to implement AlphaFold-Multimer [40].

2.6 Acknowledgements

We would like to thank Brian Peterson, Jenn Russ, and other members of the Baldridge lab past and present for insightful discussion and critical readings of the manuscript. We also thank former lab member Jiwon Hwang for helpful insights during assay optimization and critical reading of the manuscript. We thank members of the University of Michigan Flow Cytometry Core for their assistance and training. We thank the Espenshade Lab and the Li Lab for sharing Tul1 antibodies.

2.7 Author Contributions

D.D.D conceptualized and designed the project, optimized the methodology, conducted investigations, analyzed and visualized the data, drafted the original manuscript, and contributed to the review and editing of the final document. R.D.B. conceptualized and designed the project, conducted investigations, analyzed and visualized the data, drafted the original manuscript, participated in the review and editing of the final manuscript, and supervised all work.

2.8 Declaration of Interests

The authors declare that they have no conflict of interest.

2.9 Funding

Work performed by D.D.D. was supported in part by the NIH Cellular and Molecular Biology Training Grant (T32-GM007315). This work was also supported by the University of Michigan Biological Sciences Scholars Program (BSSP) and NIH/NIGMS award (R35GM128592 to R.D.B.).

2.10 Figures

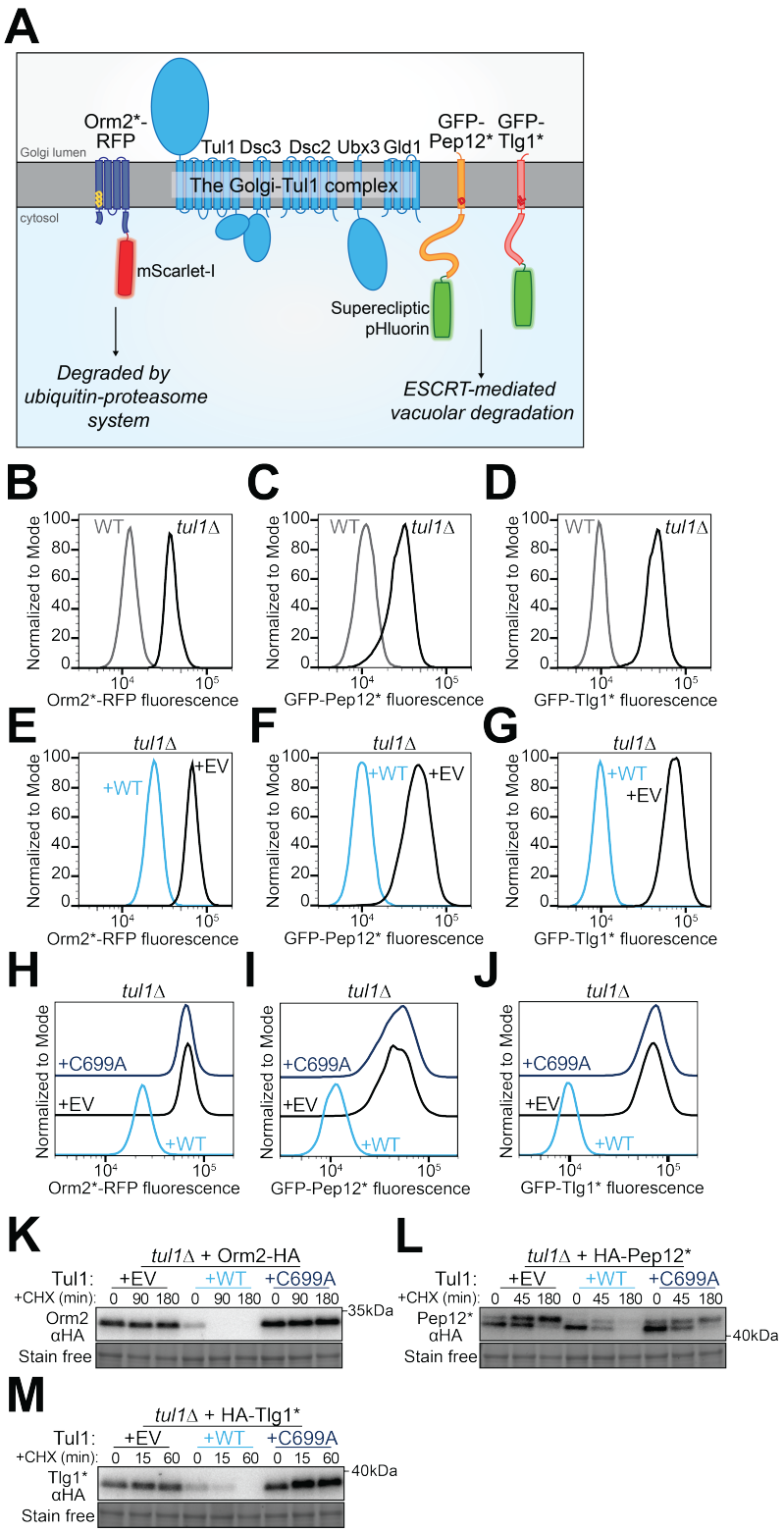

Figure 2.1: Establishing high-throughput methods to monitor Golgi-localized Tul1 function.

Figure 2.1: Establishing high-throughput methods to monitor Golgi-localized Tul1 function.

A) Schematic of the Golgi-localized Tul1 complex components and fluorescently tagged model substrates. Orm2* with a C-terminal mScarlet-I (Orm2*-RFP) is degraded by the ubiquitin-proteasome system. Pep12(D) and Tlg1(LL) with N-terminal super ecliptic pHluorin (GFP-Pep12*) and (GFP-Tlg1*) are degraded via ESCRT-mediated vacuolar degradation.
B) Degradation of the model substrate Orm2*-RFP was followed by flow cytometry two hours after addition of 50µg/mL cycloheximide. Experiments were performed in wild-type (WT, grey line) and *tul1*Δ (*tul1*Δ, black line) cells.
C) As in (B) but with model vacuolar substrate GFP-Pep12*.
D) As in (B) but with model vacuolar substrate GFP-Tlg1*.
E) As in (B), except in *tul1*Δ cells complemented with either wild-type Tul1 (WT, light blue line) or an empty vector (EV, black line).
F) As in (E) but with GFP-Pep12*.
G) As in (E) but with GFP-Tlg1*.
H) As in (E), except with the additional Tul1 RING-finger variant Tul1(C699A) (C699A, dark blue line), wild-type Tul1 (WT, light blue line), or empty vector (EV, black line).
I) As in (H) but with GFP-Pep12*.
J) As in (H) but with GFP-Tlg1*.
K) Degradation of the model substrate Orm2*-3xHA was followed by immunoblotting for Orm2*-3xHA (Orm2-HA) after cycloheximide treatment for the indicated times. Orm2-HA was expressed in *tul1*Δ cells complemented with either an empty vector (EV), wild-type Tul1 (WT), or inactive Tul1 variant (C699A). Total protein was visualized by stain-free technology and used as a loading control.
L) As in (K) but monitoring 3xHA-Pep12* (HA-Pep12*) degradation.
M) As in (K) but monitoring 3xHA-Tlg1* (HA-Tlg1*) degradation.
See also Figure S2.1.

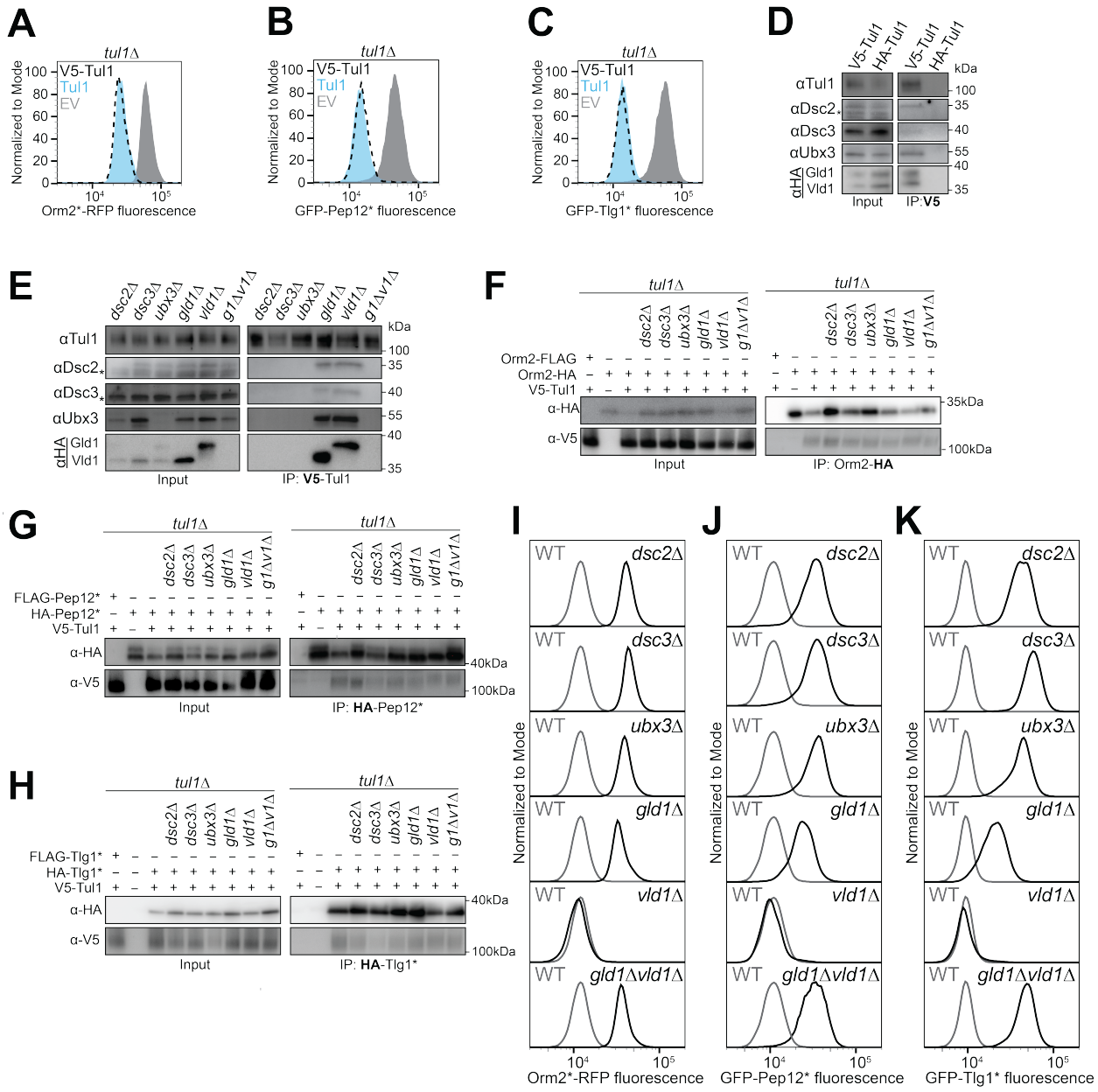

Figure 2.2: Tul1 complex assembly is not required for Tul1 substrate interaction.

Figure 2.2: Tul1 complex assembly is not required for Tul1 substrate interaction.

A) Degradation of the model substrate Orm2*-RFP was followed by flow cytometry after a two-hour treatment with 50µg/mL cycloheximide. Experiments were performed in *tul1*Δ cells complemented with 3xV5-Tul1(WT) (V5-Tul1, black dotted line with no fill), untagged Tul1 (Tul1, light blue fill), or an empty vector (EV, grey fill).
B) As in (A) but with GFP-Pep12*.
C) As in (A) but with GFP-Tlg1*.
D) Co-immunoprecipitation of the Tul1 complex was performed from *tul1*Δ cells expressing Gld1-HA and Vld1-HA, and either HA-Tul1 or V5-Tul1. Inputs were loaded at 5% and proteins were detected by immunoblotting with α-Tul1, α-Dsc2, α-Dsc3, α-Ubx3, or α-HA antibodies; * denotes off-target bands.
E) As in (D) but in *dsc2*Δ, *dsc3*Δ, *ubx3*Δ, *gld1*Δ, *vld1*Δ, and *gld1*Δ*vld1*Δ (see *g1*Δ*v1*Δ) cells.
F) Co-immunoprecipitation of the substrate HA-Orm2 expressed in *tul1*Δ, *tul1*Δ*dsc2*Δ (see *dsc2*Δ), *tul1*Δ*dsc3*Δ (see *dsc3*Δ), *tul1*Δ*ubx3*Δ (see *ubx3*Δ), *tul1*Δ*gld1*Δ (see *gld1*Δ), *tul1*Δ*vld1*Δ (see *vld1*Δ), *tul1*Δ*gld1*Δ*vld1*Δ (see *g1*Δ*v1*Δ) cells, expressing either Orm2-FLAG (FLAG) or Orm2-HA (HA) and either V5-Tul1 or an empty vector. Inputs were loaded at 5% and detected by immunoblotting using either α-HA or α-V5 antibodies.
G) As in (F) but expressing FLAG-Pep12* (FL) or HA-Pep12* (HA).
H) As in (F) but expressing FLAG-Tlg1* (FL), empty vector (-), or HA-Tlg1* (HA).
I) As in (A) but in the indicated deletion strains *dsc2*Δ, *dsc3*Δ, *ubx3*Δ, *gld1*Δ, *vld1*Δ, or *gld1*Δ*vld1*Δ cells (black lines) compared to wild-type cells (grey lines).
J) As in (I) but with GFP-Pep12*.
K) As in (I) but with GFP-Tlg1*.

See also Figure S2.2.

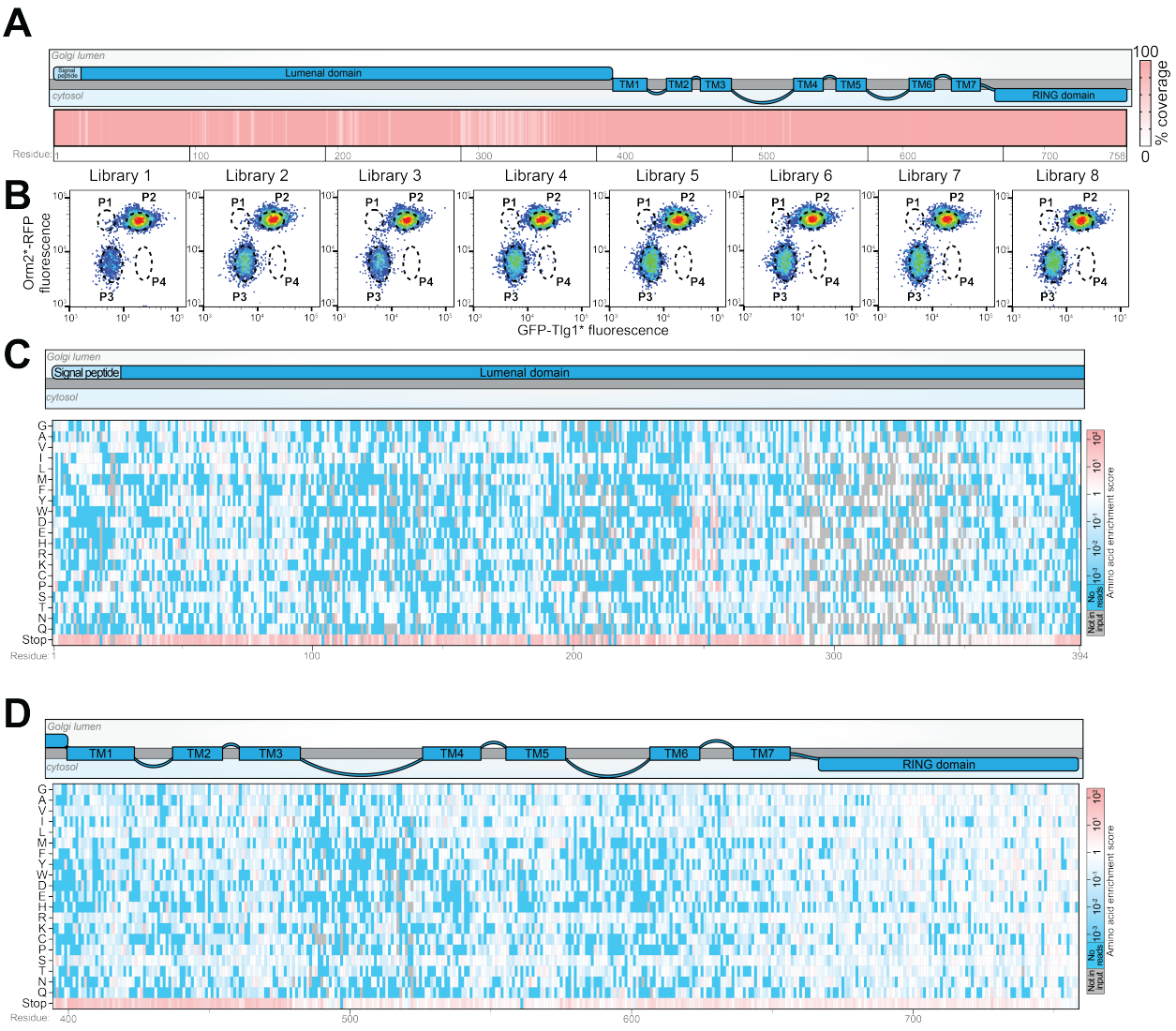

Figure 2.3: Deep mutational scanning of the Tul1 ubiquitin ligase.

Figure 2.3: Deep mutational scanning of the Tul1 ubiquitin ligase.

A) Top: Predicted topology diagram of Tul1. Bottom: Heatmap representing the amino acid variant coverage of the input libraries (of 20 possible amino acids + stop codon) for each position within Tul1.
B) Scatter plots of flow cytometry data for Tul1 variant sub-libraries expressed in *tul1*Δ cells containing Orm2*-RFP and GFP-Tlg1* and grown to saturation. The fluorescence intensity of the proteasomal substrate Orm2*-RFP is displayed on the y-axis, and the vacuolar substrate GFP-Tlg1* is displayed on the x-axis. The dashed circles represent the gates used in the fluorescence activated cell sorting to select for Tul1 variant populations that were predicted to be unable to degrade proteasomal substrates (P1), completely nonfunctional (P2), wildtype-like and functional (P3), and unable to degrade vacuolar substrates (P4).
C) Heatmap depicting individual amino acid enrichment and disenrichment, relative to the input libraries, for residues in the lumenal domain (amino acids 1-394). These data are from the completely nonfunctional populations (P2) in (B).
D) As in (C) but for amino acids 395-758 covering the Tul1 transmembrane regions and the cytosolic RING domain.
See also Figure S2.3.

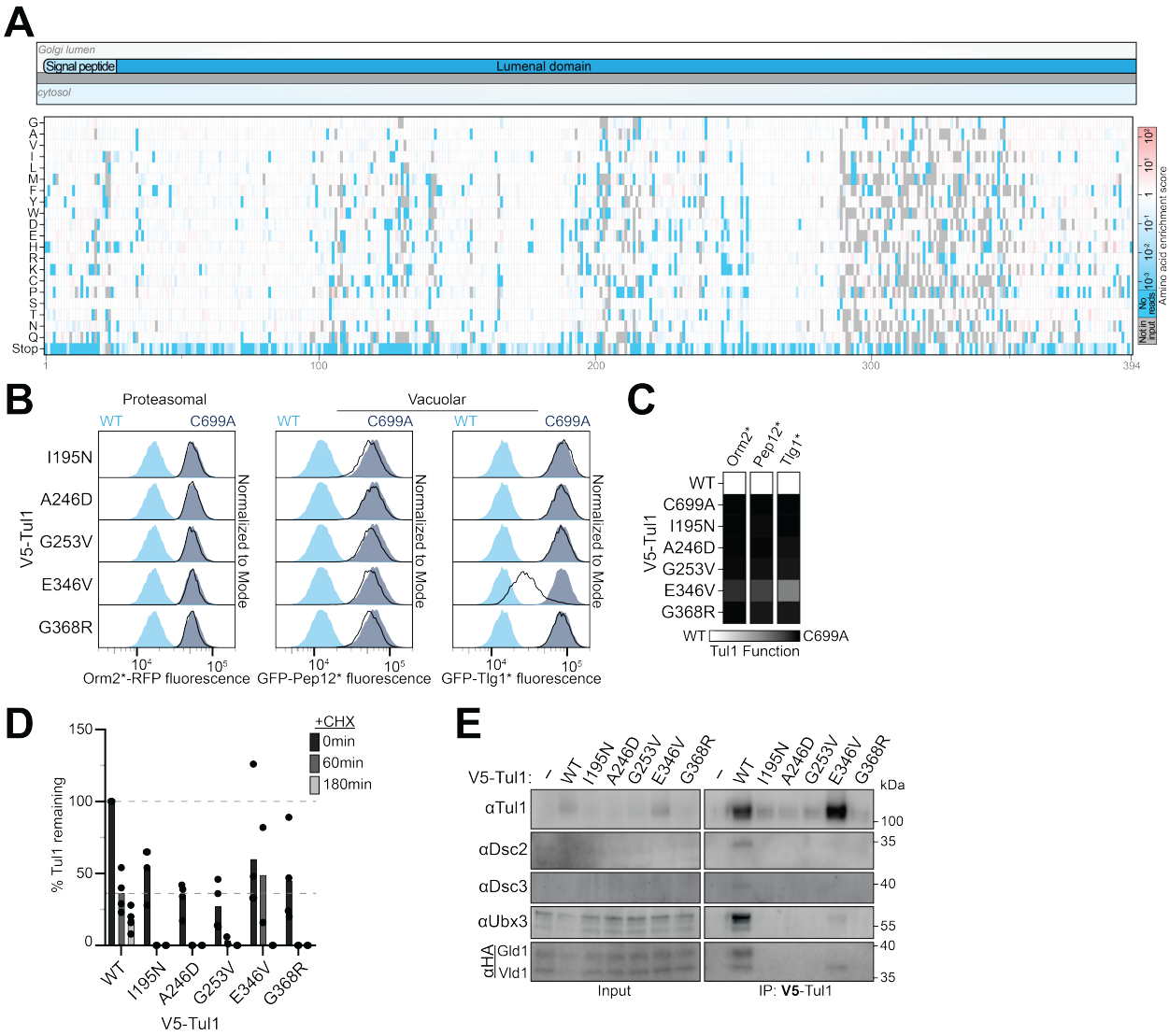

Figure 2.4: The lumenal domain is important for Tul1 complex interactions.

Figure 2.4: The lumenal domain is important for Tul1 complex interactions.

A) Top: Topology diagram of Tul1. Bottom: Heatmap depicting amino acid enrichment and disenrichment for residues within the Tul1 lumenal domain (amino acids 1-394) from wildtype-like (functional) populations.
B) Degradation of model substrates (Orm2*-RFP, GFP-Pep12*, and GFP-Tlg1*) were followed after a two-hour treatment with 50µg/mL cycloheximide. Experiments were performed in *tul1*Δ cells complemented with the indicated V5-Tul1 variants (black line with no fill), V5-Tul1 (WT, light blue fill), or an inactive Tul1(C699A) (C699A, dark blue fill).
C) Quantification of flow cytometry results in (B), depicted as a heatmap. Tul1 variant function was reported relative to wild-type Tul1 (white) and inactive Tul1(C699A) (black).
D) Degradation of wild-type Tul1 and the indicated Tul1 variants were followed by immunoblotting after treatment with cycloheximide and quantified. Values for wild-type Tul1 at time = 0, were normalized to 100%. Grey dotted lines indicate Tul1 steady state and Tul1 turnover after 60-minute cycloheximide treatment.
E) Co-immunoprecipitation of V5-Tul1 variants with complex components. V5-Tul1 variants were expressed in *tul1*Δ cells with genomically-tagged Gld1-HA/Vld1-HA. Inputs were loaded at 5% and proteins were detected by immunoblotting with α-Tul1, α-Dsc2, α-Dsc3, α-Ubx3, or α-HA antibodies.

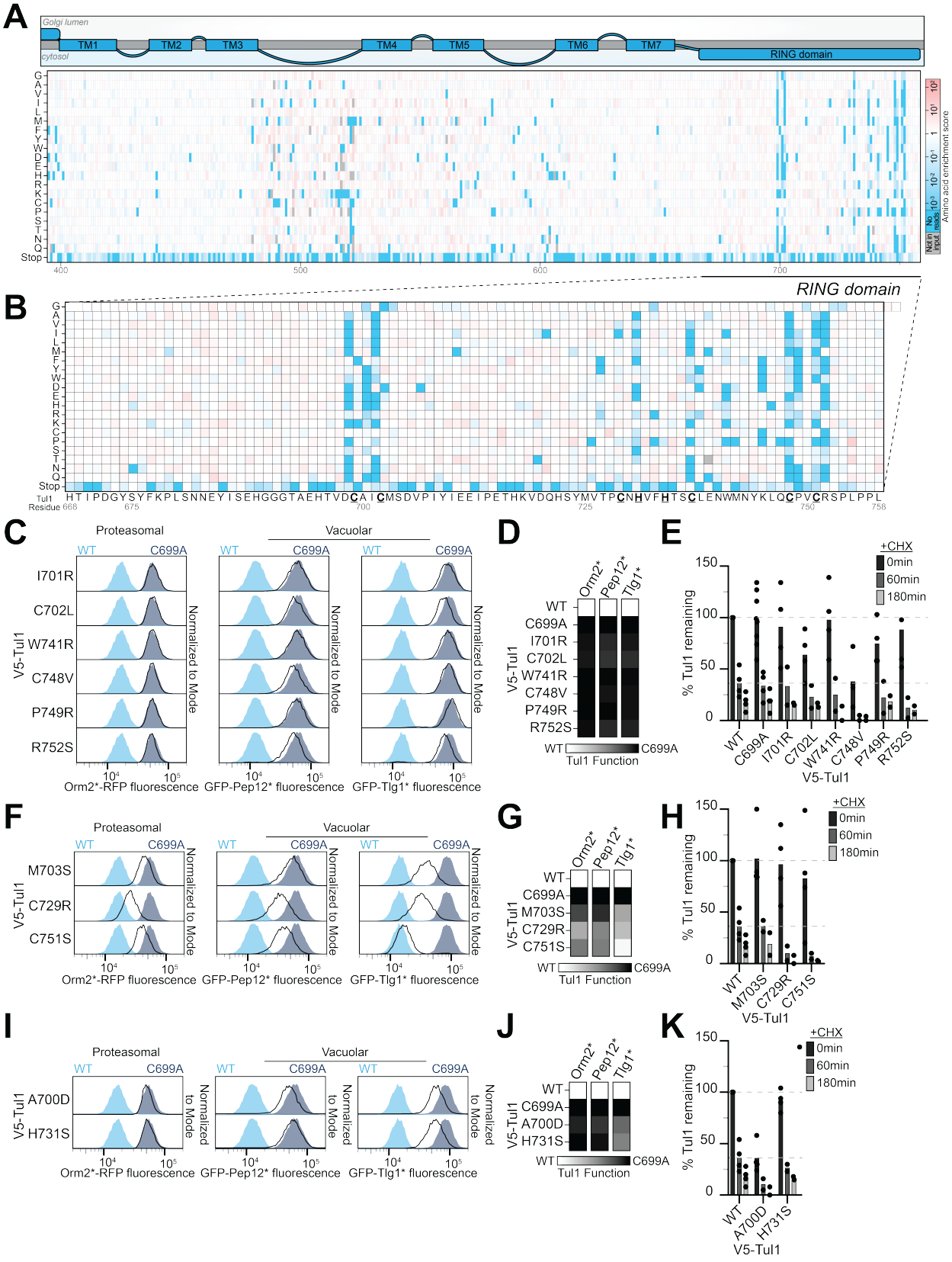

Figure 2.5: Substitutions within the Tul1-RING domain alter substrate specificity.

Figure 2.5: Substitutions within the Tul1-RING domain alter substrate specificity.

A) Top: Predicted topology diagram of Tul1 with transmembrane segments 1-7. Bottom: Heatmap depicting amino acid enrichment and disenrichment for residues spanning the Tul1 transmembrane domains and the RING domain (amino acids 395-758). These data are from the wildtype-like (functional) populations.
B) As in (A) but with focused on residues 668-758 that compose the Tul1 RING domain, with bold and underlined residues indicating canonical residues for the RING-finger fold and zinc coordination.
C) Degradation of model substrates (Orm2*-RFP, GFP-Pep12*, and GFP-Tlg1*) were followed by flow cytometry two hours after the addition of 50μg/mL cycloheximide. Experiments were performed in *tul1*Δ cells complemented with the indicated V5-Tul1 variants (black line with no fill), V5-Tul1 (WT, light blue fill), or an inactive Tul1(C699A) (C699A, dark blue fill).
D) Quantification of flow cytometry results in (C), depicted as a heatmap. Tul1 variant function was reported relative to wild-type Tul1 (white) and inactive Tul1(C699A) (black).
E) Degradation of the indicated Tul1 variants were followed by immunoblotting after treatment with cycloheximide and quantified. Values for wild-type Tul1 at time = 0, were normalized to 100%.
F) As in (C) but with the indicated V5-Tul1 variants that were found to be hypomorphic.
G) As in (D) but with the indicated V5-Tul1 variants that were found to be hypomorphic.
H) As in (E) but with the indicated V5-Tul1 variants that were found to be hypomorphic.
I) As in (C) but with the indicated V5-Tul1 variants that were found to have altered substrate specificity.
J) As in (D) but with the indicated V5-Tul1 single residue variants that were found to have altered substrate specificity.
K) As in (E) but with the indicated V5-Tul1 single residue variants that were found to have altered substrate specificity.

See also Figure S2.4.

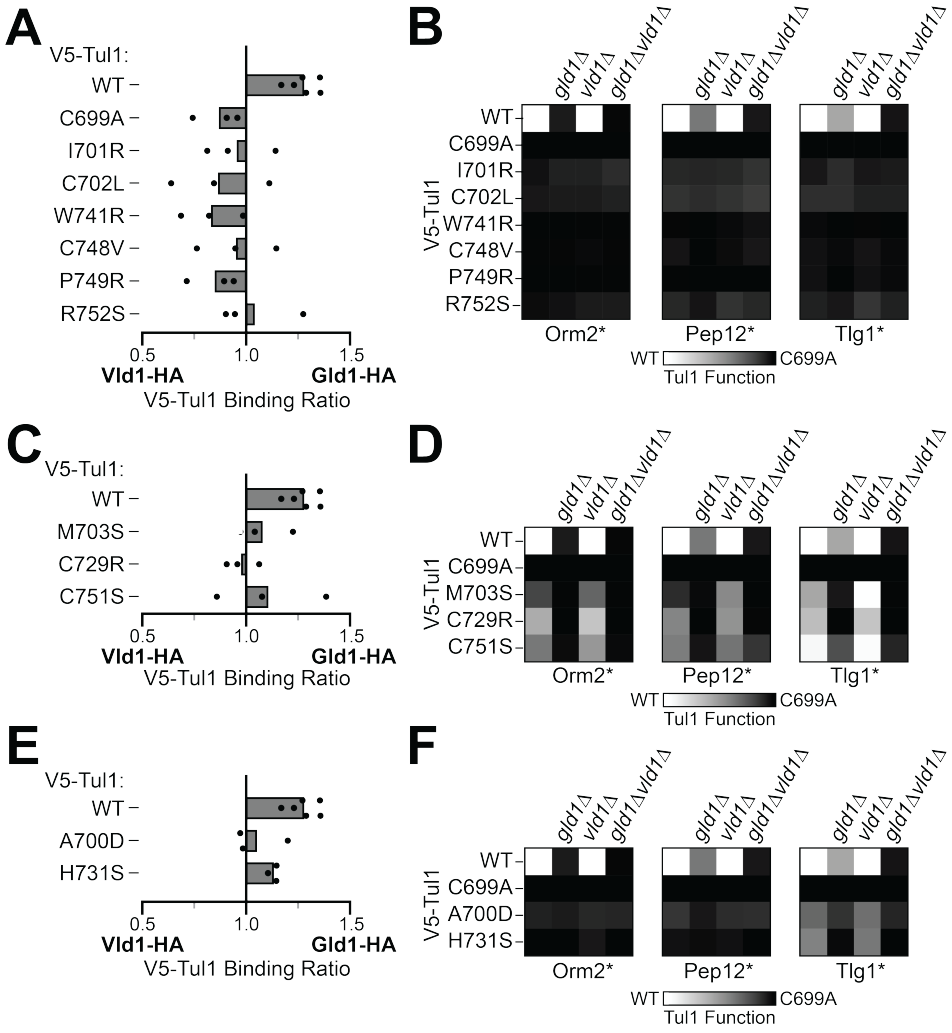

Figure 2.6: Gld1 is required for Tul1 complex function.

Figure 2.6: Gld1 is required for Tul1 complex function.

A) The indicated Tul1 variants were immunoprecipitated from strains containing Gld1-HA and Vld1-HA. The co-immunoprecipitated Gld1-HA and Vld1-HA were quantified by immunoblotting and the ratios Vld1 to Gld1 were plotted for each replicate.
B) Degradation of the model substrates Orm2*-RFP, GFP-Pep12*, and GFP-Tlg1* were followed by flow cytometry. The heatmap depicts the function of the indicated Tul1 variant relative to wild-type Tul1 in *tul1*Δ cells (in white) and inactive Tul1(C699A) in the indicated strain (in black).
C) As in (A) but with Tul1 RING variants that are hypomorphic.
D) As in (B) but with Tul1 RING variants that are hypomorphic.
E) As in (A) but with Tul1 RING variants that have altered substrate specificity.
F) As in (B) but with Tul1 RING variants that have altered substrate specificity.

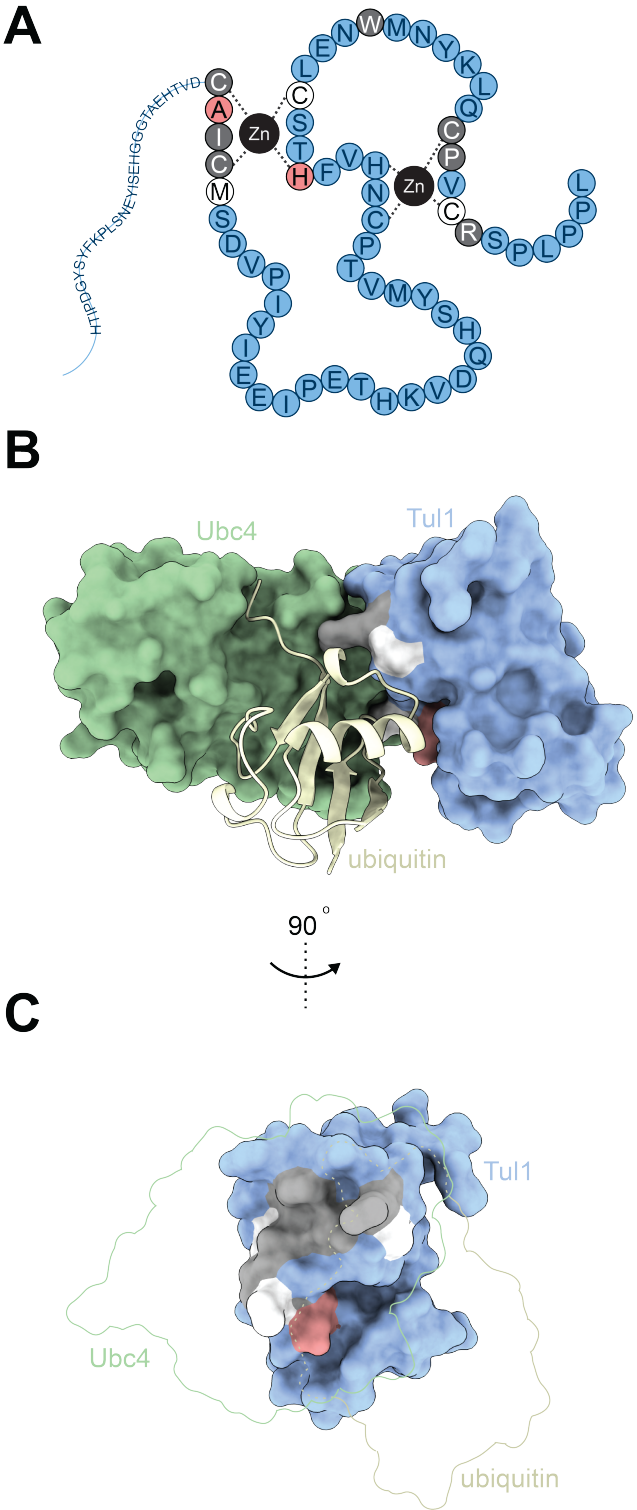

Figure 2.7: Tul1 RING domain substitutions cluster around the E2 interaction interface.

Figure 2.7: Tul1 RING domain substitutions cluster around the E2 interaction interface.

A) Schematic of the Tul1 RING domain highlighting the residues involved in zinc ion coordination. Substitutions of residues altering Tul1 function are highlighted in grey (for nonfunctional), white (for hypomorphic), and pink (for altered specificity).
B) AlphaFold multimer predicted model of the Tul1 RING domain (blue) with the ubiquitin conjugating E2 enzyme Ubc4 (green), and ubiquitin (tan). The coloring scheme follows (A).
C) As in (B) but rotated by 90˚ and the Ubc4 and ubiquitin protein shown only as outlines.

2.11 Supplemental Figures

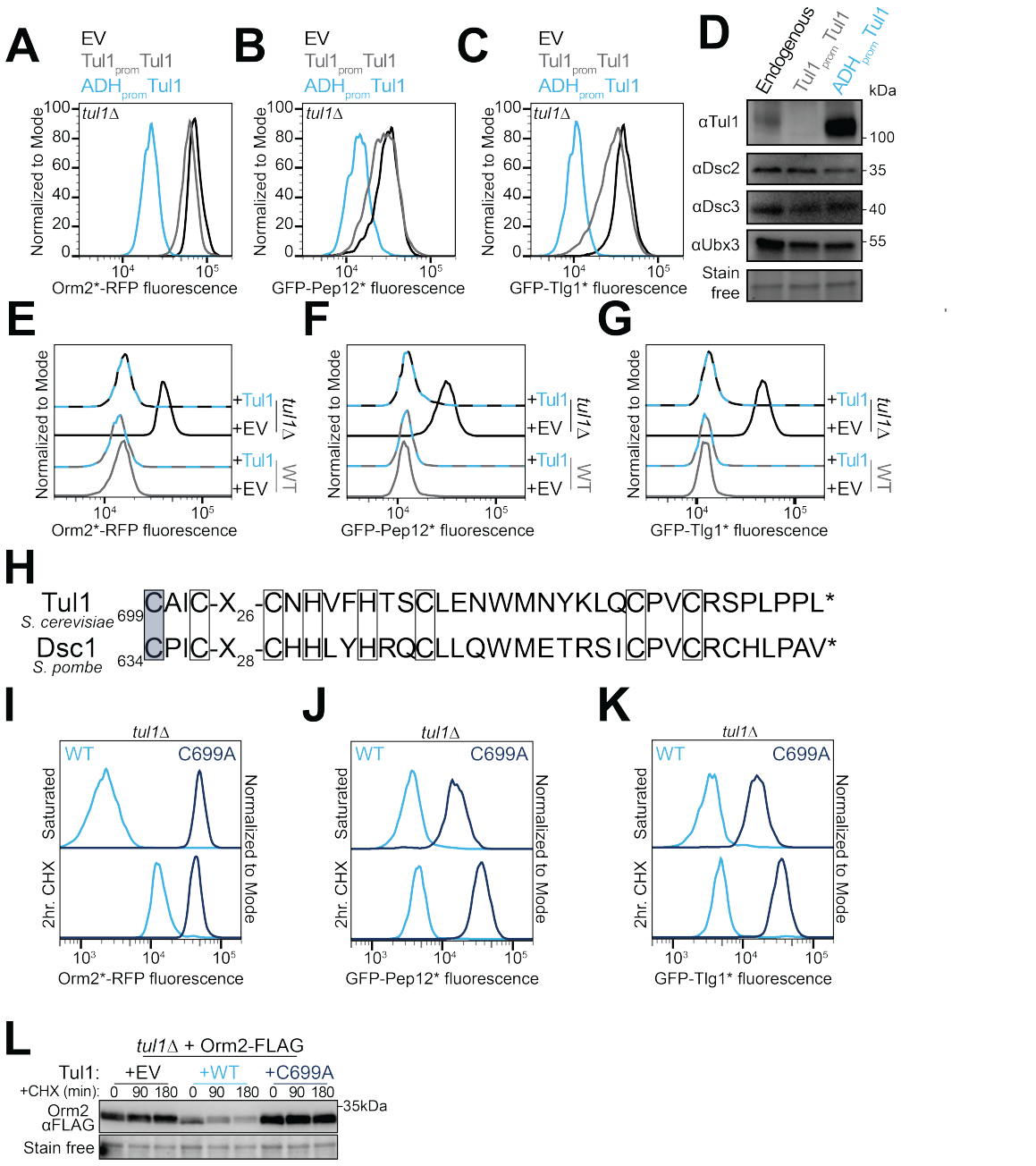

Supplemental Figure 2.1: Development of methods to monitor Golgi-localized Tul1 function.

Figure S2.1: Development of methods to monitor Golgi-localized Tul1 function.

A) Degradation of the model substrate Orm2*-RFP was followed by flow cytometry after a two-hour treatment with 50µg/mL cycloheximide. Experiments were performed in *tul1*Δ cells complemented with an empty vector (EV, black solid line), wild-type Tul1 expressed from its endogenous promoter ($Tul1_{prom}$-Tul1, grey solid line), or from the ADH1 promoter (ADH_{prom}-Tul1, light blue solid line) integrated at the exogenous *his3* locus.
B) As in (A) but with vacuolar model substrate GFP-Pep12*.
C) As in (A) but with vacuolar model substrate GFP-Tlg1*.
D) Tul1, Dsc2, Dsc3, and Ubx3 to protein expression was tested at steady state using previously-developed antibodies[25] in wild-type cells (Endogenous), *tul1*Δ cells exogenously expressing Tul1 from its native promoter at the *his3* locus ($Tul1_{prom}$-Tul1) or *tul1*Δ cells exogenously expressing Tul1 from the ADH1 promoter at the HIS3 locus (ADH_{prom}-Tul1). Stain free technology was used to follow total protein levels and was used as a loading control.
E) As in (A), but in wild-type cells and *tul1*Δ cells, containing an empty vector control (EV, solid lines) or Tul1 expressed from the ADH1 promoter at the *his3* locus (+Tul1, dashed lines).
F) As in (E) but with GFP-Pep12*
G) As in (E) but with GFP-Tlg1*
H) Alignment of the *S. cerevisiae* Tul1 RING domain with the *S. pombe* Dsc1 RING domain. The zinc coordinating residues are boxed.
I) Degradation of the model substrates Orm2*-RFP was followed by flow cytometry for cells grown for 40 hours to saturation, or treated with cycloheximide for two hours. Experiments were performed in *tul1*Δ cells complemented with wild-type Tul1 (light blue line) and inactive Tul1(C699A) (dark blue line).
J) As in (I) but with GFP-Pep12*.
K) As in (I) but with GFP-Tlg1*.
L) Degradation of the model substrate Orm2-3xFlag (Orm2-Flag) was followed by immunoblotting after cycloheximide treatment for the indicated times. Orm2-Flag was expressed in *tul1*Δ cells complemented with either an empty vector (EV), wild-type Tul1 (WT), or inactive Tul1 variant (C699A). Total protein was visualized by stain-free technology and used as a loading control.

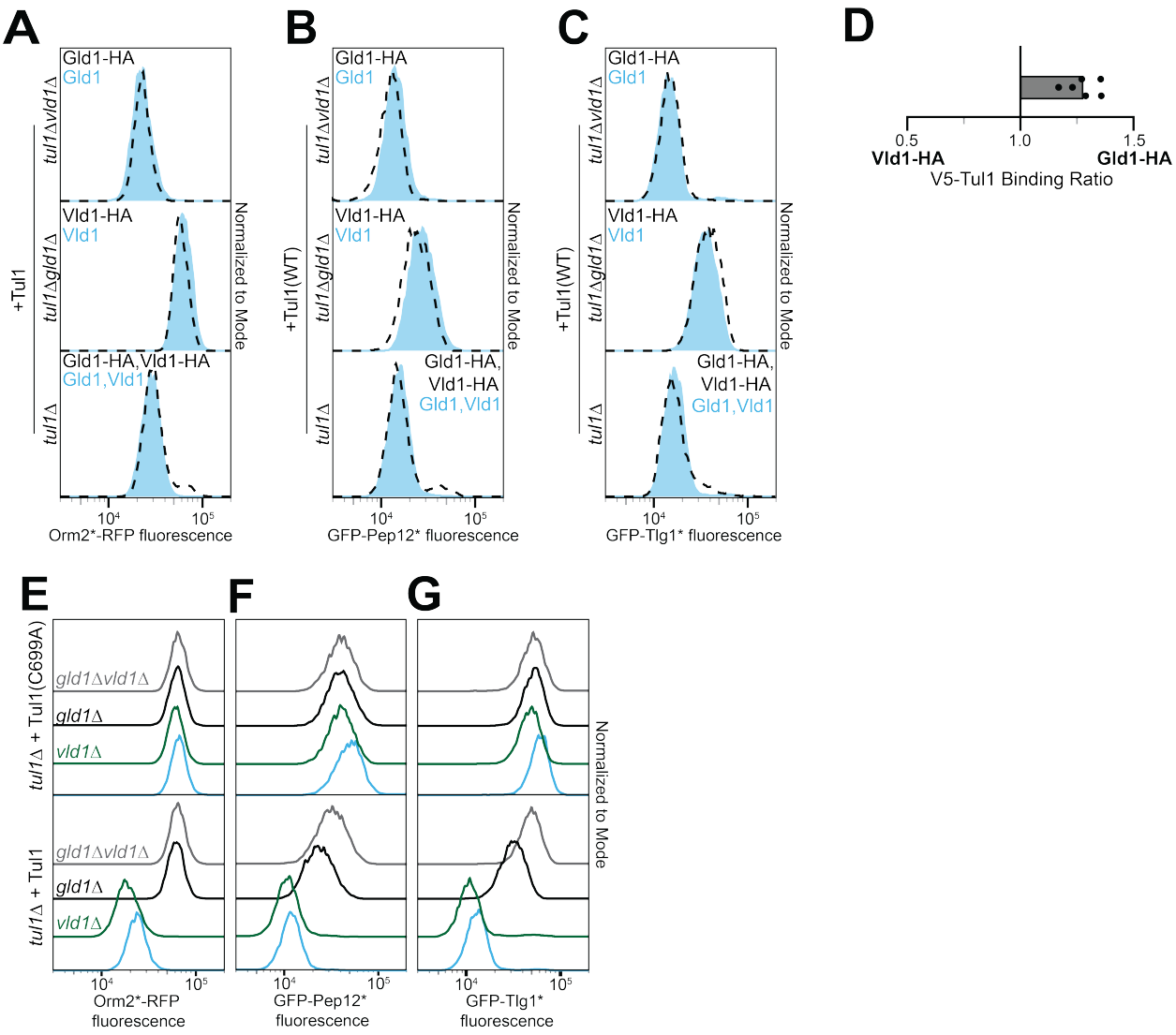

Supplemental Figure 2.2: Tul1 complex assembly is not required for Tul1 substrate interaction.

Figure S2.2: Tul1 complex assembly is not required for Tul1 substrate interaction.

A) Flow cytometry of the model proteasomal substrate Orm2*-RFP after 2-hour cycloheximide treatment of *tul1*Δ cells complemented with Tul1 and containing either untagged endogenous Gld1 and Vld1 (Gld1/Vld1, blue filled histogram) or endogenously tagged 3xHA-Gld1 and 3xHA-Vld1 (Gld1-HA/Vld1-HA, black dotted line), or *tul1*Δ*gld1*Δ complemented with Tul1 and containing untagged Vld1 (Vld1, blue histogram) or endogenously tagged 3xHA-Vld1 (HA-Vld1, black dotted line), or *tul1*Δ*vld1*Δ cells complemented with Tul1 and containing untagged Gld1 (Gld1, blue histogram) or endogenously tagged 3xHA-Gld1 (HA-Gld1, black dotted line).
B) As in (A) but with vacuolar model substrate GFP-Pep12*.
C) As in (A) but with vacuolar model substrate GFP-Tlg1*.
D) Wild-type V5-Tul1 was immunoprecipitated from strains containing Gld1-HA and Vld1-HA. The co-immunoprecipitated Gld1-HA and Vld1-HA were quantified by immunoblotting and the ratios Vld1 to Gld1 were plotted for each replicate.
E) Orm2*-RFP fluorescence intensity after 2-hour cycloheximide chase in *tul1*Δ cells (light blue solid line) complemented with either wild-type Tul1 (*tul1*Δ + Tul1) or the nonfunctional RING mutant (*tul1*Δ + Tul1 (C699A)), which are also expressed in cells with additional genetic deletions of localization signal(s) of Gld1 (*gld1*Δ, green solid line), Vld1 (*vld1*Δ, black solid line), or both Gld1 and Vld1 (*gld1*Δ*vld1*Δ, grey solid line).
F) As in (E) but with GFP-Pep12*.
G) As in (F) but with GFP-Tlg1*.

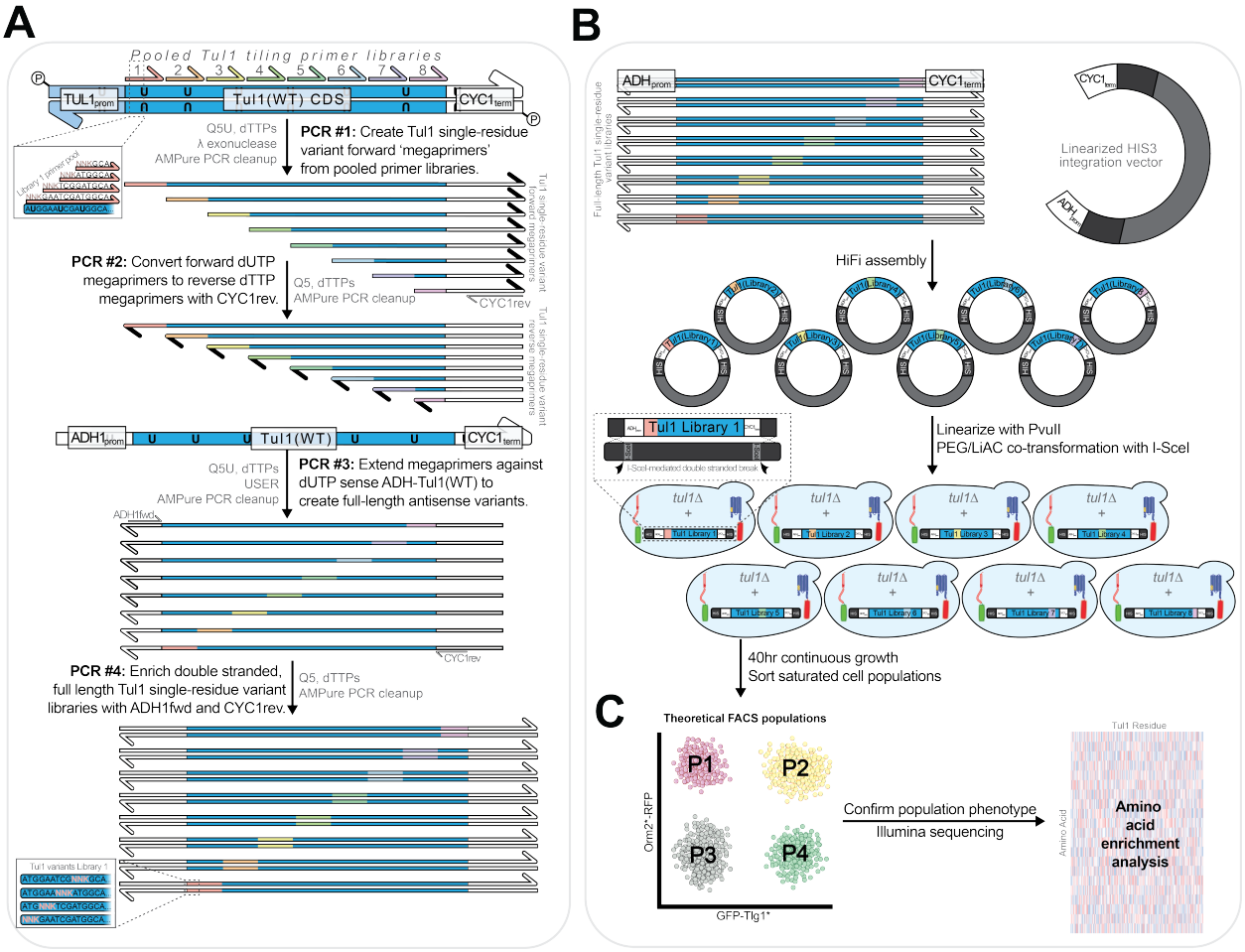

Supplemental Figure 2.3: Deep mutational scanning of the Tul1 ubiquitin ligase.

Figure S2.3: Deep mutational scanning of the Tul1 ubiquitin ligase.

A) Schematic of the tiling primer mutagenesis strategy for Tul1 library generation.
B) Schematic of the strategy for cloning the Tul1 libraries and high-efficiency genomic integration.
C) Theoretical FACS scatter plot schematic with Orm2*-RFP fluorescence intensity on the y-axis and GFP-Tlg1* fluorescence intensity on the x-axis. Libraries of cells generated in (A) and (B) would be predicted to fall within one of four groups based on Tul1 variant function. The predicted activity phenotypes would be: unable to degrade proteasomal substrates (P1), completely nonfunctional (P2), wildtype-like and functional (P3), and unable to degrade vacuolar substrates (P4).

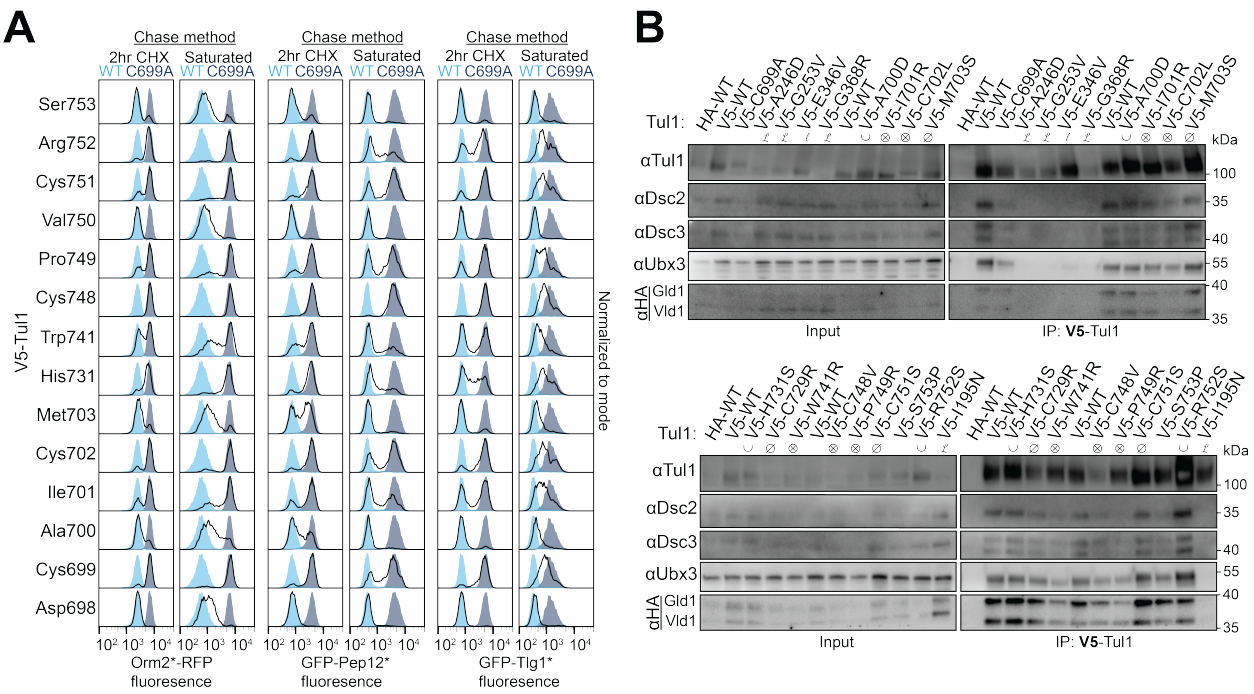

Supplemental Figure 2.4: Single-residue mutations in the Tul1-RING domain disrupt Golgi-localized Tul1 substrate degradation.

Figure S2.4: Single-residue mutations in the Tul1-RING domain disrupt Golgi-localized Tul1 substrate degradation.

A) Degradation of the model substrates (Orm2*-RFP, GFP-Pep12*, and GFP-Tlg1*) were followed by flow cytometry following cycloheximide treatment for 2 hours or growth to saturation. The experiments were performed in *tul1*Δ cells, with the function of the indicated Tul1 single-residue variant libraries covering all possible substitutions (black traces) relative to wild-type Tul1 in *tul1*Δ cells (light blue fill) or inactive Tul1(C699A) in the indicated strain (gray fill).

B) Co-immunoprecipitation of the Tul1 complex was performed from *tul1*Δ cells expressing Gld1-HA and Vld1-HA, and either HA-Tul1, V5-Tul1, or the indicated V5-Tul1 variants (⊗ marking nonfunctional RING mutants, ∅ marking hypomorphic RING mutants, ∪ marking proteasomal-nonfunctional RING mutants, L marking nonfunctional lumenal mutations and l marking hypomorphic lumenal mutants. Inputs were loaded at 5% and proteins were detected by immunoblotting with α-Tul1, α-Dsc2, α-Dsc3, α-Ubx3, or α-HA antibodies.

2.12 Tables

Table 2.1: Plasmids used in this study.

Plasmid name	Backbone, features	Reference
pRB903	Empty HIS3_Integrating_plasmid	Hwang, J., *et al. (2023*)
pRB916	Empty URA3_Integrating_plasmid	Hwang, J., *et al. (2023*)
	pFA6_Nat_NT2	Janke, C., *et al. (2004)*
	pFA6_hph_NT1	Janke, C., *et al. (2004)*
pRB824	pFA6_3xHA_TDH1term_NatNT2	This study
pRB835	pFAG_3xHA_TDH1term_hygNT1	This study
pRB953	Empty HIS3_Integrating_plasmid_KanR	This study
pDD66	pDD66_pRB905_Tul1prom_Tul1_cyc1	This study
pDD69	pDD69_pRB905_ADH_Tul1_cyc1	This study
pDD169	pDD169_pRB903_ADH_Tul1(C699A)_cyc1	This study
pDD187	pDD187_pRB916_GPD_Orm2(S46,47,48D)-mScarlet-I(BGP)_cyc1_CCW12_SEP-Pep12D_pgk1	This study
pDD188	pDD188_pRB916_GPD_Orm2(S46,47,48D)-mScarlet-I(BGP)_cyc1_CCW12_SEP-Tlg1LL_pgk1	This study
pDD189	pDD189_pRB916_Orm2prom_Orm2-3XFLAG_cyc1	This study
pDD204	pDD204_pRB903_ADH_3xV5-Tul1_cyc1	This study
pDD205	pDD205_pRB903_ADH_3xHA-Tul1_cyc1	This study
pDD214	pDD214_pRB903_ADH-3xV5_Tul1(C699A)_cyc1	This study
pDD222	pDD222_pRB903_ADH-3xV5_Tul1(C751S)_cyc1	This study
pDD228	pDD228_pRB953_ADHlong_EcoRV_cyc1	This study
pDD243	pDD243_pRB953_ADHlong_Tul1(125var)_cyc1	This study
pDD244	pDD244_pRB953_ADHlong_Tul1(137var)_cyc1	This study
pDD245	pDD245_pRB953_ADHlong_Tul1(138var)_cyc1	This study
pDD246	pDD246_pRB953_ADHlong_Tul1(195var)_cyc1	This study
pDD247	pDD247_pRB953_ADHlong_Tul1(229var)_cyc1	This study
pDD248	pDD248_pRB953_ADHlong_Tul1(246var)_cyc1	This study
pDD249	pDD249_pRB953_ADHlong_Tul1(247var)_cyc1	This study
pDD250	pDD250_pRB953_ADHlong_Tul1(248var)_cyc1	This study
pDD251	pDD251_pRB953_ADHlong_Tul1(249var)_cyc1	This study
pDD252	pDD252_pRB953_ADHlong_Tul1(250var)_cyc1	This study
pDD253	pDD253_pRB953_ADHlong_Tul1(251var)_cyc1	This study
pDD254	pDD254_pRB953_ADHlong_Tul1(252var)_cyc1	This study
pDD255	pDD255_pRB953_ADHlong_Tul1(253var)_cyc1	This study
pDD256	pDD256_pRB953_ADHlong_Tul1(254var)_cyc1	This study

pDD257	pDD257_pRB953_ADHlong_Tul1(255var)_cyc1	This study
pDD258	pDD258_pRB953_ADHlong_Tul1(325var)_cyc1	This study
pDD259	pDD259_pRB953_ADHlong_Tul1(326var)_cyc1	This study
pDD260	pDD260_pRB953_ADHlong_Tul1(327var)_cyc1	This study
pDD261	pDD261_pRB953_ADHlong_Tul1(328var)_cyc1	This study
pDD262	pDD262_pRB953_ADHlong_Tul1(329var)_cyc1	This study
pDD263	pDD263_pRB953_ADHlong_Tul1(346var)_cyc1	This study
pDD264	pDD264_pRB953_ADHlong_Tul1(368var)_cyc1	This study
pDD265	pDD265_pRB953_ADHlong_Tul1(369var)_cyc1	This study
pDD266	pDD266_pRB953_ADHlong_Tul1(370var)_cyc1	This study
pDD267	pDD267_pRB953_ADHlong_Tul1(397var)_cyc1	This study
pDD268	pDD268_pRB953_ADHlong_Tul1(398var)_cyc1	This study
pDD269	pDD269_pRB953_ADHlong_Tul1(399var)_cyc1	This study
pDD270	pDD270_pRB953_ADHlong_Tul1(400var)_cyc1	This study
pDD271	pDD271_pRB953_ADHlong_Tul1(401var)_cyc1	This study
pDD272	pDD272_pRB953_ADHlong_Tul1(402var)_cyc1	This study
pDD273	pDD273_pRB953_ADHlong_Tul1(403var)_cyc1	This study
pDD274	pDD274_pRB953_ADHlong_Tul1(404var)_cyc1	This study
pDD275	pDD275_pRB953_ADHlong_Tul1(405var)_cyc1	This study
pDD276	pDD276_pRB953_ADHlong_Tul1(406var)_cyc1	This study
pDD277	pDD277_pRB953_ADHlong_Tul1(505var)_cyc1	This study
pDD278	pDD278_pRB953_ADHlong_Tul1(506var)_cyc1	This study
pDD279	pDD279_pRB953_ADHlong_Tul1(507var)_cyc1	This study
pDD280	pDD280_pRB953_ADHlong_Tul1(508var)_cyc1	This study
pDD281	pDD281_pRB953_ADHlong_Tul1(509var)_cyc1	This study
pDD282	pDD282_pRB953_ADHlong_Tul1(510var)_cyc1	This study
pDD283	pDD283_pRB953_ADHlong_Tul1(511var)_cyc1	This study
pDD284	pDD284_pRB953_ADHlong_Tul1(512var)_cyc1	This study
pDD285	pDD285_pRB953_ADHlong_Tul1(513var)_cyc1	This study
pDD286	pDD286_pRB953_ADHlong_Tul1(514var)_cyc1	This study
pDD287	pDD287_pRB953_ADHlong_Tul1(698var)_cyc1	This study
pDD288	pDD288_pRB953_ADHlong_Tul1(699var)_cyc1	This study
pDD289	pDD289_pRB953_ADHlong_Tul1(700var)_cyc1	This study
pDD290	pDD290_pRB953_ADHlong_Tul1(701var)_cyc1	This study
pDD291	pDD291_pRB953_ADHlong_Tul1(702var)_cyc1	This study
pDD292	pDD292_pRB953_ADHlong_Tul1(703var)_cyc1	This study
pDD293	pDD293_pRB953_ADHlong_Tul1(731var)_cyc1	This study
pDD294	pDD294_pRB953_ADHlong_Tul1(737var)_cyc1	This study
pDD295	pDD295_pRB953_ADHlong_Tul1(741var)_cyc1	This study

pDD296	pDD296_pRB953_ADHlong_Tul1(747var)_cyc1	This study
pDD297	pDD297_pRB953_ADHlong_Tul1(748var)_cyc1	This study
pDD298	pDD298_pRB953_ADHlong_Tul1(749var)_cyc1	This study
pDD299	pDD299_pRB953_ADHlong_Tul1(750var)_cyc1	This study
pDD300	pDD300_pRB953_ADHlong_Tul1(751var)_cyc1	This study
pDD301	pDD301_pRB953_ADHlong_Tul1(752var)_cyc1	This study
pDD302	pDD302_pRB953_ADHlong_Tul1(753var)_cyc1	This study
pDD317	pDD317_pRB903_ADHlong_3xV5_Tul1(A700D)_cyc1	This study
pDD320	pDD320_pRB903_ADHlong_3xV5_Tul1(H731S)_cyc1	This study
pDD322	pDD322_pRB903_ADHlong_3xV5_Tul1(R752S)_cyc1	This study
pDD330	pDD330_pRB916_Orm2prom_Orm2-3xHA_cyc1	This study
pDD331	pDD331_pRB916_ADH_3xFLAG-Pep12(D)_pgk1	This study
pDD332	pDD332_pRB916_ADH_3xFLAG-Tlg1(LL)_pgk1	This study
pDD333	pDD333_pRB916_ADH_3xHA-Pep12(D)_pgk1	This study
pDD334	pDD334_pRB916_ADH_3xHA-Tlg1(LL)_pgk1	This study
pDD335	pDD335_pRB916_CCW12_Orm2(S46,47,48D)-mScarlet-I(BGP)_pgk1	This study
pDD336	pDD336_pRB916_GPD_SEP-Pep12(D)_cyc1	This study
pDD337	pDD337_pRB916_GPD_SEP-Tlg1(LL)_cyc1	This study
pDD340	pDD340_pRB903_ADH_3xV5-Tul1(I195N)_cyc1	This study
pDD341	pDD341_pRB903_ADH_3xV5-Tul1(A246D)_cyc1	This study
pDD343	pDD343_pRB903_ADH_3xV5-Tul1(G253V)_cyc1	This study
pDD345	pDD345_pRB903_ADH_3xV5-Tul1(E346V)_cyc1	This study
pDD346	pDD346_pRB903_ADH_3xV5-Tul1(G368R)_cyc1	This study
pDD348	pDD348_pRB903_ADH_3xV5-Tul1(I701R)_cyc1	This study
pDD349	pDD349_pRB903_ADH_3xV5-Tul1(C702L)_cyc1	This study
pDD350	pDD350_pRB903_ADH_3xV5-Tul1(M703S)_cyc1	This study
pDD351	pDD351_pRB903_ADH_3xV5-Tul1(T727G)_cyc1	This study
pDD352	pDD352_pRB903_ADH_3xV5-Tul1(C729R)_cyc1	This study
pDD354	pDD354_pRB903_ADH_3xV5-Tul1(W741R)_cyc1	This study
pDD355	pDD355_pRB903_ADH_3xV5-Tul1(Q747V)_cyc1	This study
pDD356	pDD356_pRB903_ADH_3xV5-Tul1(C748V)_cyc1	This study
pDD357	pDD357_pRB903_ADH_3xV5-Tul1(P749R)_cyc1	This study
pDD359	pDD359_pRB903_ADH_3xV5-Tul1(S753P)_cyc1	This study

Table 2.2: Yeast strains used in this study.

Strain name	Genotype	Source
BY4742	MATα *his3Δ1 leu2Δ0 lys2Δ0 ura3Δ0*	Dharmacon
tul1Δ	MATα *his3Δ1 leu2Δ0 lys2Δ0 ura3Δ tul1::kanR*	Dharmacon
dsc2Δ (yRB503)	MATα *his3Δ1 leu2Δ0 lys2Δ0 ura3Δ0 dsc2::kanR*	This study
dsc3Δ (yRB516)	MATα *his3Δ1 leu2Δ0 lys2Δ0 ura3Δ0 dsc3::kanR*	This study
ubx3Δ (yRB514)	MATα *his3Δ1 leu2Δ0 lys2Δ0 ura3Δ0 ubx3::kanR*	This study
*gld1*Δ (yRB510)	MATα *his3Δ1 leu2Δ0 lys2Δ0 ura3Δ0 gld1::kanR*	This study
*vld1*Δ (yRB512)	MATα *his3Δ1 leu2Δ0 lys2Δ0 ura3Δ0 vld1::kanR*	This study
*gld1*Δ*vld1*Δ (yRB518A)	MATα *his3Δ1 leu2Δ0 lys2Δ0 ura3Δ0 gld1::kanR vld1::kanR*	This study
*tul1*Δ with SceI sites at HIS3 (yRB508)	MATα *his3Δ0::I-sceI_HygB_NT3_I-SceI leu2Δ0 lys2Δ0 ura3Δ0 tul1Δ::kanMX*	This study
*tul1*Δ*dsc2Δ* (yDD92)	MATα *his3Δ1 leu2Δ0 lys2Δ0 ura3Δ0 dsc2::kanR tul1:: hphNT1*	This study
*tul1*Δ*dsc3Δ* (yDD93)	MATα *his3Δ1 leu2Δ0 lys2Δ0 ura3Δ0 dsc3::kanR tul1:: hphNT1*	This study
*tul1*Δ*ubx3Δ* (yDD94)	MATα *his3Δ1 leu2Δ0 lys2Δ0 ura3Δ0 ubx3::kanR tul1:: hphNT1*	This study
*tul1*Δ*gld1*Δ (yDD95)	MATα *his3Δ1 leu2Δ0 lys2Δ0 ura3Δ0 gld1::kanR tul1:: hphNT1*	This study
*tul1*Δ*vld1*Δ (yDD96)	MATα *his3Δ1 leu2Δ0 lys2Δ0 ura3Δ0 vld1::kanR tul1:: hphNT1*	This study
*tul1*Δ*gld1*Δ*vld1*Δ (yDD85)	MATα *his3Δ1 leu2Δ0 lys2Δ0 ura3Δ0 gld1::kanR vld1::kanR tul1:: hphNT1*	This study
tul1Δ, Gld1-HA, Vld1-HA (yDD68)	MATα *his3Δ1 leu2Δ0 lys2Δ0 ura3Δ tul1::kanR gld1-HA::hphNT1 vld1-3xHA::Nat*	This study
dsc2Δ, Gld1-HA, Vld1-HA (yDD69)	MATα *his3Δ1 leu2Δ0 lys2Δ0 ura3Δ0 dsc2::kanR gld1-HA::hphNT1 vld1-3xHA::Nat*	This study
dsc3Δ, Gld1-HA, Vld1-HA (yDD70)	MATα *his3Δ1 leu2Δ0 lys2Δ0 ura3Δ0 dsc3::kanR gld1-HA::hphNT1 vld1-3xHA::Nat*	This study
ubx3Δ, Gld1-HA, Vld1-HA (yDD71)	MATα *his3Δ1 leu2Δ0 lys2Δ0 ura3Δ0 ubx3::kanR gld1-HA::hphNT1 vld1-3xHA::Nat*	This study
*gld1*Δ, Gld1-HA, Vld1-HA (yDD72)	MATα *his3Δ1 leu2Δ0 lys2Δ0 ura3Δ0 gld1::kanR vld1-3xHA::hphNT1*	This study

*vld1*Δ, Gld1-HA, Vld1-HA (yDD73)	MATα *his3Δ1 leu2Δ0 lys2Δ0 ura3Δ0 vld1::kanR gld1-HA::hphNT1*	This study

Table 2.3: Antibodies used in this study.

Antibody	Source
THE DYKDDDDK Tag Antibody, mAb, Mouse	GenScript
Anti-HA High Affinity; Rat monoclonal antibody (clone 3F10)	Roche
THE V5 Tag Antibody, mAb, Mouse	GenScript
Goat Anti-Rat IgG, Whole Ab ECL Antibody, HRP Conjugated	Cytiva
Goat anti-Mouse IgG (H+L) Highly Cross-Adsorbed Secondary Antibody, Alexa Fluor Plus 800	Thermo Fisher Scientific
Sheep Anti-Mouse IgG - Horseradish Peroxidase	Cytiva
Donkey anti-Rat IgG (H+L) Cross-Adsorbed Secondary Antibody, DyLight 550	Invitrogen
Goat anti-Rabbit IgG (H+L) Secondary Antibody, DyLight 488	Invitrogen
Rabbit, anti-Tul1	Tong, Z., *et al., (2014)*
Rabbit, anti-Dsc2	Tong, Z., *et al., (2014)*
Rabbit, anti-Dsc3	Tong, Z., *et al., (2014)*
Rabbit, anti-Ubx3	Tong, Z., *et al., (2014)*

Table 2.4: Primers used in this study.

Name	Description	Sequence
prDD1	prDD1_SacII-insert-Gibson-KpnI-overhang	CGACTCACTATAGGGCGAATTGGGTACCCCGCGGGCCGCAAATTAAAGCCTTCGAGCGTC
prDD2	prDD2_SacII-insert-Gibson-Kpn-I-overhang	GACGCTCGAAGGCTTTAATTTGCGGCCCGCGGGGTACCCAATTCGCCCTATAGTGAGTCG
prDD3	prDD3_Tul1-SacI/SacII-T4-ligase-insert	GACCCGCGGGCCGCAAATTAAAGCCTTCGAG
prDD4	prDD4_ADHprom-3'F-seq	CTCGTTCCCTTTCTTCCTTG
prDD5	prDD5_sfpHluorin-3'F-seq	GCTGCTGGGATTACACATGG
prDD6	prDD6_FDP-5'F-seq	GCAGGTATACTAAACTCAC
prDD11	prDD11_mScarlet-Iamp_F	GCGGCCGCGGAATTCACCGGTCCATGGTCTCCAAGGGT
prDD12	prDD12_mScarlet-Iamp_R	ACTAGTCTCGAGGGAACCCTTATATAATTCGTCCATGCCTCC
prDD13	prDD13_ADH_F	CCTCGTCATTGTTCTCGTTCCC
prDD14	prDD14_SEP+322_F	CAAGAGCGGAGGTCAAATTTGAGG
prDD15	prDD15_mScar-link_F	CGGTTCAATGGTCTCCAAG
prDD16	prDD16_mScar+326_F	CAAGACACATCTCTGGAGGAC
prDD19	prDD19_-447bpTul1_F	GAACATTGAAGGTGCGGCTTG
prDD20	prDD20_+456bpTul1_R	GCCGGCTCATAGAATCTGGG
prDD21	prDD21_SEP-SpeI-insert	ACTAGTCAATTTATATAACTCGTCCATACCATGAGTG
prDD22	prDD22_Kandefconfirm_F	ATTATCGCGAGCCCATTTATACC
prDD49	prDD49_SEP-SpeI-insert_R2	CTTCCGACATACTAGtCAATTTATATAACTCGTCCATACCATGAGTG
prDD50	prDD50_Tul1del_F	GTTGCTGGTTAAATCAGATCTATTCCGTCTGGAACACGGTTCTTTGAAGTTAGACCCATCCGGATCCCCGGGTTAATTAA
prDD51	prDD51_Tul1del_R	CGGTATCTTGGATCTTGAATACAAATACAGTATATAGTTCTTAGGATCAAGAGATGCTATCGATGAATTCGAGCTCGTTTAAAC
prDD52	prDD52_pDD5-Tul1amp_F	AGATGTAGGTGTTGGCACC
prDD53	prDD53_pDD5-Tul1amp_R	TTAGCAGCCGGATCTTCTAGA
prDD60	prDD60_+202bp-natMX6_R	TCCTCCCCGTCGTCCGATT
prDD61	prDD61_+236-hphMX6_R	TCGCTGAATTCCCCAATGT
prDD62	prDD62_+196bp-kanMX6_R	AGCCAGTTTAGTCTGACCATCT

prDD63	prDD63_-150bp-Tul1del_F	TTTCCTTTGGCGGGGTAAGGGTCTGTGAACTTTAGGGAAATAGAATAAACGTAAGTTAAACGGATCCCCGGGTTAATTAAGG
prDD64	prDD64_+150bp-Tul1del_R	AAAAGGGTAACACTAAAAACCCTTGTGAATTATCCTAAGTCTAGTTTGCCTATTGTATATCGATGAATTCGAGCTCGTTTAAAC
prDD77	prDD77_-16bp-cyc1_R	GGGCGTGAATGTAAGCGTGAC
prDD88	prDD88_GPDend_F	CACCAGAACTTAGTTTCGACGG
prDD89	prDD89_mScarlet-Iend-SacI-XhoI_R	CTAATTACATGACTCGAGGTCGACGGAACCCTTATATAATTCGTCCATG
prDD90	prDD90_mNeonGreenend-SacI-XhoI_R	CTAATTACATGACTCGAGGTCGACTTGTACAATTCGTCCATACCCAT
prDD99	prDD99_3xHAseq_F	ATGTACCCATACGATGTTCCTG
prDD100	prDD100_3xHAseq_R	AGCGTAATCTGGAACGTCAT
prDD101	prDD101_3xFLAG-SalI-Gibson_F	TAGGTCACCATTACCTCCGTTGTAGGGATCCGACTACAAAGACCATGACGG
prDD102	prDD102_3xHA-SalI-Gibson_F	TAGGTCACCATTACCTCCGTTGTAGGGTTACCCATACGATGTTCCTGACT
prDD103	prDD103_3xHA-SalI-Gibson_R	ACTAATTACATGACTCGAGGTCGACCTAAGCGTAATCTGGAACGTCAT
prDD110	prDD110_CCW12-SEP-Pep12D_F	ATAGGGCGAATTGGAGCTCCACCGCGGTGGCGGCCGCTCTAGACACCCATGAACCACACG
prDD111	prDD111_CCW12-SEP-Pep12D_R	CCTCGAGGTCGACGGTATCGATAAGCTTGATATCGAATTCAACGCAGAATTTTCGAGTTA
prDD112	prDD112_GPD-Orm2-mScarlet-I_F	AATTGGAGCTCCACCGCGGTGGCGGCCGCTCTAGATCATTATCAATACTCGCCATTTCAA
prDD113	prDD113_GPD-Orm2-mScarlet-I_R	GTACCGGGCCCCCCCTCGAGGTCGACGGTATCGATAAGCTTGCAAATTAAAGCCTTCGAG
prDD114	prDD114_pDD40+NheI-site_F	TCGAAGGCTTTAATTTGCAAGCTTATCGATACCGTCGACCTCGCTAGCGGGGGGCCCGGT
prDD115	prDD115_pDD40+NheI-site_R	ACCGGGCCCCCCGCTAGCGAGGTCGACGGTATCGATAAGCTTGCAAATTAAAGCCTTCGA
prDD116	prDD116_SpeI-Tlg1_F	ATATAAATTGACTAGTATGAACAACAGTGAAGATCCG
prDD117	prDD117_Tlg1-BamHI_R	CGAGGTCGACGGATCCTCAAGCAATGAATGCCAA
prDD118	prDD118_Tlg1LL_F	GAAAAAAATAAAGAAAAATACGACGATTTGTTGATAGGACTTCTTATTGTCG

prDD119	prDD119_Tlg1LL_R	CGACAATAAGAAGTCCTATCAACAAAT CGTCGTATTTTTCTTTATTTTTTTC
prDD122	prDD122_Orm2D_F	GCCGACCATAGGAGAAGACGGTCATCC AGCGTAATATCACATGTGGAAC
prDD123	prDD123_Orm2D_R	GTTCCACATGTGATATTACGCTGGATGA CCGTCTTCTCCTATGGTCGGC
prDD129	prDD129_Tul1seq_F1prom	CAAGTTCAATCTCGTTTGTTAC
prDD130	prDD130_Tul1seq_F2	GACAATAATAATTACTTAAGGAGA
prDD131	prDD131_Tul1seq_F3	GCCACTTTGTACTTTGTCGCAGCT
prDD132	prDD132_Tul1seq_F4	GAGCATGGTGGTGGAACTGCTGA
prDD138 *	prDD138_-20bp-CYC1_R	GAGGGCGTGAATGTAAGCG
prDD139	prDD139_M13rev_F	GGCGTAATCATGGTCATAGCTG
prDD140	prDD140_Tul1prom-amp_F	CGGGGTAAGGGTCTGTGAAC
prDD141	prDD141_nextera-adapt-Tul1_F	TCGTCGGCAGCGTCAGATGTGTATAAG AGACAGGTGAGTTTTCAGCATGGCG
prDD142	prDD142_nextera-adapt-Tul1_R	CTGTCTCTTATACACATCTCCGAGCCCA CGAGACCCAAAATTCATCAACGAGTTC C
prDD143 *	prDD143_-30bp-Tul1amp_F	GGAAAGTCCTACAGCAAAAGAGG
prDD144	prDD144_pRS313-Tul1promamp_F	AATACGACTCACTATAGGGCGAATTGG AGCTCCCGTTTTGGTCCAAACCC
prDD145	prDD145_SfoI-Tul1promamp_R	TTGTCTAACTCCTTCCTTTTCGGTTAGA GCGGCGCCAAAGGAAAATCTCTATATA TACTG
prDD146	prDD146_SfoI-CYC1amp_F	GCTTCAGTATATATAGAGATTTTCCTTT GGCGCCGCTCTAACCGAAAAGG
prDD147	prDD147_CYC1amp-pRS313_R	AACAAAAGCTGGGTACCGGGCCCCCCC TCGAGGCAAATTAAAGCCTTCGAGC
prDD148 *	prDD148_Tul1prom-256bp_F	GTTGTCGTTACTGGTAATTTGC
prDD149 *	prDD149_+166-CYC1amp_R	GAGCGTCCCAAAACCTTC
prDD150	prDD150_Tul1libamp-HiFi_F	CGTCATGTTATATATTTGTTAAGCGTAG C
prDD151	prDD151_Tul1libamp-HiFi_R	GGGACCTAGACTTCAGGTTGTCTAAC
prDD152	prDD152_pRBHiFi-GPDamp_F	GAGCTCCACCGCGGTGTCTAGATCATT ATCAATACTCGCCATTTC
prDD153	prDD153_Cyc1amp+NheI-CCW12HiFi_R	ACCGTGTGGTTCATGGGTGGCTAGCGC AAATTAAAGCCTTCGAGC
prDD154	prDD154_Cyc1HiFi+NheI-CCW12amp_F	CTCGAAGGCTTTAATTTGCGCTAGCCAC CCATGAACCACACG

prDD155	prDD155_pgk1amp+EcoRI-pRBHiFi_R	GGTACCGGGCCCCCCCTCGAGGTCGGAATTCAACGCAGAATTTTCGAGTTATTAAAC
prDD156	prDD156_pRBHiFi-Orm2promamp_F	GAGCTCCACCGCGGTGTCTAGACGCTTGCCAAAGACCACA
prDD157	prDD157_Cyc1amp+NheI-ADHHiFi_R	AAAAAAAGAAAAGAAGTTGGCTAGCGCAAATTAAAGCCTTCGAGCG
prDD158	prDD158_Cyc1HiFi+NheI-ADHamp_F	CTCGAAGGCTTTAATTTGCGCTAGCCAACTTCTTTTCTTTTTTTTTCTTTTC
prDD165	prDD165_pRB903-SacI-Orm2prom_HiFi_F	TTCACACAAAGATTTGAGCTCCACGCTTGCCAAAGACCACA
prDD166	prDD166_ADH1-EcoRI-Cyc1_HiFi_R	AAAGAAGTTGAATTCGCAAATTAAAGCCTTCGAGCG
prDD167	prDD167_Cyc1-EcoRI-ADH1_HiFi_F	TTTAATTTGCGAATTCAACTTCTTTTCTTTTTTTTCTTTTC
prDD168	prDD168_Pgk1-KpnI-pRB903_HiFi_R	TTGGAGAAATATACAGGTACCAACGCAGAATTTTCGAGTTATTAAAC
prDD169	prDD169_pRB903-SacI-GPD_HiFi_F	TTCACACAAAGATTTGAGCTCCATCATTATCAATACTCGCCATTTC
prDD170	prDD170_CCW12-EcoRI-Cyc1_HiFI_R	TTCATGGGTGAATTCGCAAATTAAAGCCTTCGAGCG
prDD171	prDD171_Cyc1-EcoRI-CCW12_HiFi_F	TTTAATTTGCGAATTCACCCATGAACCACACG
prDD172	prDD172_M13F	TGTAAAACGACGGCCAGT
prDD173	prDD173_M13F43	AGGGTTTTCCCAGTCACGACGTT
prDD174	prDD174_M13R	CAGGAAACAGCTATGACC
prDD175	prDD175_M13R49	GAGCGGATAACAATTTCACACAGG
prDD176	prDD176_T3	AATTAACCCTCACTAAAGGG
prDD177	prDD177_T7	TAATACGACTCACTATAGGG
prDD178	prDD178_CYC1Reverse	GCGTGAATGTAAGCGTGAC
prDD179	prDD179_CYC1_F	GTCACGCTTACATTCACGC
prDD180	prDD180_Orm2seq_F	ATGATTGACCGCACTAAAAACG
prDD181	prDD181_CYC1Rend_R	GCAAATTAAAGCCTTCGAGCG
prDD182	prDD182_Pep12seq_F	GTCGGAAGACGAATTTTTTGG
prDD183	prDD183_Pep12seq_R	CCAAAAAATTCGTCTTCCGAC
prDD184	prDD184_Tlg1seq_F	GAACAACAGTGAAGATCCG
prDD185	prDD184_Tlg1seq_R	CGGATCTTCACTGTTGTTC
prDD186	prDD186_Tul1-C699A_F	GGAACTGCTGAACATACCGTTGATGCCGCGATATGTATGTCTGATG
prDD187	prDD187_Tul1-C699A_R	CATCAGACATACATATCGCGGCATCAACGGTATGTTCAGCAGTTCC
prDD188	prDD188_Tul1-C751S_F	GAATTATAAGTTACAATGTCCTGTGTCTAGGTCACCATTACCTCCG

prDD189	prDD189_Tul1-C751S_R	CGGAGGTAATGGTGACCTAGACACAGG ACATTGTAACTTATAATTC
prDD192	prDD192_pRB905_SacI_ADH_F	CTTAAAAAATAGAGTGAGCTCAACTTC TTTTCTTTTTTTTTCTTTTC
prDD193	prDD193_ADH_EcoRV_cyc1_R	CCTTTTCGGTTAGAGCGGATATCAGCTC TGGAACAACGAC
prDD194	prDD194_ADH_EcoRV_cyc1_F	CGTTGTTCCAGAGCTGATATCCGCTCTA ACCGAAAAGG
prDD195	prDD195_cyc1_XhoI_pRB905_R	GGTACCGGGCCCCCCCTCGAGCAAATT AAAGCCTTCGAGC
prDD196	prDD196_ADH_Tul1libamp_F	GTCGTTGTTCCAGAGCTGAT
prDD197	prDD197_Tul1libamp_cyc1_R	CCTTTTCGGTTAGAGCGGAT
prDD198	prDD198_Tul1libamp_F2	CGACAAAGACAGCACCAAC
prDD199	prDD199_Tul1libamp_R2	CCTTCCTTTTCGGTTAGAGC
prDD200	prDD200_Tul1libamp_F3	CAGATGTCGTTGTTCCAGAG
prDD201	prDD201_Tul1libamp_R3	CAGGTTGTCTAACTCCTTCC
prDD202 *	prDD202_ADHlong_F	GGTGTACAATATGGACTTCCTC
prDD203 *	prDD203_M13R49_lowertemp	GCGGATAACAATTTCACACAGG
prDD204	prDD204_Tul1lib-Plate1adapt_F	ACACTCTTTCCCTACACGACGCTCTTCC GATCTACTAGTATGGAAATCGATGG
prDD205	prDD205_Tul1lib-Plate1adapt_R	GACTGGAGTTCAGACGTGTGCTCTTCCG ATCTGTAGTTTTGATTGGGAAACCATC
prDD206	prDD206_Tul1lib-Plate2adapt_F	ACACTCTTTCCCTACACGACGCTCTTCC GATCTAATCAAAACTACATGGTTTTGCC C
prDD207	prDD207_Tul1lib-Plate2adapt_R	GACTGGAGTTCAGACGTGTGCTCTTCCG ATCTGCTATTTCGCCATGCTGAAAAC
prDD208	prDD208_Tul1lib-Plate3adapt_F	ACACTCTTTCCCTACACGACGCTCTTCC GATCTGGCGAAATAGCTATTCAAATTTC TC
prDD209	prDD209_Tul1lib-Plate3adapt_R	GACTGGAGTTCAGACGTGTGCTCTTCCG ATCTTCCTTGACATCATTAAATATTTTC TC
prDD210	prDD210_Tul1lib-Plate4adapt_F	ACACTCTTTCCCTACACGACGCTCTTCC GATCTGATGTCAAGGAACTCGTTGATG
prDD211	prDD211_Tul1lib-Plate4adapt_R	GACTGGAGTTCAGACGTGTGCTCTTCCG ATCTACCCTTTACGTTATGAAGCCC
prDD212	prDD212_Tul1lib-Plate5adapt_F	ACACTCTTTCCCTACACGACGCTCTTCC GATCTAACGTAAAGGGTACACGG
prDD213	prDD213_Tul1lib-Plate5adapt_R	GACTGGAGTTCAGACGTGTGCTCTTCCG ATCTAAGTAGCGTATTTCAAAAATAGA TG

prDD214	prDD214_Tul1lib-Plate6adapt_F	ACACTCTTTCCCTACACGACGCTCTTCCGATCTATACGCTACTTAATTTCAATTTACGC
prDD215	prDD215_Tul1lib-Plate6adapt_R	GACTGGAGTTCAGACGTGTGCTCTTCCGATCTAACGGCGTTACGGAAAATTTG
prDD216	prDD216_Tul1lib-Plate7adapt_F	ACACTCTTTCCCTACACGACGCTCTTCCGATCTCGTAACGCCGTTAAAGGTATTCC
prDD217	prDD217_Tul1lib-Plate7adapt_R	GACTGGAGTTCAGACGTGTGCTCTTCCGATCTATCCATCAGGTATTGTGTG
prDD218	prDD218_Tul1lib-Plate8adapt_F	ACACTCTTTCCCTACACGACGCTCTTCCGATCTCCTGATGGATATTCGTATTTCAAGC
prDD219	prDD219_Tul1lib-Plate8adapt_R	GACTGGAGTTCAGACGTGTGCTCTTCCGATCTGTCGACCTACAACGGAGG
prDD220	prDD220_CCW12seq_F	CCTAACATACCAAGAAATTAATCTTCTGTC
prDD231	prDD231_Tul1Plate1_Read1+F	TCGTCGGCAGCGTCAGATGTGTATAAGAGACAGNNNNNNNNCATATACAAGCGGCCGCACTAGT
prDD232	prDD232_Tul1Plate1_R+Read2	GTCTCGTGGGCTCGGAGATGTGTATAAGAGACAGNNNNNNNNTCGTTGGGCAAAACCATGTAGTT
prDD233	prDD233_Tul1Plate2_Read1+F	TCGTCGGCAGCGTCAGATGTGTATAAGAGACAGNNNNNNNNGATCGATGGTTTCCCAATCAA
prDD234	prDD234_Tul1Plate2_R+Read2	GTCTCGTGGGCTCGGAGATGTGTATAAGAGACAGNNNNNNNNGATTGCTCATATGAGAAATTTGAATAGCTAT
prDD235	prDD235_Tul1Plate3_Read1+F	TCGTCGGCAGCGTCAGATGTGTATAAGAGACAGNNNNNNNNGAGTTTTCAGCATGGCGAA
prDD236	prDD236_Tul1Plate3_R+Read2	GTCTCGTGGGCTCGGAGATGTGTATAAGAGACAGNNNNNNNNCCAAAATTCATCAACGAGTTCCTT
prDD237	prDD237_Tul1Plate4_Read1+F	TCGTCGGCAGCGTCAGATGTGTATAAGAGACAGNNNNNNNNGAATGATTATAATGAGAAAATATTTAATGATGTC
prDD238	prDD238_Tul1Plate4_R+Read2	GTCTCGTGGGCTCGGAGATGTGTATAAGAGACAGNNNNNNNNTTCGTACCGTGTACCCTT
prDD239	prDD239_Tul1Plate5_Read1+F	TCGTCGGCAGCGTCAGATGTGTATAAGAGACAGNNNNNNNNCGATTAGGGCTTCATAACGTA
prDD240	prDD240_Tul1Plate5_R+Read2	GTCTCGTGGGCTCGGAGATGTGTATAAGAGACAGNNNNNNNNCTGTGAAGCGTAAATTGAAATTAAGTA

prDD241	prDD241_Tul1Plate6_Read1+F	TCGTCGGCAGCGTCAGATGTGTATAAGAGACAGNNNNNNNNGGCATCTATTTTTGAAATACGC
prDD242	prDD242_Tul1Plate6_R+Read2	GTCTCGTGGGCTCGGAGATGTGTATAAGAGACAGNNNNNNNNGAAGGAATACCTTTAACGGC
prDD243	prDD243_Tul1Plate7_Read1+F	TCGTCGGCAGCGTCAGATGTGTATAAGAGACAGNNNNNNNNGATCCCTCAAATTTTCCGTAAC
prDD244	prDD244_Tul1Plate7_R+Read2	GTCTCGTGGGCTCGGAGATGTGTATAAGAGACAGNNNNNNNNGGGCTTGAAATACGAATATCC
prDD245	prDD245_Tul1Plate8_Read1+F	TCGTCGGCAGCGTCAGATGTGTATAAGAGACAGNNNNNNNNCCTAAGCACACAATACCTGAT
prDD246	prDD246_Tul1Plate8_R+Read2	GTCTCGTGGGCTCGGAGATGTGTATAAGAGACAGNNNNNNNNACATGACTCGAGGTCGAC
prDD265	prDD265_Gld1-3xHA_F	AATGCCATTTTAAATGACGGCAATATTAATGACAACAATGAGAATGCTAGCAATTCTGTCGGGTCTGGTTACCCATACG
prDD268	prDD268_ADH1-Gld1_R	TAAGGAAATGTAATAGAATGATATATGTAAATGTAACTCTCTATAAAATAGTGCCGATAACCGGTAGAGGTGTGGTCA
prDD269	prDD269_CYC1-Gld1_R	TAAGGAAATGTAATAGAATGATATATGTAAATGTAACTCTCTATAAAATAGTGCCGATAACTTCGAGCGTCCCAAAACC
prDD270	prDD270_Vld1-3xHA_F	CCTCAACAGGCAGACGGGGATGACGCTACAGAGATCACTCCTCTACTGAATATCGCCGAAGGGTCTGGTTACCCATACG
prDD273	prDD273_ADH1-Vld1_R	TGGGAAGGACAGTAGAAGAACCACGTATTGTTTTATTTTCTGTTCATCTTTTTTTTCCGTCCGGTAGAGGTGTGGTCA
prDD274	prDD274_CYC1-Vld1_R	TGGGAAGGACAGTAGAAGAACCACGTATTGTTTTATTTTCTGTTCATCTTTTTTTTCCGTCTTCGAGCGTCCCAAAACC
prDD280	prDD280_Gld1(+161bp)_F	CTGGACACTTATAACAAGAGC
prDD281	prDD281_Vld1(+75bp)_F	CTCCAGGGAAAGAAAGGG
prDD283	prDD283_3xHA_R	CTAAGCGTAATCTGGAACG
prDD286	prDD286_TEFprom(+325bp)_F	CACATCCGAACATAAACAAC
prDD287	prDD287_Gld1term_R	GGAAGAGTGAGGAACCAC
prDD288	prDD288_Vld1term_R	GTCGGATGTGATTTCCAG
prDD290	prDD290_gbDD18_F	CAATTTACGCTTCACAGGTTGCCGAACAGAATGTTGGGATTA

prDD291	prDD291_gbDD18_R	TAATCCCAACATTCTGTTCGGCAACCTG TGAAGCGTAAATTG
prDD292	prDD292_gbDD30_F	ATAAGTTACAATGTCCTGTGCATAGGTC ACCATTACCTCCGTTGTAGGTC
prDD293	prDD293_gbDD30_R	GACCTACAACGGAGGTAATGGTGACCT ATGCACAGGACATTGTAACTTAT
prDD294	prDD294_gbDD31_F	ATAAGTTACAATGTCCTGTGTGTAGTTC ACCATTACCTCCGTTGTAGGTC
prDD295	prDD295_gbDD31_R	GACCTACAACGGAGGTAATGGTGAACT ACACACAGGACATTGTAACTTAT
prDD296	prDD296_gbDD32_F	ATAAGTTACAATGTCCTGTGTGTATTTC ACCATTACCTCCGTTGTAGGTC
prDD297	prDD297_gbDD32_R	GACCTACAACGGAGGTAATGGTGAAAT ACACACAGGACATTGTAACTTAT
prDD298	prDD298_Orm2-3xHA_F	GTGCTCAAATTAGTGGATCCTACCCATA CGATGTTC
prDD299	prDD299_3xHA-STOPcyc1_R	TAACTAATTACATGACTCGAGGTCGAC TTAAGCGTAATCTGGAAC
prDD300	prDD300_ADH-3xFLAG_F	ACTATCTCATATACAAGCGGCCGCATG GACTACAAAGACCATGAC
prDD301	prDD301_3xFLAG-Pep12_R	TCGTCTTCCGACATACTAGTCTTGTCAT CGTCATCC
prDD302	prDD302_3xFLAG-Tlg1_R	TCACTGTTGTTCATACTAGTCTTGTCAT CGTCATCC
prDD303	prDD303_mScarMod1_R	TACCCCGTCTTCGGGGTACAACCTCTCA ACTGAAGCCTCCCACCC
prDD325	prDD325_mScarMod2_F	AAGAAGACTATGGGGTGGGAGGCTTCA GTTGAGAGGTTGTACCCCG
prDD326	prDD326_mScarMod2_R	AATCTTCGTTATGAGACGTGATAGTCA ATTGACGATCTACGTTGTATGC
prDD327	prDD327_+215bpHygR_R	GCGGCCGATGCAAAGTG
prDD328	prDD328_-854bpTul1_F	CCGCTTGTGGTGCTGC
prDD329	prDD329_-1025bpDsc2_F	CCCATTTGACCATCTTTCCCAG
prDD330	prDD330_-1405bpDsc3_F	CATATCAGGTGCCGTCGC
prDD331	prDD331_-1133bpUbx3_F	CTTTGGTGGAGGTCCTGGC
prDD332	prDD332_-1563bpGld1_F	GGAAGCGGCAAAGTTATTGGTC
prDD333	prDD333_-1688bpVld1_F	CCAGAACAAGACGAATTAGATGCC
prDD334	prDD334_KpnI-ADH_F	CTTTAATTTGCGGCCGGTACCGGTGTAC AATATGGACTTCC
prDD335	prDD335_pgk1-KpnI_R	TTGGCAGAAAGACTGCTGGTACCCAAC GCAGAATTTTCGAGTTATTAAAC

2.13 References

1. Sun, Z. & Brodsky, J. L. Protein quality control in the secretory pathway. *J. Cell Biol.* **218**, 3171–3187 (2019).
2. Arvan, P., Zhao, X., Ramos-Castaneda, J. & Chang, A. Secretory Pathway Quality Control Operating in Golgi, Plasmalemmal, and Endosomal Systems: Post-ER Quality Control Pathways. *Traffic* **3**, 771–780 (2002).
3. Ruggiano, A., Foresti, O. & Carvalho, P. ER-associated degradation: Protein quality control and beyond. *J. Cell Biol.* **204**, 869–879 (2014).
4. Gregersen, N., Bross, P., Vang, S. & Christensen, J. H. Protein Misfolding and Human Disease. *Annu. Rev. Genomics Hum. Genet.* **7**, 103–124 (2006).
5. Labbadia, J. & Morimoto, R. I. The Biology of Proteostasis in Aging and Disease. *Annu. Rev. Biochem.* **84**, 435–464 (2015).
6. Kincaid, M. M. & Cooper, A. A. Misfolded Proteins Traffic from the Endoplasmic Reticulum (ER) Due to ER Export Signals. *Mol. Biol. Cell* **18**, 455–463 (2007).
7. Coughlan, C. M., Walker, J. L., Cochran, J. C., Wittrup, K. D. & Brodsky, J. L. Degradation of mutated bovine pancreatic trypsin inhibitor in the yeast vacuole suggests post-endoplasmic reticulum protein quality control. *J. Biol. Chem.* **279**, 15289–15297 (2004).
8. Wang, S. & Ng, D. T. W. Evasion of Endoplasmic Reticulum Surveillance Makes Wsc1p an Obligate Substrate of Golgi Quality Control. *Mol. Biol. Cell* **21**, 1153–1165 (2010).
9. Suyama, K., Hori, M., Gomi, K. & Shintani, T. Fusion of an intact secretory protein permits a misfolded protein to exit from the endoplasmic reticulum in yeast. *Biosci. Biotechnol. Biochem.* **78**, 49–59 (2014).
10. Sato, K., Sato, M. & Nakano, A. Rer1p, a retrieval receptor for ER membrane proteins, recognizes transmembrane domains in multiple modes. *Mol. Biol. Cell* **14**, 3605–3616 (2003).
11. Park, H.-J., Ryu, D., Parmar, M., Giasson, B. I. & McFarland, N. R. The ER retention protein RER1 promotes alpha-synuclein degradation via the proteasome. *PLOS ONE* **12**, e0184262 (2017).
12. Bowers, K. & Stevens, T. H. Protein transport from the late Golgi to the vacuole in the yeast Saccharomyces cerevisiae. *Biochim. Biophys. Acta BBA - Mol. Cell Res.* **1744**, 438–454 (2005).
13. Reggiori, F. & Pelham, H. R. B. A transmembrane ubiquitin ligase required to sort membrane proteins into multivesicular bodies. *Nat. Cell Biol.* **4**, 117–123 (2002).
14. Schmidt, O. *et al.* Endosome and Golgi-associated degradation (EGAD) of membrane proteins regulates sphingolipid metabolism. *EMBO J.* **38**, (2019).
15. Schwabl, S. & Teis, D. Protein quality control at the Golgi. *Curr. Opin. Cell Biol.* **75**, 102074 (2022).
16. Valdez-Taubas, J. & Pelham, H. Swf1-dependent palmitoylation of the SNARE Tlg1 prevents its ubiquitination and degradation. *EMBO J.* **24**, 2524–2532 (2005).
17. Li, M., Koshi, T. & Emr, S. D. Membrane-anchored ubiquitin ligase complex is required for the turnover of lysosomal membrane proteins. *J. Cell Biol.* **211**, 639–652 (2015).
18. Dobzinski, N., Chuartzman, S. G., Kama, R., Schuldiner, M. & Gerst, J. E. Starvation-Dependent Regulation of Golgi Quality Control Links the TOR Signaling and Vacuolar Protein Sorting Pathways. *Cell Rep.* **12**, 1876–1886 (2015).
19. Schäfer, J.-H. *et al.* Structure of the ceramide-bound SPOTS complex. *Nat. Commun.* **14**, 6196 (2023).

20. Stewart, E. V. *et al.* Yeast SREBP Cleavage Activation Requires the Golgi Dsc E3 Ligase Complex. *Mol. Cell* **42**, 160–171 (2011).
21. Stewart, E. V. *et al.* Yeast Sterol Regulatory Element-binding Protein (SREBP) Cleavage Requires Cdc48 and Dsc5, a Ubiquitin Regulatory X Domain-containing Subunit of the Golgi Dsc E3 Ligase. *J. Biol. Chem.* **287**, 672–681 (2012).
22. Lloyd, S. J.-A., Raychaudhuri, S. & Espenshade, P. J. Subunit Architecture of the Golgi Dsc E3 Ligase Required for Sterol Regulatory Element-binding Protein (SREBP) Cleavage in Fission Yeast. *J. Biol. Chem.* **288**, 21043–21054 (2013).
23. Raychaudhuri, S. & Espenshade, P. J. Endoplasmic Reticulum Exit of Golgi-resident Defective for SREBP Cleavage (Dsc) E3 Ligase Complex Requires Its Activity. *J. Biol. Chem.* **290**, 14430–14440 (2015).
24. Hwang, J. *et al.* A Golgi rhomboid protease Rbd2 recruits Cdc48 to cleave yeast SREBP. *EMBO J.* **35**, 2332–2349 (2016).
25. Tong, Z., Kim, M.-S., Pandey, A. & Espenshade, P. J. Identification of Candidate Substrates for the Golgi Tul1 E3 Ligase Using Quantitative diGly Proteomics in Yeast. *Mol. Cell. Proteomics* **13**, 2871–2882 (2014).
26. Yang, X., Arines, F. M., Zhang, W. & Li, M. Sorting of a multi-subunit ubiquitin ligase complex in the endolysosome system. *eLife* **7**, e33116 (2018).
27. Sankaranarayanan, S., De Angelis, D., Rothman, J. E. & Ryan, T. A. The Use of pHluorins for Optical Measurements of Presynaptic Activity. *Biophys. J.* **79**, 2199–2208 (2000).
28. Kitzman, J. O., Starita, L. M., Lo, R. S., Fields, S. & Shendure, J. Massively parallel single-amino-acid mutagenesis. *Nat. Methods* **12**, 203–206, 4 p following 206 (2015).
29. Bloom, J. D. An Experimentally Determined Evolutionary Model Dramatically Improves Phylogenetic Fit. *Mol. Biol. Evol.* **31**, 1956–1978 (2014).
30. Dingens, A. S., Haddox, H. K., Overbaugh, J. & Bloom, J. D. Comprehensive Mapping of HIV-1 Escape from a Broadly Neutralizing Antibody. *Cell Host Microbe* **21**, 777-787.e4 (2017).
31. Peterson, B. G. *et al.* Deep mutational scanning highlights a role for cytosolic regions in Hrd1 function. *Cell Rep.* **42**, 113451 (2023).
32. Sharninghausen, R., Hwang, J., Dennison, D. & Baldridge, R. D. *Identification of ERAD-dependent degrons for the endoplasmic reticulum lumen*. https://elifesciences.org/reviewed-preprints/89606v1 (2023) doi:10.7554/eLife.89606.1.
33. Hwang, J., Peterson, B. G., Knupp, J. & Baldridge, R. D. The ERAD system is restricted by elevated ceramides. *Sci. Adv.* **9**, eadd8579 (2023).
34. Eckert-Boulet, N., Rothstein, R. & Lisby, M. Cell biology of homologous recombination in yeast. *Methods Mol. Biol. Clifton NJ* **745**, 523–536 (2011).
35. Rubin, A. F. *et al.* A statistical framework for analyzing deep mutational scanning data. *Genome Biol.* **18**, 150 (2017).
36. Deshaies, R. J. & Joazeiro, C. A. P. RING Domain E3 Ubiquitin Ligases. *Annu. Rev. Biochem.* **78**, 399–434 (2009).
37. Metzger, M. B., Pruneda, J. N., Klevit, R. E. & Weissman, A. M. RING-type E3 ligases: Master manipulators of E2 ubiquitin-conjugating enzymes and ubiquitination. *Biochim. Biophys. Acta BBA - Mol. Cell Res.* **1843**, 47–60 (2014).
38. Sakamaki, J.-I. *et al.* Ubiquitination of phosphatidylethanolamine in organellar membranes. *Mol. Cell* **82**, 3677-3692.e11 (2022).
39. Cianfrocco, M. A., Wong-Barnum, M., Youn, C., Wagner, R. & Leschziner, A. COSMIC2: A Science Gateway for Cryo-Electron Microscopy Structure Determination. in *Proceedings of*

the Practice and Experience in Advanced Research Computing 2017 on Sustainability, Success and Impact 1–5 (ACM, 2017). doi:10.1145/3093338.3093390.
40. Evans, R. *et al. Protein complex prediction with AlphaFold-Multimer*. http://biorxiv.org/lookup/doi/10.1101/2021.10.04.463034 (2021) doi:10.1101/2021.10.04.463034.
41. Lips, C. *et al.* Who with whom: functional coordination of E2 enzymes by RING E3 ligases during poly-ubiquitylation. *EMBO J.* **39**, e104863 (2020).
42. Swatek, K. N. & Komander, D. Ubiquitin modifications. *Cell Res.* **26**, 399–422 (2016).
43. Ye, Y. *et al.* Ubiquitin chain conformation regulates recognition and activity of interacting proteins. *Nature* **492**, 266–270 (2012).
44. Rodrigo-Brenni, M. C., Foster, S. A. & Morgan, D. O. Catalysis of lysine 48-specific ubiquitin chain assembly by residues in E2 and ubiquitin. *Mol. Cell* **39**, 548–559 (2010).
45. Grice, G. L. & Nathan, J. A. The recognition of ubiquitinated proteins by the proteasome. *Cell. Mol. Life Sci.* **73**, 3497–3506 (2016).
46. Schaefer, J. B. & Morgan, D. O. Protein-linked ubiquitin chain structure restricts activity of deubiquitinating enzymes. *J. Biol. Chem.* **286**, 45186–45196 (2011).
47. Kolla, S., Ye, M., Mark, K. G. & Rapé, M. Assembly and function of branched ubiquitin chains. *Trends Biochem. Sci.* **47**, 759–771 (2022).
48. Christensen, D. E., Brzovic, P. S. & Klevit, R. E. E2–BRCA1 RING interactions dictate synthesis of mono- or specific polyubiquitin chain linkages. *Nat. Struct. Mol. Biol.* **14**, 941–948 (2007).
49. Nathan, J. A., Tae Kim, H., Ting, L., Gygi, S. P. & Goldberg, A. L. Why do cellular proteins linked to K63-polyubiquitin chains not associate with proteasomes? *EMBO J.* **32**, 552–565 (2013).
50. Renz, C. *et al.* Ubc13-Mms2 cooperates with a family of RING E3 proteins in budding yeast membrane protein sorting. *J. Cell Sci.* **133**, jcs244566 (2020).
51. Seufert, W. & Jentsch, S. Ubiquitin-conjugating enzymes UBC4 and UBC5 mediate selective degradation of short-lived and abnormal proteins. *EMBO J.* **9**, 543–550 (1990).
52. Causton, H. C. *et al.* Remodeling of Yeast Genome Expression in Response to Environmental Changes. *Mol. Biol. Cell* **12**, 323–337 (2001).
53. Carvalho, P., Stanley, A. M. & Rapoport, T. A. Retrotranslocation of a Misfolded Luminal ER Protein by the Ubiquitin-Ligase Hrd1p. *Cell* **143**, 579–591 (2010).
54. Baldridge, R. D. & Rapoport, T. A. Autoubiquitination of the Hrd1 Ligase Triggers Protein Retrotranslocation in ERAD. *Cell* **166**, 394–407 (2016).
55. Assainar, B. M., Ragunathan, K. & Baldridge, R. D. *Direct observation of autoubiquitination for an integral membrane ubiquitin ligase in ERAD*. http://biorxiv.org/lookup/doi/10.1101/2023.06.20.545802 (2023) doi:10.1101/2023.06.20.545802.
56. Peterson, B. G., Glaser, M. L., Rapoport, T. A. & Baldridge, R. D. Cycles of autoubiquitination and deubiquitination regulate the ERAD ubiquitin ligase Hrd1. *eLife* **8**, e50903 (2019).
57. Altschul, S. F. *et al.* Gapped BLAST and PSI-BLAST: a new generation of protein database search programs. *Nucleic Acids Res.* **25**, 3389–3402 (1997).
58. Altschul, S. F. *et al.* Protein database searches using compositionally adjusted substitution matrices. *FEBS J.* **272**, 5101–5109 (2005).

59. Engel, S. R. *et al.* New data and collaborations at the Saccharomyces Genome Database: updated reference genome, alleles, and the Alliance of Genome Resources. *Genetics* **220**, iyab224 (2022).
60. Janke, C. *et al.* A versatile toolbox for PCR-based tagging of yeast genes: new fluorescent proteins, more markers and promoter substitution cassettes. *Yeast* **21**, 947–962 (2004).
61. Gietz, R. D. & Schiestl, R. H. High-efficiency yeast transformation using the LiAc/SS carrier DNA/PEG method. *Nat. Protoc.* **2**, 31–34 (2007).
62. Munder, M. C. *et al.* A pH-driven transition of the cytoplasm from a fluid- to a solid-like state promotes entry into dormancy. *eLife* **5**, e09347 (2016).
63. Fuxman Bass, J. I., Reece-Hoyes, J. S. & Walhout, A. J. M. Zymolyase-Treatment and Polymerase Chain Reaction Amplification from Genomic and Plasmid Templates from Yeast. *Cold Spring Harb. Protoc.* **2016**, pdb.prot088971 (2016).
64. Lõoke, M., Kristjuhan, K. & Kristjuhan, A. Extraction of genomic DNA from yeasts for PCR-based applications. *BioTechniques* **50**, 325–328 (2011).
65. Martin, M. Cutadapt removes adapter sequences from high-throughput sequencing reads. *EMBnet.journal* **17**, 10 (2011).
66. Masella, A. P., Bartram, A. K., Truszkowski, J. M., Brown, D. G. & Neufeld, J. D. PANDAseq: paired-end assembler for illumina sequences. *BMC Bioinformatics* **13**, 31 (2012).
67. Shen, W., Le, S., Li, Y. & Hu, F. SeqKit: A Cross-Platform and Ultrafast Toolkit for FASTA/Q File Manipulation. *PLOS ONE* **11**, e0163962 (2016).
68. Wickham, H. *ggplot2: Elegant Graphics for Data Analysis*. (Springer-Verlag New York, 2016).

Chapter 3
Conclusions

3.1 Overview

Eukaryotic protein quality control is a conglomerate of interconnected systems that function within the cytosol and at all organelles to prevent or assuage cell stress by maintaining proteostasis, as detailed in Chapter 1 of this thesis. Systems that operate within the secretory pathway compose one critical branch of eukaryotic protein quality control, as they surveil organelles that receive membrane and secretory proteins that leave the ER. Post-ER quality control can respond by either distributing aberrant protein, to be dealt with by systems localized to other organelles, or by simply degrading substrates using a localized system that facilitates lysosomal or proteasomal degradation [1,2]. As highlighted in Chapter 1, the complete inventory of systems and mechanisms specifically involved in degradative quality control in the eukaryotic secretory pathway are not well-characterized and are almost all restricted to those that facilitate lysosomal degradation. This is due to the fact that most of our current understandings of post-ER quality control systems come merely from observing the result of their function: proteins localized to lysosomal compartments in mammalian cells or to the vacuole in yeast for degradation [1–5].

The work in this thesis focuses on the Golgi-localized Tul1 ubiquitin ligase complex found in *S. cerevisiae*, which recognizes and ubiquitinates integral membrane proteins for degradation via ESCRT-mediated delivery to the vacuole. The Golgi-localized Tul1 complex is unique in that it is a post-ER quality control system that can also degrade substrate via the ubiquitin-proteasome system [6] and remains to be the only clearly defined post-ER ubiquitin ligase system in the secretory pathway to do so [1–5]. Furthermore, Golgi-localized Tul1 is the only known integral membrane ubiquitin ligase system across all organelles that can send substrates to both degradation pathways. Importantly, there is a fixed specificity to which Tul1 substrates are sent to the vacuole for degradation and which Tul1 substrates are degraded by the cytosolic proteasome [6–10]. Investigating the unknown mechanism(s) that direct Tul1 selective substrate degradation was the basis of the

work presented in Chapter 2 and led us to discover a role for the namesake ubiquitin ligase, Tul1, in directing a protein to either degradation pathway.

We began by creating high-throughput tools that surveyed the function of the Golgi-localized Tul1 system. We developed fluorescence-based cellular assays that concurrently monitored model vacuolar and proteasomal substrate degradation, which we applied to deep mutational scanning of the ubiquitin ligase Tul1. We focused our first deep mutational scanning efforts on Tul1 in part because co-immunoprecipitation experiments in Chapter 2 revealed that Tul1 interacts directly with both classes of substrate in the absence of each known complex component. This was the first evidence in the field suggesting that Tul1 plays a role in bringing substrates to the complex, and we reasoned that these interactions could play a role in how a substrate is degraded though the evidence from our screen did not contribute to this hypothesis.

To test the necessity of each residue within Tul1, we generated single-residue variant libraries that spanned the Tul1 protein and screened 96% of all possible Tul1 substitutions by their functional phenotype. From our efforts, we identified functionally important residues in the Tul1 lumenal and RING domains. Most notably, our screening efforts revealed several particularly interesting Tul1 RING mutants that we were surprised to find altered the specificity of the Tul1 system. These change-of-specificity variants were unable to degrade the model proteasomal substrate but were hypomorphic for model vacuolar substrate degradation. We concluded in Chapter 2 that Tul1 plays an important role in directing substrate fate and began to explore the possible mechanism(s) responsible for this function.

Our structure-function analysis of Tul1 RING mutants mapped each substitution to a predicted ubiquitin conjugating enzyme (Ubc4) interaction site based on a predicted AlphaFold model, in which we folded the Tul1 RING domain, Ubc4, and ubiquitin [11,12]. Unsurprisingly, the majority of our defined nonfunctional RING mutants comprised conserved residues required for the characteristic RING domain fold, and therefore proper Ubc4 engagement with Tul1 [13,14]. In contrast, RING-domain mutants that were hypomorphic or changed the specificity of the Tul1 complex mapped to a different plane of the modeled Tul1 RING domain. These residues were not predicted to directly orient towards Ubc4 like nonfunctional substitutions, but instead bordered this region and oriented closer to the ubiquitin moiety. We interpreted this data to mean that the ubiquitin ligase Tul1 directs a protein for vacuolar versus proteasomal degradation by mediating

different types of substrate ubiquitination specific to each degradation pathway, models of which will be discussed in depth in Section 3.2.1.

Our screening efforts also revealed several residues in the Tul1 lumenal domain that were critical for Tul1 function. We found that mutating these residues abolished or impaired Tul1 from interacting with known integral membrane complex components. Most of these lumenal mutations completely abolished Tul1 interaction with all known complex components and were nonfunctional, though we defined one hypomorphic lumenal mutant that had attenuated complex interaction. These findings were consistent with previous characterizations [15,10,6,14,16] that Tul1 must form a complex to function and that Tul1 requires all known components (Dsc2, Dsc3, Ubx3, and a localization signal Gld1 or Vld1) for proper complex interaction, which we also confirmed via cellular and biochemical assays in Chapter 2.

Previous studies of Tul1 substrate degradation proposed that Tul1 subcomplexes do not share protein substrates [6,10]. It was proposed that Gld1-containing/Golgi-localized Tul1 only targeted integral membrane proteins localized to Golgi and endosomal compartments and Vld1-containing/vacuole-localized Tul1 only targeted vacuolar integral membrane proteins [6,10]. Equally important to note, and as we confirmed in Chapter 2, is that Golgi-localized Tul1 substrates are degraded in the vacuole or by the proteasome while vacuole-localized substrates are only degraded in the vacuole [6,10]; the possible role of substrate localization in directing Tul1 selective degradation is further explored in Section 3.2.2. However, while validating our Golgi-localized Tul1 functional assays in Chapter 2, we defined the first examples of Tul1 substrates that are degraded in the vacuole by both Gld1- and Vld1-containing complexes. Based on previous profiling of a different Golgi-localized Tul1 vacuolar substrate [10], we had expected to find that only Gld1-Tul1 complexes targeted mutant t-SNAREs Pep12(D) and Tlg1(LL) (hereafter referred to as Pep12* and Tlg1*, respectively) for ESCRT-mediated vacuolar degradation. We were therefore surprised to find that in the absence of Gld1, Vld1-Tul1 complexes could poorly degrade both mutant SNAREs. Similar to these shared protein substrates, a recent study found that Gld1- and Vld1-Tul1 both ubiquitinate the non-protein substrate phosphatidylethanolamine (PE) at endosomal compartments and the vacuole [14], a phenomenon that will be detailed later in this chapter.

In contrast to the vacuolar substrates Pep12* and Tlg1*, previous work [6] that we also confirmed in Chapter 2 found that only Gld1-Tul1 complexes can degrade the Tul1 proteasomal substrate Orm2. This is despite the fact that, like Pep12* and Tlg1*, Vld1-Tul1 complexes can

exist in the same space as Orm2 in the Golgi membrane [6,10] and that co-immunoprecipitation assays in Chapter 2 demonstrated that Vld1-Tul1 interacts with Orm2. There is a clear necessity for Gld1 in Orm2 proteasomal degradation, perhaps implicating an important function specific to Tul1 participation with the ubiquitin-proteasome system; Section 3.2.3 explores this potential role of Gld1 in Tul1 substrate selectivity mechanisms.

In conclusion, work in Chapter 2 revealed that the Golgi-localized Tul1 ubiquitin ligase plays a role in specifying a substrate's fate. Structure-function analyses and predictive modeling indicated that Tul1 function in the ubiquitination cascade is the likely mechanism responsible for directing substrates to a specific degradation pathway. However, there are clearly other factor(s) involved in Tul1 substrate selection. Whether these factors are known, or even unknown, complex components can be investigated using or adapting cellular functional assays established in this thesis. It is also possible that screening larger Tul1 mutations, rather than single-residue substitutions as tested in Chapter 2, could reveal multi-residue regions within Tul1 that are singularly important to proteasomal or vacuolar degradation. A good place to start any larger-scale investigation of Tul1 would be to return to the deep mutational scanning data collected in the experiments shown in Chapter 2 and mine for regions that cannot tolerate multi-residue mutations. The importance of these regions can then be validated using our established Tul1 structure-function analysis tools. Such discoveries would reveal a more direct role for Tul1 in substrate selection outside of our proposed ubiquitination-based mechanisms.

Regardless, Golgi-localized Tul1 functional screening assays, structure-function analyses of important Tul1 residues revealed by deep mutational scanning, and biochemical characterizations of Tul1 complex interactions in Chapter 2 suggest several plausible models for how the Golgi-localized Tul1 system selectively degrades a substrate and are discussed in detail in the next section. Each of these proposed models can be tested in the future by adapting the cellular and biochemical readouts established in this thesis.

3.2 Golgi-localized Tul1 selective substrate degradation models

The fate of Golgi-localized Tul1 substrates seems to be specific to a degradation pathway, meaning previous work from other groups have indicated a proteasomal substrate is not degraded in the vacuole and vacuolar substrates are not degraded by the 26S proteasome [6,7,9,16]. This suggests that there is a mechanism within the Golgi-localized Tul1 system that designates a protein for

degradation by each pathway. Our structure-function analysis of Tul1 suggested that the ubiquitin ligase Tul1 plays a role in designating a substrate for the proteasome versus the vacuole, but that there are certainly other factors involved. Based off work presented in Chapter 2 and in consideration of known mechanisms of other RING-type ubiquitin ligase systems, several possible models are proposed for Golgi-localized Tul1 selective substrate degradation.

3.2.1 Golgi-localized Tul1 selectively conjugates different types of ubiquitin onto substrates

While findings in Chapter 2 suggested that the ubiquitin ligase Tul1 is not the only factor involved in designating a substrate for the proteasome versus the vacuole, we propose several possible features and functions of Tul1 that could play a main role in regulating substrate degradation fates [17,18]. Based on results in Chapter 2, Tul1 variants with altered substrate selectivity contained substitutions in the RING domain that bordered, but did not compose, the modeled Ubc4 interaction site. This suggests that these Tul1 variants can engage with ubiquitination machinery, but perhaps these mutations impair the ability and/or efficiency of Tul1 to mediate the addition of specific types or lengths of polyubiquitin chains. Specifically, these mutations might alter or even impede discreet Tul1 intermolecular interactions with substrates and/or engaged Ubc enzymes. This led us to consider a model that Golgi-localized Tul1 plays a role in selective substrate degradation by directing specific types of ubiquitin conjugation(s) onto each class of substrate for exclusive engagement with either the 26S proteasome or ESCRT-mediated vacuolar degradation (Figure 3.1).

As discussed in Chapter 1, certain types of polyubiquitin linkages are characteristically associated with either degradation pathway [19,20]. With this in mind, perhaps Tul1 selectively conjugates proteasomal substrates with K48-polyubiquitin chains and vacuolar substrates specifically with K63-polyubiquitin chains at the Golgi membrane (Figure 3.1A). For the sake of clarity, we are simply characterizing K48- and K63-linkages to either class of substrate, with the understanding that future studies of this model should take into consideration other types of ubiquitin conjugations, including K11-linkages, branched chains, and mono/multi-ubiquitination [17–20]. Our simplified proposed model relies on the fact that K48-linkages are canonical to 26S proteasomal degradation and that K63-ubiquitin directs proteins to ESCRT-mediated vacuolar degradation [21–24]. Clear mechanism(s) that describe how proteins containing K48- or K63-ubiquitin conjugations are specific to either degradation pathway requires further investigation in

the ubiquitin field in general, but is likely due to preferential interactions with components of each pathway, as summarized in Chapter 1 [19,21,25]. Briefly, K48-chains strongly interact with the 19S regulatory cap of the 26S proteasome while K63-chains strongly interact with ESCRT-0 components [21,26]. Both K48-chains and K63-chains interact with ESCRT-0 components in a reconstituted system [26], however K48-polyubiquitinated substrates in cells might be too rapidly degraded to engage with ESCRT-0 and/or could simply just preferentially bind the proteasome. K63-polyubiquitin can also associate with the 19S cap in reconstituted systems [27,28], but it is proposed that strong interactions between K63-linked ubiquitin and ESCRT-0 components, or other ubiquitin binding domain proteins, inhibit K63-conjugated proteins from being recognized by the 19S cap or extracted for degradation by the proteasome, leading to a specificity for vacuolar degradation in cells [21–23].

There are several possible Tul1-based mechanisms that are relevant when considering how proteasomal or vacuolar substrates might be selectively conjugated with K48- versus K63-polyubiquitin, respectively. Interactions during the final step of the ubiquitination cascade determine the characteristics of ubiquitin conjugated onto a protein, including 1) what Ubc enzyme is recruited by the ubiquitin ligase, 2) how the ubiquitin ligase engages with the Ubc enzyme, and 3) how a ubiquitin ligase positions a substrate for ubiquitin conjugation [17,18,20]. As a RING-type ubiquitin ligase, Tul1 coordinates the transfer of ubiquitin directly from a Ubc enzyme to a substrate through intermolecular interactions with both components [17,18], therefore Tul1 plays a role in determining the type of ubiquitin conjugated onto a substrate.

Ubiquitin ligases can interact with multiple Ubc enzymes; different Ubc enzymes can be recruited by a RING-type ubiquitin ligase to conjugate specific types of ubiquitin onto a substrate [18,25,29]. It is therefore logical to speculate that Golgi-localized Tul1 selectively recruits different Ubc enzymes to ubiquitinate either class of substrate, resulting in specific polyubiquitin linkages that direct the protein for proteasomal or vacuolar degradation. Published yeast two-hybrid screens find that Tul1 interacts with Ubc1, Ubc4, Ubc5, Ubc6 (which is integrated into the ER-membrane [30] and is not discussed as it seems unlikely to be involved with a post-ER ubiquitin ligase system), and Ubc13 [7,31]. Of these, Ubc1 and Ubc13 are interesting candidates to consider in a model of selective Ubc enzyme recruitment by Tul1 to direct differential substrate degradation. Ubc1 exclusively conjugates K48-linked ubiquitin [32] while Ubc13-Mms2 (a heterodimeric complex with Ubc13 and the ubiquitin-conjugating enzyme variant protein Mms2 [33]) exclusively conjugates

K63-ubiquitin chains [33,34]. Though Ubc13-Mms2 is most commonly associated with DNA damage repair [33], it was recently discovered to play a role in ESCRT-mediated vacuolar degradation of an integral membrane protein by the soluble RING-type ubiquitin ligase Pib1, which associates to endosomal compartments and the vacuole in yeast [5,31]. Therefore, it is possible that Ubc1 is recruited by Tul1 to selectively ubiquitinate a proteasomal substrate with K48-linkages while Ubc13-Mms2 is recruited to ubiquitinate a vacuolar substrate with K63-linkages. If so, the RING-domain mutations discovered in Chapter 2 that changed Tul1 substrate selectivity might completely disrupt Tul1-Ubc1 engagement, resulting in stabilized proteasomal substrate, but only impair Ubc13-Mms2 interactions, allowing for some vacuolar substrate degradation.

It should be noted that, outside of suggested interactions from a published yeast two-hybrid screening study [31], there is no evidence that Ubc1 nor Ubc13-Mms2 ubiquitinate Tul1 substrates. However, our preliminary (Figure 3.2) and another group's published [14] *in vitro* reconstitution experiments do confirm the *in vivo* yeast two-hybrid studies [7,31] that suggested Ubc4 and Ubc5 are active in the Tul1 system. Using purified components, we found that Tul1 can be auto-ubiquitinated by Ubc4 and Ubc5 (Figure 3.2A) and, interestingly, can also ubiquitinate noncanonical protein substrates CPY and CPY* in the presence of either Ubc enzyme (Figure 3.2B). We do not conclude from this work that CPY, nor CPY*, are substrates of Tul1, but rather interpreted this data to show that Ubc4 and Ubc5 are active in the Tul1 system. Recently published reconstitution experiments also found that the non-protein substrate phosphatidylethanolamine (PE) was ubiquitinated by Tul1 with Ubc4 or Ubc5 [14]. It should be noted that Ubc4 and Ubc5 are paralogs, as Ubc5 arose from a chromosomal duplication and is generally thought to be expressed specifically under high-stress conditions [7,35]. We therefore consider Ubc4 and Ubc5 synonymous in further discussions of Ubc-related mechanisms (Figure 3.2).

Ubc4/Ubc5 can conjugate both K48-and K63-ubiquitin chains [36] and therefore, at face-value, are not easy candidates to consider in a model proposing that Tul1 selectively recruits different Ubc enzymes to ubiquitinate proteasomal substrates with K48-linkages and vacuolar substrates with K63-linkages. However, after a Ubc enzyme is recruited, intermolecular interactions with the ubiquitin ligase influences how the Ubc enzyme is positioned for substrate ubiquitination, which can also determine what type(s) of polyubiquitin linkage(s) are formed [17,18]. This leads us to consider another mechanism, in which Tul1 selectively conjugates proteasomal substrates with K48-linkages and vacuolar substrates with K63-linkages not by recruiting different

Ubc enzymes, but rather by how it positions a Ubc enzyme for substrate ubiquitination. Tul1 might recruit the same Ubc enzyme regardless of the substrate, for which Ubc4/5 seem the likely candidate [7,14,36] (Figure 3.2), but specifically position Ubc4/5 to only conjugate of K48- or K63-linkages on proteasomal or vacuolar substrates, respectively. In the context of this mechanism, perhaps the altered-substrate-selectivity RING mutants abrogated discreet intermolecular interactions that position Ubc4/5 for K48-linkages, but only attenuated interactions required for K63-linkages to be built, resulting in stabilized proteasomal substrate but slight vacuolar substrate degradation.

It is certainly possible that a parallel mechanism, in which Tul1 specifically positions each class of substrate for ubiquitin conjugation by a common Ubc enzyme, determines if they will contain either K48- or K63-linkages. This would posit that Tul1-substrate recruitment and interaction(s), not Ubc enzyme engagement, are the primary factors in selectively conjugating each ubiquitin-linkage type [17,18]. While it is likely that discreet intermolecular interactions between Tul1 and its substrates influence if/how proteins are ubiquitinated, evidence we have collected in Chapter 2 does not indicate that differential interactions alter Tul1 substrate selectivity. The altered-specificity mutations we characterized fall around zinc-coordinating residues in the RING domain [13,17,18], which are involved in Ubc enzyme recruitment and engagement. We therefore favor mechanisms for differential Tul1 substrate ubiquitination models that center on interactions with ubiquitination machinery.

In our discussion of two ubiquitination-machinery based mechanisms for how Tul1 directs substrate selectivity, we proposed that K48- and K63-chains are built on proteasomal and vacuolar substrates, respectively (Figure 3.1A). However, we so far omitted other known characteristics of polyubiquitin chains that can direct proteins to proteasomal or vacuolar pathways. First, we simplified our model by implying substrates are conjugated with homotypic K48- or K63-linkages, but it is important to recognize that heterotypic K48/K63 linkages are often associated with protein degradation, perhaps even accounting for ~50% of all ubiquitin linkages associated with proteasomal degradation [37]. One mechanism that can build these heterotypic chains is through sequential Ubc enzyme engagement, during which a ubiquitin ligase will first engage one Ubc enzyme to place initial ubiquitin(s) onto a substrate, which then acts as a ‘seed’ for extending the ubiquitin chain by engaging a different Ubc enzyme. Sequential Ubc enzyme activity is required for the Doa10 ubiquitin ligase-centric ERAD system to proteasomally degrade substrates from the

ER membrane, though this activity is also associated with many other cellular functions including non-degradative pathways [38–41]. Therefore, a combination of both proposed mechanisms is interesting to consider, in which Tul1 might recruit the same Ubc enzyme for initial ubiquitination of both classes of Tul1 substrate, but divergent sequential engagement of specific Ubc enzyme(s) leads to different types of ubiquitin linkages that direct substrates to each degradation pathway.

Contributing to this theory is the discovery that Ubc1, Ubc4, and Ubc5, all of which we referenced in earlier mechanisms of this model, are considered to be in a Ubc enzyme family with overlapping functions; haploid *ubc1*Δ*ubc4*Δ cells are inviable and Ubc4 and Ubc1 are found to act sequentially on protein substrates to build different types of polyubiquitin chains [40,42]. Specifically, the soluble ubiquitin ligase anaphase-promoting complex (APC) in yeast recruits Ubc4 to monoubiquitinate substrate before engaging Ubc1 to build K48-ubiquitin chains for proteasomal degradation [40]. Ubc1 also contains a ubiquitin-associating (UBA) domain, which was found to specifically interact with K63-polyubiqutin to build K48/K63 chains on a target protein in yeast [43]. With this in mind, one could speculate that all Tul1 substrates are first conjugated with a monoubiquitin or short K63-ubiquitin chains by Ubc4. Tul1 might then selectively recruit Ubc1 to extend K48/K63 linkages on a proteasomal substrate, while Tul1 restricts ubiquitination of vacuolar substrates by Ubc1, causing them to remain in a monoubiquitinated or K63-polyubiquitianted state. As we observed in the AlphaFold-predicted interaction between Tul1 and Ubc4, altered-substrate-selectivity Tul1 RING mutations do not seem to interfere with Ubc4 interactions, therefore perhaps allowing it to add the 'seed' K63-chains or monoubiquitin, but, as suggested in previous mechanisms, perhaps these mutations only interrupt Ubc1 interactions, resulting in specific stabilization of the proteasomal substrate.

The idea that perhaps proteasomal substrates are specifically conjugated with longer polyubiquitin chains while vacuolar substrates are mono/multiubiquitinated or contain shorter polyubiquitin chains introduces another important characteristic of the ubiquitin proteasome system that we have yet to discuss in our Tul1 selective-substrate-ubiquitination model. In addition to the type of linkages, the length of a polyubiquitin chain is also important for specifically engaging the proteasome [27]. This requirement is traditionally considered to be at least four K48-linked ubiquitin chains, though other types of polyubiquitin chains containing greater than four moieties, including K63-polyubiquitin, have been shown to sufficiently cause proteins to be degraded by the proteasome in reconstitution experiments [21,27]. Meanwhile, monoubiquitin is

found to be sufficient for entry into ESCRT-mediated degradation in the vacuole, though short chains containing up to four K63-linked ubiquitin increases affinity for ESCRT components [7,23,26,44].

This introduces another model in which Tul1 selectively conjugates different lengths of ubiquitin chains, not different linkage-types, onto each class of substrate (Figure 3.1B). Tul1 might direct proteasomal substrates to be conjugated with long polyubiquitin chains, allowing for recognition by the 26S proteasome, while vacuolar substrates are mono/multiubiquitinated or contain short chains of ubiquitin that are not preferred by the proteasome, but can be engaged by ESCRT. For example, perhaps proteasomal Tul1 substrates are conjugated with K63-pentamer chains, which have been shown to result in protein degradation by the proteasome [27], while vacuolar substrates contain K63-tetraubiquitin chains [26], allowing for recognition specifically by ESCRT-0 and facilitating vacuolar degradation. The Tul1 RING mutations that altered substrate specificity might be unable to build long chains of ubiquitin, which would specifically impair degradation of a proteasomal substrate if the short linkages are not compatible with 19S recognition. This is especially true if these mutants only facilitate monoubiquitination of substrates by Ubc4/5. Monoubiquitin is sufficient for ESCRT-mediated degradation of proteins in the vacuole, though previous studies observed that a Tul1 vacuolar substrate is less efficiently targeted to the vacuole if restricted to monoubiquitination [7], which is a phenomenon observed with other non-Tul1 vacuole-fated proteins due to reduced affinity for ESCRT-0 components [26]. Restricted functionality of the altered-specificity Tul1 RING mutants to only monoubiquitinate substrates offers a clear explanation for why proteasomal substrate degradation was inhibited while vacuolar substrates were degraded, though not at wild-type levels.

There are several mechanisms that could fall into our ubiquitin-length model for Tul1 substrate selectivity. Previously introduced Ubc enzyme-based mechanisms, that could allow Tul1 to selectively conjugate different types of ubiquitin linkages, also apply to this model that Tul1 ubiquitinates each class of substrate with different chain lengths. For the sake of brevity, they will not be repeated in the context of our ubiquitin-chain-length model, outside of stating that what Ubc enzyme is recruited and how a Ubc enzyme engages with the ubiquitin ligase can modulate the lengths of ubiquitin conjugated onto a substrate [17,18].

A new possible mechanism, that applies specifically to our ubiquitin-length model, posits that the rates of proteasomal and vacuolar substrate ubiquitination by Tul1 differ, which could be

regulated by intermolecular interactions between Tul1 and each class of substrate and/or the recruited Ubc enzyme. The efficiency with which ubiquitin chains are built is proposed to play a role in regulating substrate degradation, lending to the idea that a 'ubiquitination threshold' exists in cells to prevent premature or mistaken degradation of proteins by the proteasome [17,19]. Tul1 might rapidly ubiquitinate a proteasomal substrate to build sufficiently long polyubiquitin chains upon entry in the early Golgi, allowing for 26S proteasome engagement (Figure 3.3A). Conversely, a vacuolar substrate might be slowly ubiquitinated by Tul1, resulting in monoubiquitin or short polyubiquitin chains that are not recognized by the 19S regulatory cap for proteasomal degradation, allowing it to traffic to endosomal compartments where the chains can be recognized by ESCRT-0 (Figure 3.3A). If our altered-specificity RING mutants have generally impaired substrate ubiquitination efficiency, this would explain why the proteasomal substrate Orm2 is stabilized while there is some vacuolar substrate degradation. Specifically, if Orm2 is not degraded by Tul1 at the Golgi membrane, it was found to cycle back to the ER membrane instead of trafficking to endosomal compartments [6], where it might have been recognized by ESCRT and degraded in the vacuole. Meanwhile, reduced ubiquitination efficiency might only slightly impair recognition of the vacuolar substrates by ESCRT, resulting in the slight degradation of these proteins.

The length of polyubiquitin on a substrate can also be modulated by the activity of deubiquitinating enzymes (DUBs), which can selectively edit or trim polyubiquitinated proteins based on length, and even linkage-type [45–47]. The DUB Doa4 was found to be active in a Tul1 reconstituted system for non-protein substrate PE deubiquitination, [14] and loss of Doa4 is synthetic-lethal under heat stress conditions when deleted from the genome concurrently with Tul1 [15]. Doa4 plays an important role in ubiquitin recycling at the endosome for proper MVB formation, as well as in the ubiquitin proteasome system, though any linkage 'editing' function of this enzyme has not been documented [14,48,49]. Overall, the mechanisms of DUB regulation in degradative quality control systems are still quite unclear, which makes this a hard model to consider [45–47].

The altered-selectivity Tul1 mutants that we discovered in Chapter 2 resulted from substitutions in RING domain residues and we therefore have focused our attention in this section on considering the role of Tul1 in the ubiquitination cascade and how it might influence substrate selectivity. The proposed models in this section highlight several mechanisms that allow Tul1 to direct substrates to proteasomal or vacuolar degradation pathways by selectively conjugating

different linkages and/or lengths of ubiquitin chains by differential engagement with Ubc enzymes. However, while investigating the Tul1 system, it is hard to ignore the fact that proteasomal substrates and vacuolar substrates localize to different organelles in the secretory pathway. As explored in the next section, this observation invites other models that bring into consideration that substrate localization might play a role in the Tul1 system's selectivity (Figure 3.3).

3.2.2 Substrate localization plays a role in Golgi-localized Tul1 selectivity

The Golgi-localized Tul1 proteasomal substrate Orm2 is an ER resident protein that dissociates from the SPOTS complex and traffics to the Golgi when it is phosphorylated under low sphingolipid cellular environments [6]. It is thought that Orm2 is rapidly ubiquitinated and degraded at the Golgi membrane, suggesting that Tul1 ubiquitinates Orm2 in early Golgi compartments, though whether Tul1 responsible for Orm2 extraction from the Golgi membrane for proteasomal degradation is not exactly clear, but is speculated on later in Section 3.3 [6]. Genetic deletion of Tul1 results in Orm2 retrograde trafficking to the ER membrane, suggesting that it does not continue in or engage with other components further on in the secretory pathway, including ESCRT, if not degraded at the Golgi; Orm2 does not traffic through the VPS pathway to the vacuole for degradation [6].

In contrast, all known vacuolar substrates of the Golgi-localized Tul1 system are mutant or modified forms of proteins that normally localize to the Golgi and early or late endosomal compartments [7–10,16]. For example, the work performed in Chapter 2 used previously characterized Tul1 substrates Pep12* and Tlg1* to monitor Tul1 vacuolar degradation. Both of these SNARE proteins are involved in vesicle fusion events across the VPS pathway; Pep12 cycles between late endosomal and vacuolar compartments and Tlg1 cycles through late Golgi and early endosomal compartments [50–52]. Genetic deletion of Tul1 results in Pep12* and Tlg1* accumulation in late endosomal/Class E compartments [7,8]. This indicates that these proteins fail to engage ESCRT in the absence of Tul1 [7,8,53,54], but equally reveals that these mutant SNAREs traverse the VPS pathway, where they might continue to interact with Gld1-containing Tul1 complexes [10] unlike Orm2 which seemingly only interacts with Tul1 at the early Golgi [6].

With this in mind, we recall one of the mechanisms that we previously introduced in Section 3.2.1, in which Tul1 substrate ubiquitination rates are different between vacuole- and proteasome-fated proteins, resulting in different lengths of ubiquitin being conjugated for

recognition by a specific pathway and driving substrate selectivity. As previously proposed, perhaps all Tul1 substrates are recognized and ubiquitinated by Tul1 upon entry into the Golgi, but that Tul1 affinity for vacuolar substrates is lower, resulting in reduced ubiquitination rates (Figure 3.3A). Putting this mechanism in the context of known substrate localization characteristics, it is logical to assume that Orm2 is rapidly ubiquitinated for proteasomal degradation in the Golgi given it does not move beyond the Golgi in the secretory pathway [6]. Meanwhile, Pep12* and Tlg1* continue to traverse the VPS pathway along with Gld1-containing Tul1 complexes [7,8,10], which could allow continued ubiquitination events to occur and potentially the eventual conjugation of sufficient polyubiquitin length(s) for efficient ESCRT engagement, once localized to endosomal compartments (Figure 3.3A). Again, if our altered-specificity mutants have reduced, but not disrupted, substrate ubiquitination rates, this would prevent rapid Orm2 ubiquitination at the Golgi which could fail to engage the proteasome and result in stabilization, while still somewhat ubiquitinating the mutant SNAREs, allowing for some vacuolar substrate degradation for reasons already discussed in Section 3.2.1.

Alternatively, moving away from a ubiquitin-based mechanism, perhaps endogenous binding partners of vacuolar substrates prevent their extraction from the Golgi membrane, therefore inhibiting proteasomal degradation and trapping them a ubiquitinated state for later recognition by ESCRT in endosomal compartments (Figure 3.3B). Pep12 and Tlg1 have several known binding partners required for trafficking through the VPS pathway, for example GGA adaptors are thought be involved with Pep12 endosomal localization [55] and Ent5 with proper localization of Tlg1 to endosomes [56]. Given that Pep12* and Tlg1* are still trafficked via the VPS pathway [7,8], and that Pep12* is also still functional if not degraded by Tul1 [7], it is logical to think that these clathrin adaptor proteins still interact with these mutant SNAREs and perhaps equally prevent their extraction from the Golgi membrane and subsequent degradation by the cytosolic proteasome (Figure 3.3B). ESCRT functions in late endosomes and these adaptors are likely naturally recycled upon entry into late endosomes, and therefore should not impede ESCRT participation. Even if these components are not recycled before ESCRT engagement, internalization of proteins into multivesicular bodies does not require them to be extracted from the membrane. Therefore, it is not unreasonable to propose that the trafficking factors involved with sending mutant SNAREs to late endosomes make them natural candidates for specific entry into the ESCRT pathway by preventing extraction for proteasomal degradation.

Similarly, but returning to a ubiquitin-based mechanism, it is possible that Tul1 facilitates vacuolar substrate entry into the ESCRT pathway by ubiquitinating PE at endosomes and the vacuole, which is proposed to stimulate ESCRT and MVB formation (Figure 3.3C) [14]. If certain residues in Tul1 (or complex components, discussed next in Section 3.2.3) are required for PE ubiquitination but not protein substrate ubiquitination, mutations in these regions could specifically impair vacuolar but not proteasomal degradation. It should be noted that none of the phenotypes of the Tul1 mutants we identified in Chapter 2 would support this model, but we also did not test the identified Tul1 mutants for their ability to ubiquitinate PE. Further investigation of the function(s) associated with of Tul1 PE ubiquitination, in general, are also required.

Another important difference between Orm2 and the mutant SNAREs that tangentially relates to substrate localization is that Orm2 is exclusively degraded by Gld1-Tul1 complexes. Though Pep12* and Tlg1* are primarily degraded by Gld1-Tul1 complexes, we observed some degradation by Vld1-Tul1 complexes, which were thought to only be functional at vacuolar membrane [10]. This observation might be due to the different trafficking pathways used by either subcomplex from the Golgi; Vld1-Tul1 complexes are trafficked to the vacuole via the AP3 pathway while Gld1-Tul1 complexes are trafficked to endosomal compartments via the VPS pathway [10]. Co-immunoprecipitation assays in Chapter 2 found that Pep12* and Tlg1* interact with both Vld1-Tul1 and, unsurprisingly, Gld1-Tul1. Perhaps Vld1-Tul1 is active before it is localized to the vacuole, and therefore somewhat ubiquitinates Pep12* or Tlg1* while occupying the same space in the Golgi membrane, resulting in the observed inefficient degradation of these substrates in the absence of Gld1-Tul1. Meanwhile, Gld1-Tul1 complexes traverse the same trafficking pathway and cycle through the same organelles as Pep12* and Tlg1* [7,8,10], thus increased access to substrates across the VPS pathway perhaps results in Gld1-Tul1 primary degradation. However, the exclusivity of Gld1-Tul1 complexes to degrade the proteasomal substrate Orm2 indicates a potential role for Gld1 in proteasome-specific Tul1 system function, which will be discussed in the next section.

3.2.3 Other Tul1 complex component(s) direct substrate fates

We have so far posited several Tul1-dependent and Tul1-independent mechanisms describing how the Tul1 system might direct selective substrate degradation, focusing on models operating within the ubiquitination cascade and substrate localization (Figures 3.1 & 3.3). Each of

these models focused on potential roles of various cytosolic and lumenal soluble proteins, of which most are mostly not proven interactors with the Tul1 system, aside from several Ubc enzymes and obviously the Tul1 ubiquitin ligase itself. Golgi-localized Tul1 is in complex with four other integral membrane proteins, Dsc2, Dsc3, Ubx3, and Gld1. The function(s) of each component within the complex are unknown, despite the annotated domains, outlined in Chapter 1 and summarized in Table 3.1. It is quite possible that these known integral membrane components of the Tul1 complex play an important role in substrate selection, including playing a potential role in positioning substrates for specific ubiquitination, but that such function(s) are overshadowed by their necessity to correctly assemble the Tul1 complex.

Functional assays in Chapter 2 confirmed that Dsc2, Dsc3, and Ubx3 are indispensable for the degradation of proteasomal and vacuolar substrates, though this is likely because full Tul1 complex construction is required for trafficking from the ER to the Golgi membrane [6,10,16]. Localization to the Golgi appears to be a prerequisite for complex function and therefore might preclude additional function(s) of the known Tul1 complex components that could be specific to proteasomal or vacuolar degradation [6,10,16]. The role of other known Tul1 complex components in selective degradation is worth exploring. For example, Dsc2 contains a UBA domain, which can characteristically bind to ubiquitin chains. Therefore, Dsc2 could bind specifically to K63 linkages on a vacuolar substrate, instead of ESCRT-0 components previously proposed to have this function, to prevent their degradation by the proteasome and specifically allow vacuolar substrate entry into ESCRT [28].

Importantly, outside the Tul1 RING mutants found in Chapter 2, Gld1 is only clear factor in the known core complex that, when genetically deleted, resulted in altered Tul1 substrate specificity. Outside of the requirement for trafficking Golgi-localized Tu1l complexes through the VPS pathway [10], our functional assays and work from other groups demonstrated that Gld1 is absolutely required for degradation of the Tul1 proteasomal substrate Orm2 [6]. As mentioned, we discovered in Chapter 2 that vacuolar substrates were still slightly degraded in a *gld1*Δ cell, suggesting that vacuole-localized Tul1 complexes (containing Vld1 instead of Gld1) are also able to inefficiently degrade Golgi-Tul1 vacuolar substrates. This potentially implicates a role for Gld1 specific to Tul1 proteasomal substrate degradation; studying Gld1 is an obvious next candidate to dissect to understand why it is necessary for Tul1 proteasomal substrate degradation.

There are no homologous domains within Gld1 that indicate how it could specifically direct substrates for proteasomal degradation [10], but this component could play a role in orienting proteasomal substrates for ubiquitin conjugation or chain building, reflecting back to the differential ubiquitin-type models introduced in Section 3.2.1. Gld1 could also have undefined cytosolic domains that assist in interaction with proteasomal machinery, such as adaptors that help recruit the proteasome to the Golgi membrane. There is a plethora of mechanisms that could be speculated on due to a lack of annotated domains in the protein, however a good first step is to determine whether specific residues and/or regions within Gld1 are essential to proteasomal versus vacuolar substrate degradation. This, along with explorations of every other known complex component, can be accomplished by performing deep mutational scanning experiments using the pipeline and the functional assays established in this thesis. It is worth mentioning that perhaps unknown components that are part of the core Tul1 complex also play a role in Tul1 substrate selectivity but have yet to be discovered. Again, the tools established in this thesis can be adapted to determine if novel undefined complex components are important to either or both classes of Tul1 substrates.

3.2.4 Proposed Tul1 selective substrate degradation model

This section introduced several models that could direct how Golgi-localized Tul1 substrates are designated for the proteasome versus the vacuole. Many of these models incorporated observations from other ubiquitin ligases and their substrates in eukaryotic systems, however the specific mechanisms and functions of these systems are also relatively unknown. As such, further exploration into the selectivity of Golgi-localized Tul1 substrate degradation will equally contribute to understanding the mechanisms of other ubiquitin ligase systems in the eukaryotic secretory pathway. Based on data presented in Chapter 2, and in conversation with published Tul1 studies from other groups, we favor that Tul1 conjugates different lengths of ubiquitin chains onto vacuolar versus proteasomal substrates to direct proteins to specific degradation pathways (Figure 3.3A). RING mutants with altered specificity are clustered at the RING/Ubc4/ubiquitin interaction site, but do not likely prohibit Ubc4 engagement. These mutations could alter intermolecular interactions by Tul1 and Ubc4 that build linkages differently on proteasomal versus vacuolar substrates. Published work from the groups of Hugh Pelham (Pep12 and Tlg1) and David Teis (Orm2) lend support to this model: Pep12* was successfully

targeted to the vacuole when conjugated with monoubiquitin [7]. Anti-ubiquitin immunoblotting of un-palmitoylated Tlg1 (a consequence of the di-leucine mutation in Tlg1*) seems to contain short di-ubiquitin chains [8], while Orm2 smearing in insoluble and soluble fractions indicates conjugation with longer poly-ubiquitin chains [6]. Before continuing to speculate on which potential mechanism(s) we introduced earlier in this section might be involved, however, we should first focus on determining if this model is correct by adapting the biochemical and cellular assays established in Chapter 2.

3.3 Implications of the ERAD Hrd1 complex function on Tul1 complex function

While considering the function of the Tul1 system, it is hard to disregard the high levels of similarity between components of Golgi-localized Tul1 and the Hrd1 ERAD systems. These complexes both center on integral membrane ubiquitin ligases, with other components sharing many of the same conserved functional domains (Table 3.1), and both can degrade integral membrane proteins via the ubiquitin-proteasome system. It is therefore tempting to propose that Tul1 and Hrd1 systems share similar degradation mechanics and functions. Though the work in this thesis does not directly test any of these shared features, this section will explore the possible implications that published studies of the Hrd1 system could have on our understanding of the Golgi-localized Tul1 system and how they might direct future Tul1 studies.

All currently defined Tul1 protein substrates are integral membrane proteins [6–9,16] while Hrd1 degrades both integral membrane and soluble/lumenal proteins [57]. The transient nature of Golgi soluble/lumenal proteins likely impedes our ability to easily define if and how these proteins are degraded by Golgi-localized protein quality control systems. However, analysis of published quantitative proteomic data sets from previous studies suggest the existence of potential soluble Tul1 substrates, though these proteins remain to be characterized as direct targets of Tul1 for degradation from the Golgi lumen [6,15]. Furthermore, the experiments that generated these data sets used indirect methods to survey potential Tul1 substrates, defining candidates based on those with reduced levels of ubiquitination [22] or increased protein stability [6] in *tul1*Δ cells. Work in Chapter 2 reveals many amino acids within the Tul1 lumenal domain that are tolerant to mutations, making them candidates for substitution of an unnatural amino acid residue, which could be used for cross-linking experiments and mass spectrometry [58]. This could lead to characterization of more Tul1

substrates with highly transient interactions, including potentially soluble/lumenal proteins, or even new complex components given the role of the lumenal domain defined in Chapter 2.

Exploration of whether Golgi-localized Tul1 can degrade soluble/lumenal substrates from the Golgi could potentially address a major open question in the field of ubiquitin-dependent protein quality control in the secretory pathway. There are currently no clear eukaryotic quality control system that recognizes and degrades soluble/lumenal proteins via the ubiquitin-proteasome system outside of the Hrd1 complex, which operates at the ER. For a ubiquitin ligase system to recognize and degrade soluble/lumenal proteins at the Golgi, it must 1) be able to access and interact with proteins in the Golgi lumen and 2) have the capability to retrotranslocate and expose substrates to the cytosol for ubiquitination and engagement with the 26S proteasome. The Golgi-localized Tul1 complex is an interesting potential candidate for this question not only because it bears striking similarities to the Hrd1 complex (Table 3.1), but because predicted Tul1 structures suggested that it can meet these criteria.

Like Hrd3 in the Hrd1 complex, Tul1 has a predicted large lumenal domain (which composes half of the entire protein), meaning it could have access to these soluble/lumenal proteins, and is known to ubiquitinate and degrade substrates in the secretory pathway. Another structural/functional implication of Tul1 we can gather from studies of the Hrd1 complex is the potential formation of a Tul1 retrotranslocon, therefore meeting the second requirement introduced for Tul1 to be able to degrade soluble/lumenal proteins. Hrd1 forms a retrotranslocon channel to move substrates through the ER membrane into the cytosol for ubiquitination and/or for proteasomal degradation [59–61]. Comparison of AlphaFold multimer models of the Golgi-localized Tul1 complex [11,12] to the experimentally-determined cryoEM model of the ERAD complex [61,] would suggest that Tul1 and Gld1 might align to where the probable channel is formed by Hrd1/Der1 (data not shown) [11,12]; it is also possible Tul1 can homodimerize to serve as this channel, like Hrd1 [59,62].

Continuing in speculation of a putative Tul1 retrotranslocon, it is important to note that the Hrd1 channel is regulated by the DUB Ubp1 [63]. Perhaps DUB(s) also regulate Tul1 function and this hypothetical Tul1 retrotranslocon. Outside of AlphaFold predictive modeling, there is currently no experimental evidence indicating if or how Tul1 forms a channel for proteasomal substrate extraction and degradation. That being said, if the altered-specificity RING mutations impair the ability of a hypothetical retrotranslocon to form, or for a DUB to interact with and

regulate this channel, it would most dramatically impair proteasomal substrate degradation, as these proteins would fail to be extracted for degradation by the 26S proteasome. ESCRT-mediated vacuolar degradation does not require substrates to be extracted from the membrane, but vacuolar substrate degradation might be attenuated as loss of DUB regulation could lead to increased turnover of Tul1, like in the Hrd1 system [63]. This would align to the functional phenotype of these altered-specificity RING mutants, especially considering that we observed decreased stability for one of these mutants. However, further investigation into the role(s) and regulation(s) of Tul1 proteasomal substrate extraction first requires a better understanding of the Tul1 system, including experimentally defining the hypothetical Tul1 retrotranslocon, outside of speculation invited by the Hrd1 ERAD system.

3.4 Conclusion

Protein quality control in the eukaryotic secretory pathway requires continued studies to understand the important mechanisms that maintain cellular proteostasis. The under-studied nature of these pathways subject them to analysis based mostly on speculation, though the function(s) of these systems have clear implications and future applications in human health and disease. The work presented in this thesis contributes to our understanding of the Tul1 protein quality control system that operates at the Golgi membrane in *S. cerevisiae*. It furthers our understanding of domain functions within the integral membrane ubiquitin ligase Tul1 and introduces tools that can be used to continue exploration of the mechanisms by which this system selectively designates a substrate for degradation by the proteasome versus the vacuole. Future work, built on the results and tools presented in this thesis, holds implications for our understanding of how ubiquitination machinery plays a selective role in designating substrate degradation fate through eukaryotic secretory pathway quality control.

3.5 Figures

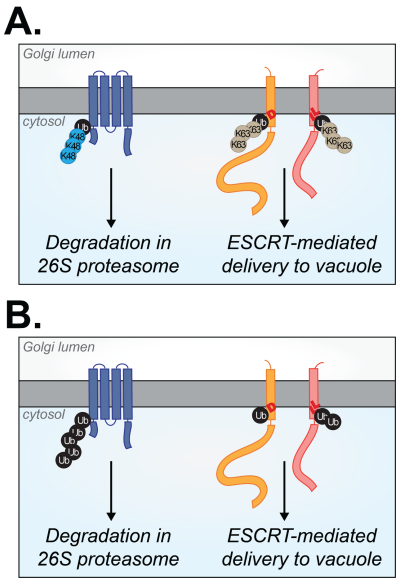

Figure 3.1: The type of ubiquitin linkages specifically conjugated by Golgi-localized Tul1 could direct substrates to the proteasome versus the vacuole.

Figure 3.1: The type of ubiquitin linkages specifically conjugated by Golgi-localized Tul1 could direct substrates to the proteasome versus the vacuole.

A) Tul1 recruits Ubc enzyme(s) to specifically conjugate proteasomal substrates with K48-linked ubiquitin and vacuolar substrates with K63-linked ubiquitin.
B) Tul1 recruits Ubc enzyme(s) to specifically conjugate long ubiquitin chains onto proteasomal substrates for degradation while vacuolar substrates are conjugated with shorter ubiquitin chains.

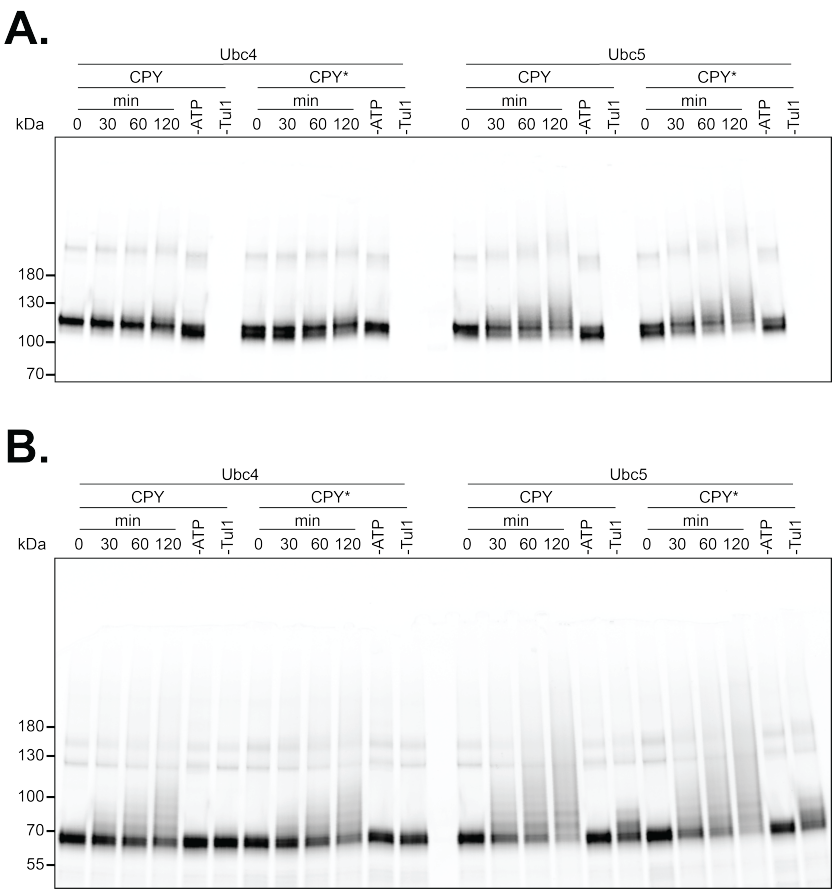

Figure 3.2: Ubc4 and Ubc5 are active in reconstituted Tul1 ubiquitination assays.

Figure 3.2: Ubc4 and Ubc5 are active in reconstituted Tul1 ubiquitination assays.

A) Tul1 was purified and sortase-labeled with Dylight680. Purified Dylight680-Tul1 was incubated with purified ubiquitin, Uba1 (E1 enzyme), Ubc4 or Ubc5 (E2 enzymes), FAM-labeled CPY or FAM-labeled CPY* (potential substrates), and ATP to allow *in vitro* ubiquitination (as described in [59]). The reactions were separated by SDS-PAGE and Tul1 autoubiquitination was visualized by in-gel fluorescence scanning. -ATP served as a negative control for the reaction and -Tul1 served as negative control for ubiquitin ligase activity for potential substrates.

B) As in (A) but with fluorescence scanning of the FAM-labeled CPY or CPY* in the ubiquitination reactions. In these *in vitro* reactions, Ubc5 without Tul1 (-Tul1) showed some levels of CPY and CPY* ligase-independent ubiquitination, which are likely a phenomenon associated with these reconstitution assays due to combining high concentrations of the purified components.

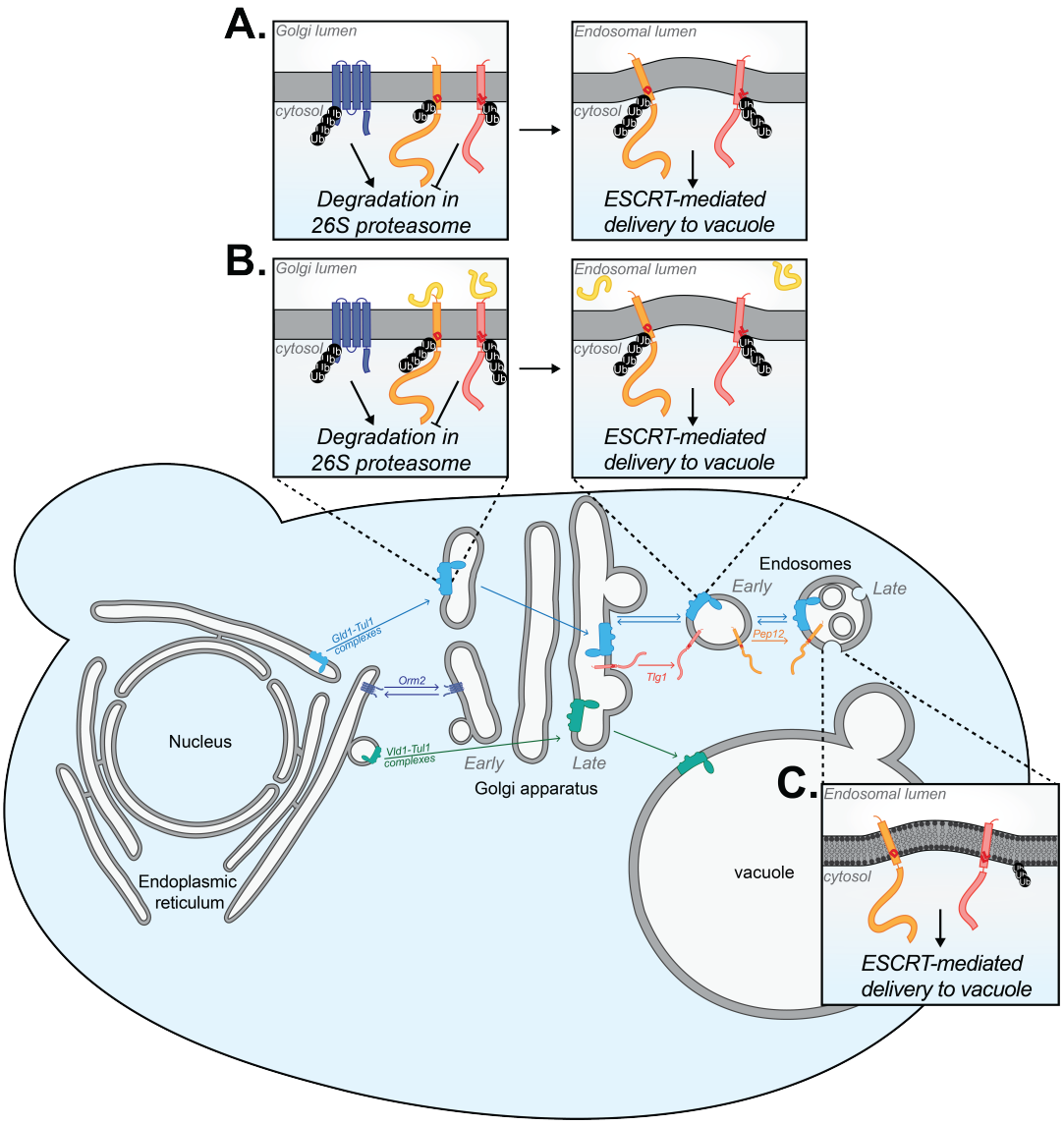

Figure 3.3: Substrate localization could play a role in Tul1 substrate specificity.

Figure 3.3: Substrate localization could play a role in Tul1 substrate specificity.

A) Ubiquitination of Tul1 proteasomal substrates could be more efficient, allowing for rapid engagement and degradation by the 26S proteasome at the Golgi membrane. Ubiquitination of Tul1 vacuolar substrates could less efficient, resulting in a slower building of chains, which are not recognized by degradative machinery until they are trafficked to endosomal compartments, where they are recognized by ESCRT components for vacuolar degradation.
B) Tul1 substrates might share the same ubiquitination profile, but proteins that interact with vacuolar substrates could prevent their extraction from the Golgi membrane for proteasomal degradation, which would leave them in a ubiquitinated state upon entry into endosomal compartments where they would then be recognized by ESCRT machinery for vacuolar degradation.
C) Polyubiquitination of PE in the endosomal lipid bilayer promotes ESCRT interaction and degradation of substrates via ESCRT-mediated degradation in the vacuole.

3.6 Tables

Table 3.1: Comparing features of Tul1 and Hrd1 complex components.

Tul1 ***S. cerevisiae***	**Hrd1 ERAD** ***S. cerevisiae*** [64]	**Shared Features**
Tul1 [7]	Hrd1	Integral membrane RING-type E3 ligase [7,64,65]
Tul1	Hrd3	Large lumenal domain
Dsc2 [15]	Der1	Contains ubiquitin-associated (UBA) domain; resembles a rhomboid pseudoprotease [15,64,65]
Dsc2	Dfm1	Rhomboid pseudoprotease
Dsc3 [15]	Usa1	Contains ubiquitin-like (UBL) domain [15,64,65]
Gld1[10]	---	Essential for complex function at the Golgi, though components lack notable homology; localizes Tul1 to Golgi [10,64,65]
Vld1 [10]	---	Essential for vacuole-Tul1 localization and function; considered related to Dsc4 though components lack homology and localize to different organelles
Ubx3 [15]	Ubx2	Contains a ubiquitin regulatory X (UBX) domain; facilitates Cdc48 association to each complex [15,16,64,65]

3.7 References

1. Sun, Z. & Brodsky, J. L. Protein quality control in the secretory pathway. *J. Cell Biol.* **218**, 3171–3187 (2019).
2. Arvan, P., Zhao, X., Ramos-Castaneda, J. & Chang, A. Secretory pathway quality control operating in Golgi, plasmalemmal, and endosomal systems. *Traffic Cph. Den.* **3**, 771–780 (2002).
3. Schwabl, S. & Teis, D. Protein quality control at the Golgi. *Curr. Opin. Cell Biol.* **75**, 102074 (2022).
4. Buzuk, L. & Hellerschmied, D. Ubiquitin-mediated degradation at the Golgi apparatus. *Front. Mol. Biosci.* **10**, 1197921 (2023).
5. Sardana, R. & Emr, S. D. Membrane Protein Quality Control Mechanisms in the Endo-Lysosome System. *Trends Cell Biol.* **31**, 269–283 (2021).
6. Schmidt, O. *et al.* Endosome and Golgi-associated degradation (EGAD) of membrane proteins regulates sphingolipid metabolism. *EMBO J.* **38**, (2019).
7. Reggiori, F. & Pelham, H. R. B. A transmembrane ubiquitin ligase required to sort membrane proteins into multivesicular bodies. *Nat. Cell Biol.* **4**, 117–123 (2002).
8. Valdez-Taubas, J. & Pelham, H. Swf1-dependent palmitoylation of the SNARE Tlg1 prevents its ubiquitination and degradation. *EMBO J.* **24**, 2524–2532 (2005).
9. Dobzinski, N., Chuartzman, S. G., Kama, R., Schuldiner, M. & Gerst, J. E. Starvation-Dependent Regulation of Golgi Quality Control Links the TOR Signaling and Vacuolar Protein Sorting Pathways. *Cell Rep.* **12**, 1876–1886 (2015).
10. Yang, X., Arines, F. M., Zhang, W. & Li, M. Sorting of a multi-subunit ubiquitin ligase complex in the endolysosome system. *eLife* **7**, e33116 (2018).
11. Cianfrocco, M. A., Wong-Barnum, M., Youn, C., Wagner, R. & Leschziner, A. COSMIC2: A Science Gateway for Cryo-Electron Microscopy Structure Determination. in *Proceedings of the Practice and Experience in Advanced Research Computing 2017 on Sustainability, Success and Impact* 1–5 (ACM, New Orleans LA USA, 2017). doi:10.1145/3093338.3093390.
12. Evans, R. *et al. Protein Complex Prediction with AlphaFold-Multimer*. http://biorxiv.org/lookup/doi/10.1101/2021.10.04.463034 (2021) doi:10.1101/2021.10.04.463034.
13. Garcia-Barcena, C., Osinalde, N., Ramirez, J. & Mayor, U. How to Inactivate Human Ubiquitin E3 Ligases by Mutation. *Front. Cell Dev. Biol.* **8**, 39 (2020).
14. Sakamaki, J.-I. *et al.* Ubiquitination of phosphatidylethanolamine in organellar membranes. *Mol. Cell* **82**, 3677-3692.e11 (2022).
15. Tong, Z., Kim, M.-S., Pandey, A. & Espenshade, P. J. Identification of Candidate Substrates for the Golgi Tul1 E3 Ligase Using Quantitative diGly Proteomics in Yeast. *Mol. Cell. Proteomics* **13**, 2871–2882 (2014).
16. Li, M., Koshi, T. & Emr, S. D. Membrane-anchored ubiquitin ligase complex is required for the turnover of lysosomal membrane proteins. *J. Cell Biol.* **211**, 639–652 (2015).
17. Deshaies, R. J. & Joazeiro, C. A. P. RING Domain E3 Ubiquitin Ligases. *Annu. Rev. Biochem.* **78**, 399–434 (2009).
18. Metzger, M. B., Pruneda, J. N., Klevit, R. E. & Weissman, A. M. RING-type E3 ligases: Master manipulators of E2 ubiquitin-conjugating enzymes and ubiquitination. *Biochim. Biophys. Acta BBA - Mol. Cell Res.* **1843**, 47–60 (2014).
19. Swatek, K. N. & Komander, D. Ubiquitin modifications. *Cell Res.* **26**, 399–422 (2016).

20. Zheng, N. & Shabek, N. Ubiquitin Ligases: Structure, Function, and Regulation. *Annu. Rev. Biochem.* **86**, 129–157 (2017).
21. Grice, G. L. & Nathan, J. A. The recognition of ubiquitinated proteins by the proteasome. *Cell. Mol. Life Sci.* **73**, 3497–3506 (2016).
22. Zhao, L., Zhao, J., Zhong, K., Tong, A. & Jia, D. Targeted protein degradation: mechanisms, strategies and application. *Signal Transduct. Target. Ther.* **7**, 113 (2022).
23. Lauwers, E., Jacob, C. & André, B. K63-linked ubiquitin chains as a specific signal for protein sorting into the multivesicular body pathway. *J. Cell Biol.* **185**, 493–502 (2009).
24. Erpapazoglou, Z. *et al.* A dual role for K63-linked ubiquitin chains in multivesicular body biogenesis and cargo sorting. *Mol. Biol. Cell* **23**, 2170–2183 (2012).
25. Komander, D. & Rape, M. The Ubiquitin Code. *Annu. Rev. Biochem.* **81**, 203–229 (2012).
26. Ren, X. & Hurley, J. H. VHS domains of ESCRT-0 cooperate in high-avidity binding to polyubiquitinated cargo. *EMBO J.* **29**, 1045–1054 (2010).
27. Martinez-Fonts, K. *et al.* The proteasome 19S cap and its ubiquitin receptors provide a versatile recognition platform for substrates. *Nat. Commun.* **11**, 477 (2020).
28. Nathan, J. A., Tae Kim, H., Ting, L., Gygi, S. P. & Goldberg, A. L. Why do cellular proteins linked to K63-polyubiquitin chains not associate with proteasomes? *EMBO J.* **32**, 552–565 (2013).
29. Christensen, D. E., Brzovic, P. S. & Klevit, R. E. E2–BRCA1 RING interactions dictate synthesis of mono- or specific polyubiquitin chain linkages. *Nat. Struct. Mol. Biol.* **14**, 941–948 (2007).
30. Sommer, T. & Jentsch, S. A protein translocation defect linked to ubiquitin conjugation at the endoplasmic reticulum. *Nature* **365**, 176–179 (1993).
31. Renz, C. *et al.* Ubc13-Mms2 cooperates with a family of RING E3 proteins in budding yeast membrane protein sorting. *J. Cell Sci.* **133**, jcs244566 (2020).
32. Rodrigo-Brenni, M. C., Foster, S. A. & Morgan, D. O. Catalysis of lysine 48-specific ubiquitin chain assembly by residues in E2 and ubiquitin. *Mol. Cell* **39**, 548–559 (2010).
33. Hofmann, R. M. & Pickart, C. M. Noncanonical MMS2-Encoded Ubiquitin-Conjugating Enzyme Functions in Assembly of Novel Polyubiquitin Chains for DNA Repair. *Cell* **96**, 645–653 (1999).
34. Pastushok, L., Moraes, T. F., Ellison, M. J. & Xiao, W. A Single Mms2 “Key” Residue Insertion into a Ubc13 Pocket Determines the Interface Specificity of a Human Lys63 Ubiquitin Conjugation Complex. *J. Biol. Chem.* **280**, 17891–17900 (2005).
35. Seufert, W. & Jentsch, S. Ubiquitin-conjugating enzymes UBC4 and UBC5 mediate selective degradation of short-lived and abnormal proteins. *EMBO J.* **9**, 543–550 (1990).
36. Hochstrasser, M. Ubiquitin-dependent protein degradation. *Annu. Rev. Genet.* **30**, 405–439 (1996).
37. French, M. E., Koehler, C. F. & Hunter, T. Emerging functions of branched ubiquitin chains. *Cell Discov.* **7**, 6 (2021).
38. Weber, A. *et al.* Sequential Poly-ubiquitylation by Specialized Conjugating Enzymes Expands the Versatility of a Quality Control Ubiquitin Ligase. *Mol. Cell* **63**, 827–839 (2016).
39. Ohtake, F., Saeki, Y., Ishido, S., Kanno, J. & Tanaka, K. The K48-K63 Branched Ubiquitin Chain Regulates NF-κB Signaling. *Mol. Cell* **64**, 251–266 (2016).
40. Rodrigo-Brenni, M. C. & Morgan, D. O. Sequential E2s Drive Polyubiquitin Chain Assembly on APC Targets. *Cell* **130**, 127–139 (2007).

41. Lips, C. *et al.* Who with whom: functional coordination of E2 enzymes by RING E3 ligases during poly-ubiquitylation. *EMBO J.* **39**, e104863 (2020).
42. Seufert, W., McGrath, J. P. & Jentsch, S. UBC1 encodes a novel member of an essential subfamily of yeast ubiquitin-conjugating enzymes involved in protein degradation. *EMBO J.* **9**, 4535–4541 (1990).
43. Pluska, L. *et al.* The UBA domain of conjugating enzyme Ubc1/Ube2K facilitates assembly of K48/K63-branched ubiquitin chains. *EMBO J.* **40**, e106094 (2021).
44. Katzmann, D. J., Babst, M. & Emr, S. D. Ubiquitin-Dependent Sorting into the Multivesicular Body Pathway Requires the Function of a Conserved Endosomal Protein Sorting Complex, ESCRT-I. *Cell* **106**, 145–155 (2001).
45. Schaefer, J. B. & Morgan, D. O. Protein-linked ubiquitin chain structure restricts activity of deubiquitinating enzymes. *J. Biol. Chem.* **286**, 45186–45196 (2011).
46. Ye, Y. *et al.* Ubiquitin chain conformation regulates recognition and activity of interacting proteins. *Nature* **492**, 266–270 (2012).
47. Nielsen, C. P. & MacGurn, J. A. Coupling Conjugation and Deconjugation Activities to Achieve Cellular Ubiquitin Dynamics. *Trends Biochem. Sci.* **45**, 427–439 (2020).
48. Amerik, A. Y., Nowak, J., Swaminathan, S. & Hochstrasser, M. The Doa4 Deubiquitinating Enzyme Is Functionally Linked to the Vacuolar Protein-sorting and Endocytic Pathways. *Mol. Biol. Cell* **11**, 3365–3380 (2000).
49. Papa, F. R., Amerik, A. Y. & Hochstrasser, M. Interaction of the Doa4 Deubiquitinating Enzyme with the Yeast 26S Proteasome. *Mol. Biol. Cell* **10**, 741–756 (1999).
50. Holthuis, J. C. M. Two syntaxin homologues in the TGN/endosomal system of yeast. *EMBO J.* **17**, 113–126 (1998).
51. Reggiori, F., Black, M. W. & Pelham, H. R. Polar transmembrane domains target proteins to the interior of the yeast vacuole. *Mol. Biol. Cell* **11**, 3737–3749 (2000).
52. Becherer, K. A., Rieder, S. E., Emr, S. D. & Jones, E. W. Novel syntaxin homologue, Pep12p, required for the sorting of lumenal hydrolases to the lysosome-like vacuole in yeast. *Mol. Biol. Cell* **7**, 579–594 (1996).
53. Raymond, C. K., Howald-Stevenson, I., Vater, C. A. & Stevens, T. H. Morphological classification of the yeast vacuolar protein sorting mutants: evidence for a prevacuolar compartment in class E vps mutants. *Mol. Biol. Cell* **3**, 1389–1402 (1992).
54. Babst, M. Endosomal transport function in yeast requires a novel AAA-type ATPase, Vps4p. *EMBO J.* **16**, 1820–1831 (1997).
55. Black, M. W. & Pelham, H. R. A selective transport route from Golgi to late endosomes that requires the yeast GGA proteins. *J. Cell Biol.* **151**, 587–600 (2000).
56. Hung, C.-W. & Duncan, M. C. Clathrin binding by the adaptor Ent5 promotes late stages of clathrin coat maturation. *Mol. Biol. Cell* **27**, 1143–1153 (2016).
57. Ruggiano, A., Foresti, O. & Carvalho, P. ER-associated degradation: Protein quality control and beyond. *J. Cell Biol.* **204**, 869–879 (2014).
58. Piersimoni, L., Kastritis, P. L., Arlt, C. & Sinz, A. Cross-Linking Mass Spectrometry for Investigating Protein Conformations and Protein–Protein Interactions─A Method for All Seasons. *Chem. Rev.* **122**, 7500–7531 (2022).
59. Baldridge, R. D. & Rapoport, T. A. Autoubiquitination of the Hrd1 Ligase Triggers Protein Retrotranslocation in ERAD. *Cell* **166**, 394–407 (2016).
60. Carvalho, P., Stanley, A. M. & Rapoport, T. A. Retrotranslocation of a Misfolded Luminal ER Protein by the Ubiquitin-Ligase Hrd1p. *Cell* **143**, 579–591 (2010).

61. Wu, X. *et al.* Structural basis of ER-associated protein degradation mediated by the Hrd1 ubiquitin ligase complex. *Science* **368**, eaaz2449 (2020).
62. Mehrtash, A. B. & Hochstrasser, M. Ubiquitin-dependent protein degradation at the endoplasmic reticulum and nuclear envelope. *Semin. Cell Dev. Biol.* **93**, 111–124 (2019).
63. Peterson, B. G., Glaser, M. L., Rapoport, T. A. & Baldridge, R. D. Cycles of autoubiquitination and deubiquitination regulate the ERAD ubiquitin ligase Hrd1. *eLife* **8**, e50903 (2019).
64. Thibault, G. & Ng, D. T. W. The endoplasmic reticulum-associated degradation pathways of budding yeast. *Cold Spring Harb. Perspect. Biol.* **4**, (2012).
65. Stewart, E. V. *et al.* Yeast SREBP Cleavage Activation Requires the Golgi Dsc E3 Ligase Complex. *Mol. Cell* **42**, 160–171 (2011).